VILNIUS UNIVERSITY
CENTER FOR PHYSICAL SCIENCES AND TECHNOLOGY

ALEKSEJUS KONONOVIČIUS

Applications of Statistical Physics in Modeling of Financial Markets and Social Processes

Doctoral Dissertation
Physical Sciences, Physics (02P)

Vilnius, 2015

The research was performed in 2011–2015 at Vilnius university, Institute of Theoretical Physics and Astronomy

Scientific supervisor:
dr. Vygintas Gontis (Vilnius University, physical sciences, physics – 02 P)

VILNIAUS UNIVERSITETAS
FIZINIŲ IR TECHNOLOGIJOS MOKSLŲ CENTRAS

ALEKSEJUS KONONOVIČIUS

Finansų rinkų ir socialinių procesų modeliavimas statistinės fizikos metodais

Daktaro disertacija
Fiziniai mokslai, fizika (02 P)

Vilnius, 2015

Disertacija rengta 2011–2015 m. Vilniaus universitete, Teorinės fizikos ir astronomijos institute.

Mokslinis vadovas:
dr. Vygintas Gontis (Vilniaus universitetas, fiziniai mokslai, fizika – 02 P)

Contents

List of abbreviations

ABM	Agent-based model
ARCH	Auto-regressive conditional heteroskedasticity
CEV	Constant elasticity of variance
COGARCH	Continuous time generalized auto-regressive conditional heteroskedasticity
EMH	Efficient Market Hypothesis
GARCH	Generalized auto-regressive conditional heteroskedasticity
FIGARCH	Fractionaly integrated generalized auto-regressive conditional heteroskedasticity
MMM	Ticker symbol for The 3M Company
NYSE	New York Stock Exchange
ODE	Ordinary differential equation
PDF	Probability density function
PSD	Power spectral density
SDE	Stochastic differential equation
USD	United States dollar
VSE	Vilnius Stock Exchange
WSE	Warsaw Stock Exchange

1 Introduction

Financial "quakes" are not uncommon phenomena in the financial markets – large stock price jumps often occur without any apparent reason [1–3]. These "quakes" are also commonly observed in other social systems – sometimes the popularity behind works of art and fiction, such as books or movies, or trademarks has no rational explanation [4]. Similar observations are also made by the experimental biologists [5–7] and sociologists [8, 9]. These observations may be related to the concepts of peer pressure and herding behavior [10]. Although the herding behavior enables creation of social institutions, it also poses a threat – increased economic and social risks.

So far the discussion seems to be detached from the traditional physical point of view. Let us develop this topic further by looking for the parallels between physics and social sciences from the historical retrospective.

1.1 Historical retrospective

In the beginning of the 19th century, ideal gas laws, such as Boyle's law (discovered around the middle of the 17th century), Charles's law (around 1780s) or Gay–Lussac's law (around the 1800s), were known purely from the experiments [11]. At that time, classical mechanics was a well-developed theoretical framework, but it was ill-suited to provide an answer in this case. No one was (and, most probably, still is) capable to solve equations of motion for every gas particle jittering in a realistic volume.

At the same time mathematicians, philosophers and statesmen were analyzing demographic data [12]. As well as physicists, they were quickly overwhelmed with the amounts of variables describing each distinct person and his behavior. In order to deal with large amounts of data, it was decided to drop irrelevant variables and calculate the averages of the relevant ones over each person. Around the 1850s–1870s, this idea was introduced into physics, mainly by James Clerk Maxwell and Ludwig Boltzmann, and used to explain ideal gas laws. The possibility that social sciences had an impact on Boltzmann's work is frequently highlighted in most historical reviews (e.g., [13, 14]) by providing the following quote:

"The molecules are like so many individuals, having the most various

states of motion, and the properties of gases only remain unaltered because the number of these molecules which on the average have a given state of motion is constant."

Thus, once in the past experience from social sciences enriched physics facilitates the emergence of statistical physics.

In the first decade of the 20th century Albert Einstein and Marian Smoluchowski independently had shown that atoms are not just an abstract concept, that atoms' jittering might cause apparently erratic motion of larger particles [15, 16]. Namely, their theoretical and experimental work served as a proof of the kinetic theory of gases, as well as the explanation for the Brownian motion. But the first work on the Brownian motion was a doctoral dissertation defended in the 1900 by French mathematician Louis Bachelier who derived it by assuming that stock prices fluctuate randomly [17]. The simple model proposed by Bachelier may be seen as an early precursor to modern risk management models based on the stochastic calculus, such as Black-Scholes [18] or Heston [19] models.

In the mid 1900s the young British hydrologist Harold E. Hurst came to Egypt. The young hydrologist was given a task to predict floods of the Nile based on the past data. While analyzing the collected data Hurst noted significant long-range auto-correlations. In the following years, he faced other similar problems and consequently developed a time series analysis framework which is now known as rescaled range analysis [20], to detect the presence and qualities of long-range correlations. Hurst published his results only after retiring in the early 1950s [21]. His work was well received and in the next decades became recognized as a fundamental work opening the discussion on the detection of long-range memory.

In the 1920s, Ernst Ising in his PhD dissertation analyzed a simple model of magnetization which is now known as the Ising model [22]. This model was one of the first models to exhibit the pattern formation. In the 1950s, Edward Lorenz noted that pattern formation was important in weather forecasting, and in the next fifteen years he developed and proposed his own weather forecasting model which was nonlinear. Due to the inherent nonlinearity the model exhibited a chaotic behavior, as Lorenz wrote [23]:

"Two states differing by imperceptible amounts may eventually evolve into two considerably different states... If, then, there is any error whatever in observing the present state – and in any real system such errors

> seem inevitable – an acceptable prediction of an instantaneous state in the distant future may well be impossible... In view of the inevitable inaccuracy and incompleteness of weather observations, precise very-long-range forecasting would seem to be nonexistent."

Nowadays this is summarized as a butterfly effect: a single unpredictable flap of butterfly's wings may set off a storm in another part of the globe. Now this is somewhat reminiscent of risk in social systems: a small, unaccounted for or completely unexpected event may cause a sudden significant change in the weather pattern. Around this interesting notion, chaos theory, complexity theory, synergetics emerge [24–26], emphasizing the nonlinear nature of our world. Physicists, mathematicians and other representatives of the "hard" sciences take up interest in open systems which often tend to exhibit pattern formation and emergent behavior.

In the meantime, economics developed in its own way. As in most social sciences, the human nature of "particles" in question, actual people, was taken into account. But it is hard to take the full complexity of human behavior and social interactions into account, thus neoclassical economical theories neglected some of these features in order to obtain analytically tractable mathematical models. This lead to mathematically simpler models and other tools to deal with the inherent risk, but with some essential features being left out.

A major oversimplification of human behavior is done by introducing the concept of *homo economicus*. This economic man, by definition, is well informed, rational and self-interested [27]. Neither of these assumptions appear to be realistic, but in physics we also tend to make simplifying approaches which usually work. In this case, one of the major problems lies in the fact that individual rationality does not necessarily imply collective rationality which is rather well-known from the voting paradox, or the Condorcet paradox [28]. A deeper problem, of course, is that individual rationality itself does not exist or might be useless while solving certain simple problems, such as the El Farol bar problem [29]. While "The End of Economic Man", namely, its insufficiency to model endogenous risk, was predicted a long time ago, originally by P. Drucker in 1939 (see more recent edition of the same book [30]), yet despite even more critique followed since then, the concept is still alive in the core of mainstream economics [31–35].

The idea about rational agents is not inherently wrong. It might actually be used to simplify mathematical logic behind certain models. Similar ideas work well

in the game theory [36] and may be applied in practice [37]. The key problem here is that mainstream economics uses the concept of *homo economicus* as an excuse to reduce what should be seen as multi-agent problems to single, representative, agent problems [38]. This idea is at odds with physical thought, with what was done by Boltzmann and Maxwell when laying the foundation of statistical mechanics.

Market efficiency is another key idea in the core of mainstream economics [1–3]. It assumes that traders are able to incorporate information about a tradable object (e.g., stock, commodity, service) into its market price, namely, that the market price reflects the true value of the object. Evidently this ought to be true, if traders in the market behave at least somewhat like *homo economicus*. However, the frequency with which local and global economic crises occur suggests that tradeable objects are often over-valued or under-valued causing those market bubbles and crashes [1–3, 31–33, 39–43].

Frequently the mainstream economics consider large economical fluctuations as outliers of the otherwise normal, following the Gaussian distribution, financial fluctuations. Logic here is rather simple: as agents are rational and markets are efficient, price fluctuations should follow the exogenous information flow. As the exogenous information flow is composed of many random events, due to the central limit theorem it should lead to the Gaussian fluctuations. Indeed, most of the time, or in most cases, the Gaussian distribution fits the empirical data rather well, but it does not fit a large portion of the extreme cases. However, they may be fitted using power-law distributions,

$$p(x) \sim x^{-\lambda}. \tag{1.1}$$

Interestingly enough, the power-law distribution was first considered by the Italian engineer (by education) and economist Vilfredo Pareto in the end of the 19th century [44, 45]. In his work Pareto shows that the wealth distribution in a stable economy follows the power-law distribution. He is also quoted to say that this result is rather general and applies to nations "as different as those of England, of Ireland, of Germany, of the Italian cities, and even of Peru." Nowadays Pareto is more commonly known for the 80–20 rule which is actually related to the power-law distribution in the sense that it highlights the importance of the outliers. Originally, in his analysis V. Pareto had shown that ~80% of land in Italy was owned by the ~20% of population. Though the rule itself was not conceived by V. Pareto, it was done a couple decades later by J. Juran [46].

Power-law distributions remained mostly forgotten until the works by P. Levy [47], H. E. Stanley [48], B. Mandelbrot [49], and P. Bak [50], who have shown that the counter-intuitive scale-free power-law behavior may be observed in open systems and generally in systems at their critical points. Now it is accepted that power-law distributions, as well as other power-law statistical features (such as cross-correlations, auto-correlations, PSD and return intervals), are common to socio-economic systems [51–65]. This doctoral dissertation is mostly concerned with the statistical features of absolute return which is defined as

$$r_T(t) = \ln P(t) - \ln P(t - T), \tag{1.2}$$

where $P(t)$ is price. In some papers, econometric and empirical papers $|r(t)|^\alpha$, usually $\alpha = 2$, is considered (e.g., [66–68]), although raising to power may distort the properties of the time series for small and large values, and thus physicists often choose to model and study $\alpha = 1$. In Figure 1.1, you can see one-minute absolute return PDF (a) and PSD (b) of a randomly selected stock (ticker symbol MMM) from NYSE approximated by the power-law functions.

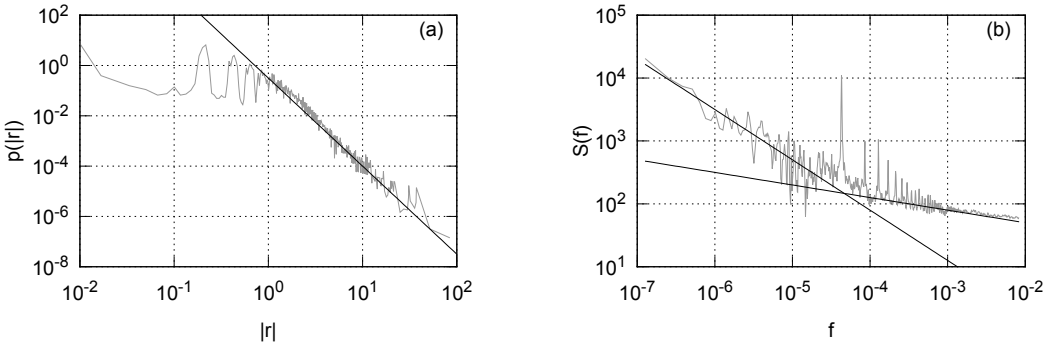

Figure 1.1: PDF (a) and PSD (b) of normalized absolute one-minute return of the MMM stock time series, time period from January 2005 to March 2007 (gray curves) fitted by power-law functions (black curves). Power-law functions: $p(|r|) \sim |r|^{-\lambda}$ with $\lambda = 3.6$ (a), $S(f) \sim f^{-\beta_i}$ with $\beta_1 = 0.8$ and $\beta_2 = 0.2$ (b).

The empirical confirmation of power-law statistics serves as a direct indication that conventional risk management tools, and also conventional models, underestimate the probability of extremely large deviations. Extremely large deviations are noticeably more probable in power-law distribution than in exponential, such as Gaussian, distributions. This kind of underestimation may lead to severe consequences, and the recent financial crisis is seen as an example [31–33, 69–71]. So, instead of using mathematically convenient concepts of the rational economic man and market

efficiency, one needs to work on the idea that human behavior is highly irrational, prone to brain bugs, as well as highly heterogeneous. One needs to embrace the idea that the human behavior is complex and non-linear, the presence of the emergent behavior and self-organization, the extreme importance of social interactions as well as the idea underlying statistical physics, that the peculiarities of a single individual are not important, all that matters is the statistical description of the interactions.

1.2 Methods

Besides methods and ideas common to physics in general and statistical physics in particular, some of which were mentioned while providing the historical context (such as the statistical and stochastic analysis), we will also use two contemporary frameworks, agent-based modeling and network theory, designed specifically to model socio-economic systems. Further in this section, we provide a brief introduction into the three main frameworks, agent-based modeling, network theory and stochastic analysis, used in this dissertation.

1.2.1 Agent-based modeling

One of the best contemporary frameworks to work with in this context is known as agent-based modeling [72–76]. As the naming of the framework implies the key concept in it is the concept of an agent. Agents are basically highly stylized objects which use simple rules to emulate essential behavioral features of real entities (e.g., firms, people, etc.) acting in the modeled system. Interestingly enough, this simplicity is still able to reproduce distinctive features of a complex behavior.

Historically, it might be reasonable to see J. von Neumann's cellular automaton as an early precursor of modern cellular automata and agent-based modeling [77]. It featured a grid and certain rules on how cells present on the grid should behave. The problem was that J. von Neumann's automaton was rather complex: cells could be found in 29 different states and, as should be expected, the transition rules were somewhat convoluted. J. von Neumann's work inspired the mathematician J. H. Conway to create a simpler automaton which is now widely known as the Game of Life [78]. The Game of Life featured only two possible cell states ("alive" or "dead") and simple state switching rules which were based only on the number of immediate neighbors in the "alive" state. Surprisingly, the Game of Life exhibits a variety of still, oscillat-

ing and moving patterns which serve as an excellent showcase of emergent complexity. Numerous authors are fascinated with the idea and lots of books are dedicated to cellular automata (with the most recent and prominent example being [79]).

This historic retrospective into cellular automata is useful in order to draw direct parallels to physical modeling. From the physicist's point of view, the Ising model might be seen to have a strongest relation to these pioneering works. First of all, in the classical handbook version of the Ising model [22], in this model the particles are aligned in a square lattice. These particles possess an intrinsic property of a magnetic spin, the orientation of which is chosen according to certain simple probabilistic rules. These rules take just a neighboring spin orientation and the global magnetic field orientation into account. But this model is able to exhibit a complex behavior, phase transitions observed in real magnetic materials. Some works [80–83] use ideas from the Ising model directly to build and enhance ABMs. In this type of works, the physical concept of particle and its spin is replaced with a more general concept of agent and its state.

Unlike for cellular automata, for most ABMs placing agents on a grid is a redundant component. Namely, in a significant fraction of contemporary ABMs, agents interact in an abstract or undefined topology. It appears that it may not matter as long as there is some other way of observing a system state or interacting with other agents.

Excellent examples of models with an undefined interaction topology are models inspired by the kinetic theory of gases [84]. In these models, the interacting agents are usually chosen randomly from the whole population. The picked agents, usually two, interact among themselves and afterwards are returned to the population with their energies changed according to simple rules. Kinetic models have found their applications in modeling wealth distributions [85–88], although there are applications to other fields of economics [89–92].

Some of the models are inspired by the traditional frameworks of economics. One of the most prominent models is the model proposed by Lux and Marchesi [93]. In this model, agents evaluate their trading strategy by comparing the prospective profits that could be generated by any of the three trading strategies. This evaluation is formulated using utility functions (an essential concept in the economical rational choice theory [94]), but, in stochastic interpretation, increased utility means an increase in the probability to switch to that trading strategy. A similar model, relevant

in context of the dissertation, was proposed by Kirman and Teyssiere [95].

At the same time, some are built around general ideas about the social interactions themselves. The Minority Game was conceived as a simple thought experiment building atop the idea that belonging to minority might benefit the agent in certain economic scenarios [29]: if significantly more people are willing to buy, then it is highly likely that the minority willing to sell could ask for unreasonably high prices and still be able to sell. Some of the works note that people are not ideally rational nor ideally informed and thus try to compensate their own shortcomings by imitating the behavior of the others [96–99]. Interestingly enough, in a recent paper by J. Touloub it was shown that these two radically different approaches might lead to equivalent behavior [100]. Namely, the results presented in the paper imply that acting as a non-conformist (trying to be in the minority) might lead to the emergence of conformism (actually belonging to the majority).

Recent reviews by Cristelli et al. [73] and Sornette [76] provide a broad outlook into the contemporary agent-based modeling. Both of the reviews emphasize different problems related to agent-based modeling, but suggest a similar idea on how to move the field forward. Sornette [76] emphasizes that there is a huge variety of the proposed ABMs which are able to reproduce some stylized facts reasonably well, however most of these ABMs being incomparable and most of them lacking possibilities to be calibrated. Thus, according to Sornette [76], the agent-based modeling as a whole appears to lack robustness. Cristelli et al. [73] emphasize the "collision" between the attempts to reproduce realism and recover the analytical tractability of the proposed models. Cristelli et al. [73] state that the ideal model should posses both of these qualities, but it might be extremely hard to achieve. Thus, Cristelli et al. [73] encourage to look for simple yet realistic and analytically tractable ABMs. We see "Emerging Intelligence Market Hypothesis", proposed by Sornette [76] as an alternative to the classical EMH, being essentially the same idea phrased using other words. Their ideas can be brought to a common denominator by formulating the following requirements for ABMs: ABMs should be as simple as possible, ABMs should be analytically tractable, and ABMs should allow important realistic market properties to emerge from the interaction among the agents.

1.2.2 Network theory

As mentioned in the previous sections ABMs and cellular automata agents may be placed on a two-dimensional square grid and assumed to interact with their immediate four (or eight) neighbors. Yet in real social life, the interaction topology is not like that at all. The increasing dimensionality or changing symmetry properties of the grid (switching to a hexagonal or a triangular grid) usually doesn't significantly change things. As it was discussed previously, in some cases it doesn't matter, but there are also cases where the interaction topology is extremely important. These cases are considered by a framework known as the network theory [101–104].

The network theory views the world as graphs, both static and evolving. Graphs consist of vertices (alternatively referred to as nodes) and edges (alternatively referred to as links). Edges connecting vertices might be weighted to show how important the given edge is: e.g., not all social contacts have the same impact on the social life. Edges might be also directed to show the directional nature of relationship: e.g., in a scientific paper citation network it is rather clear which paper was cited by which paper.

The most straightforward example of the network would be the Internet. We could even view it at two different perspectives. The first perspective is that of the organization of the online content. Namely, most of the web pages cite other web pages and in this way help users to navigate and find the desired information. In this context, it is easy to view a web page as a node and hyperlinks as edges connecting nodes. Google robots crawl and index the Internet to monitor this, later this information is used to estimate the importance of each node and may be the quality of its content. When the user enters a keyword in Google search, complex algorithms use this information to present the most relevant results. Another possible perspective is the hardware perspective. We could see every more or less sophisticated hardware (personal computer, server, router, etc.) as a network node and wiring (or established direct connections in case of WiFi) as edges.

There are three classic handbook models in the network theory [101–104]: the Erdos–Renyi, Watts–Strogatz and Barabasi–Albert models.

The Erdos–Renyi (also known as the random graph) model [105] is the simplest random network model. In this model, the link between a pair of nodes is present with certain probability p. The Erdos–Renyi model does not exhibit any

interesting features, with the exception of short path lengths. This model, being the simplest random network model, now serves as a benchmark tool for other random network models. It is worth noting that the Erdos–Renyi model is related to the percolation theory [106]. Namely, it produces an identical result as solving the percolation problem on a fully connected graph.

The Watts–Strogatz model [107] is dedicated to showing that a couple of random links (via addition or rewiring) can significantly contribute to a decrease of average path lengths in regular (e.g., grid, ring) networks. Shorter average path lengths imply a smaller world, thus the model is often referred to as a small world model, which is a rather surprising property to observe in networks as localized as human society. In the 1960s group led by S. Milgram performed an experiment: some people from Omaha (Nebraska, USA) and Wichita (Kansas, USA) were asked to pass a letter to a person living in Boston. The experimenters made sure that people would not know the addressee, but asked them to send the letter to the person who was most likely to know the addressee. When the letters arrived to Boston researchers found that it has reached the destination in at most 6–7 hops [108]. Apparently random social contacts outside the usual social circle helped to achieve this result.

The Barabasi–Albert model [109] is the most recent of the three classical network theory handbook models. This model explains the power-law degree (the number of links that connect to the node) distribution observed in numerous real networks. The examples include scientific citation, Internet hyperlink, Internet hardware, sexual interaction, Facebook friend and Twitter follower networks. The power-law degree distribution is explained by the preferential attachment mechanism: nodes having a large degree are likely to attract more links from new nodes.

Yet neither of the three main models cover an interesting feature (in terms of this dissertation) observed in gaming communities, their nonlinear densification [110–114]. Namely, it is observed that the number of links in densifying networks grows faster than linearly with the increasing number of nodes. In other words, as network grows (in terms of nodes), the average degree of nodes in the network also increases. There are numerous models [110–114] exhibiting this feature, but the universal mechanism has still not been uncovered.

1.2.3 Stochastic modeling

Both the ABM framework and the network theory provide insights into interactions among the individual agents (microscopic level interactions). Stochastic modeling (stochastic calculus) is much older framework used to deal with the dynamics happening on a global scale (macroscopic level). Evidently it is inferior in comparison with the previously discussed frameworks in the sense that stochastic models do not provide direct insights into individual level interactions: in most cases they just reproduce the desired phenomena. Stochastic calculus is superior in the sense that it is more or less analytically tractable, while it may be hard in case of complex ABMs or network models.

In the beginning of the 19th century, the Scottish botanist Robert Brown observed the jittery movement of pollen in a solution [115]. Initially, he thought that pollen moved due to being alive, but repeating the experiment with a clearly inanimate matter (metal dust) he understood that it was not the case. Almost a century later this phenomenon was explained independently by A. Einstein and M. Smoluchowski [15, 16] who predicted that the Brownian motion could serve as a proof for the existence of atoms. The jittery motion of pollen happens due to a large number of random collisions with atoms and molecules in a solution.

Inspired by these results, Paul Langevin, a couple of years later, proposed an equation to describe the Brownian motion [116]:

$$m\frac{\mathrm{d}^2\vec{x}}{\mathrm{d}t^2} = -\lambda\frac{\mathrm{d}\vec{x}}{\mathrm{d}t} + \vec{\eta}(t). \tag{1.3}$$

The proposed equation has almost the same form as equations of motion in classical mechanics, with the exception that $\vec{\eta}$ represents a random force which is assumed to be uncorrelated and following the Gaussian distribution. As the derivatives of x do not exist in the usual sense, the equation needs to be interpreted by other means: here the Ito and Stratonovich integrals are used to give meaning to this equation. The main difference between the interpretations is the moment when the random force acts upon the particle, during a time tick (the Ito sense) or in-between time ticks (the Stratonovich sense). This has some interesting consequences, such as the chain rule of calculus holding only for the Stratonovich integral, but they do not matter in terms of this dissertation as there are straightforward ways to convert SDEs from one interpretation to other.

In the general case, the Langevin equation, also referred to as the SDE, in the Ito sense may be written as [117–119]

$$\mathrm{d}\,x = f(x,t)\,\mathrm{d}\,t + g(x,t)\,\mathrm{d}\,W, \tag{1.4}$$

where $f(x,t)$ (drift) and $g(x,t)$ (diffusion) are generalized functions driving the evolution of the modeled system, while W is a Wiener process which is equivalent to the one-dimensional Brownian motion. Interestingly enough, $f(x,t)$ and $g(x,t)$ may be estimated from the empirical data by observing the means and the standard deviations of the subsequent observed values. The SDE might be also obtained from the Fokker–Planck equation which means that it might be derived from microscopic (individual level) considerations as long as they are simple enough to be analytically tractable.

1.3 Objective of the dissertation

The objective of this dissertation is to construct models of financial markets and social processes by applying ideas and tools inherent to statistical physics, econophysics and nonmainstream economics.

1.4 Main tasks of the dissertation

1. To analyze the statistical properties of the bursting behavior observed in empirical and model absolute return time series.

2. To examine the possible relation between the general class of SDEs reproducing power-law PDF and PSD and models from other frameworks,such as GARCH, agent-based modeling and network theory.

3. To propose a minimal ABM which would generate a time series exhibiting the power-law PDF and PSD characteristic to the general class of SDEs.

4. To propose a financial market model which would generate the absolute return time series exhibiting power-law PDF and PSD characteristic to the financial markets.

5. To analyze the opportunities to prevent extreme events arising from the proposed ABMs.

1.5 Scientific statements

1. The analyzed empirical and model absolute return time series exhibit statistically similar burst duration PDF as well as statistically similar power-law scaling in the geometric properties of bursts.

2. The nonlinear modifications of the GARCH(1,1) model generate the volatility time series exhibiting the power-law PDF and PSD, including $1/f$ noise.

3. A continuous transition from the nonextensive to extensive statistics is observed when interactions become more localized.

4. The derived, from ABM based on herding behavior, SDE for long-term variation of return belongs to the general class of SDEs reproducing power-law PDF and PSD.

5. Three-state financial market ABM generate a time series exhibiting a double power-law, with two characteristic exponents, PSD.

6. The empirical absolute return PDF and PSD is reproduced by the consentaneous model which includes three-state dynamics as well as the external noise.

7. The controlled agents, interacting on the global scale, are able to decrease the probability of extreme events. The effect persists in the three-state model when the controlled agents trade randomly.

1.6 Scientific novelty

Agent-based modeling is an important framework in social and economic modeling as ABMs provide important insights into the nature of interactions inside the modeled systems. Using this framework allows to understand how individual level interactions cause the observed stylized facts [72,73,120], though the exact statistical features frequently are far more complex than stylized facts, and ABMs aiming to reproduce exact statistical features often become too complex to be tractable [73]. Stochastic modeling, on the other hand, allows to generate a time series exhibiting statistical features close to those observed empirically. However stochastic models do not provide any direct insights into the process they are used to model. Thus, in

the recent decade there were numerous calls [32] and attempts [83, 121, 122] to find relationships among these frameworks.

In the given context, the research presented in this dissertation stands out, because we, by using the previous works on agent-based modeling by other research groups [96, 123–126], derive simple financial market ABMs compatible with stochastic models derived in previous works by our research group [127–131]. The financial market ABMs proposed in this dissertation are special in the sense that their complexity is gradually built up: some are able to generate the time series exhibiting stylized facts of the absolute return, while others are able to generate the time series exhibiting exact empirical statistical features of the absolute return.

The research presented in this dissertation also covers the topic of extreme event prevention. Previously this topic was developed by considering only very simple models [132, 133] or sophisticated experimental setups [8, 9]. We are the first to test the extreme event prevention strategies in the financial market model which is able to reproduce empirical statistical features of absolute return.

1.7 Outline of the dissertation

The list of abbreviations used in this dissertation is given in the chapter previous to the introductory chapter.

In Chapter 2, we briefly review previous works related to the general class of SDEs reproducing power-law PDF and PSD as well as analytical and numerical techniques used to deal with SDEs. These techniques are important in other chapters of the dissertation. Some of the discussed novel results were published by the author of this dissertation in [A13-A15].

In Chapter 3, we provide an empirical, numerical, and analytical analysis of the bursting behavior of absolute return in the financial markets. The original results were published in [A10].

In Chapter 4, we propose two nonlinear modifications of the GARCH(1,1) volatility process which generate the time series exhibiting power-law PDF and PSD. In essence, the modified nonlinear GARCH(1,1) volatility process proves to be similar to the general class of SDEs reproducing power-law PDF and PSD. The original results were published in [A2].

In Chapter 5, we provide a description of Kirman's two-state ABM of the herd-

ing behavior. In this chapter, we discuss the implications of interaction topology on the population dynamics of this two-state ABM. The original results were published in [A3].

In Chapter 6, we provide an interpretation of financial markets in terms of ABM based on the herding behavior. Starting from the ABM and including features important to the financial markets, we build a model which is able to reproduce empirically observed PDF and PSD of absolute return. The original results were published in [A4, A6-A9, A11, A12].

In Chapter 7, we discuss the opportunities of the financial extreme event prevention which appears to be possible from the perspective of ABMs presented in other chapters of this dissertation. The original results were published in [A1, A5].

In Chapter 8, we gather up the main results presented in this dissertation.

The numbered chapters are followed by a list of bibliographical references, a list of publications and presentations by the author of this dissertation, and acknowledgments.

2 General class of SDEs exhibiting power-law statistics

A general class of nonlinear SDEs generating signals exhibiting power-law statistical features was previously proposed, starting from the point process, in a series of papers by Kaulakys, Ruseckas, Gontis and Alaburda [127–131]. A general expression for this class of Ito SDEs is given by

$$\mathrm{d}\, x = \sigma^2 \left(\eta - \frac{\lambda}{2} \right) x^{2\eta - 1} \,\mathrm{d}\, t + \sigma x^{\eta} \,\mathrm{d}\, W, \tag{2.1}$$

where σ sets timescale, η is noise multiplicativity (nonlinearity) parameter, λ is exponent of power law PDF of x and W is a Wiener process, one-dimensional Brownian motion.

Different modifications of this general class of SDEs were successfully used to model trading activity and absolute return of the financial markets [134–136]. This general class of SDEs was also successfully used to model observables from other socio-economic systems (e.g., internet traffic [137, 138]) as well as other, not socio-economic, systems (e.g., music [139], word occurrences [140], diffusion in non-homogeneous media [141, 142]) suggesting that the modeled phenomena is rather general and that the SDE, given by Eq. (2.1), captures the general essence of $1/f$ noise.

SDE (2.1) is mostly identical to SDE proposed in earlier work by Marsh and Rosenfeld [143]. Furthermore this SDE may be also transformed, using Ito variable substitution formula [119] or simply fixing certain parameter values, into other well known stochastic processes, such as Bessel, Cox-Ingersoll-Ross or CEV processes [144]. The important difference from these previous works is that Kaulakys, Ruseckas, Gontis and Alaburda in their works considered $\eta > 1$, while established econometrical models tend to consider $\eta \leq 1$ [145].

2.1 Numerical solution of SDEs

2.1.1 Euler-Maruyama and Milstein methods for SDEs

Let us write a general form of SDE as:

$$\mathrm{d}\,x = A(x)\,\mathrm{d}\,t + B(x)\,\mathrm{d}\,W, \tag{2.2}$$

here $A(x)$ is a drift function and $B(x)$ is a diffusion function. The simplest method used to numerically solve SDE is based on a simple method used to numerically solve ODEs, Euler method [146]. Application of Euler method to SDEs is referred to as Euler-Maruyama method [118, 147]. The iterative difference equation, when using this method, might take the following form:

$$x_{i+1} = x_i + A(x_i)\Delta t + B(x_i)\Delta W. \tag{2.3}$$

The iterative difference equation above has similar form, compared to the iterative difference equation obtained for ODE, with the only difference being W process. We known that it stands for a Wiener process, or in other words one-dimensional Brownian motion, it describes path (time evolution of coordinate) of the one-dimensional particle hit by some random force. Central limit theorem suggest that collective influence of many independent random factors follows the Gaussian distribution, thus it is expected that the changes of particles coordinate will also follow the Gaussian distribution. The standard deviation of the distribution will depend on the size of time step, Δt, actually it is known that the standard deviation will increase as a square root of time step width. In such case we can write the difference equation, which is identical in distribution to Eq. (2.3), as follows [118, 147]:

$$x_{i+1} = x_i + A(x_i)\Delta t + B(x_i)\sqrt{\Delta t}\zeta_i, \tag{2.4}$$

where ζ_i is a Gaussian random variable with zero mean and unit variance. In handbooks this difference equation is frequently referred to as Euler-Maruyama approximation, or Euler-Maruyama method for SDEs, [118, 147].

Another classical handbook method is Milshtein method [118, 147]. Using this method iterative difference equation takes the following form,

$$x_{i+1} = x_i + A(x_i)\Delta t + B(x_i)\sqrt{\Delta t}\zeta_i + \frac{1}{2}B(x_i)\left(\left.\frac{\mathrm{d}\,B(x)}{\mathrm{d}\,x}\right|_{x=x_i}\right)\left(\zeta_i^2 - 1\right)\Delta t. \tag{2.5}$$

The fourth term on the right hand side provides enhanced precision. Using this method the error scales with Δt instead of $\sqrt{\Delta t}$ as in Euler-Maruyama method. Yet solving Eq. (2.1) using them or higher-order methods would still require use of extremely small Δt which would increase computation times beyond the feasible.

2.1.2 Variable time step method

Note that in Eq. (2.1) both drift, $A(x)$, and diffusion, $B(x)$, functions are power-law. Thus while solving Eq. (2.1) numerically using Euler-Maruyama or Milshtein methods it appears that time series of x at some point "explode". Although decreasing Δt appears to provide stability to numerical computations. But one cannot decrease Δt indefinitely as computation times grow unreasonably large.

Based on these observation it is rather natural to propose to scale Δt based on the value of x. Namely, if x is small, then its changes are small (the value changes slower), thus larger Δt values are able to provide sufficient precision. If x is large, then its changes become larger (the value changes faster), thus Δt should grow smaller. Thus in general case, building on the Euler method,

$$x_{i+1} = x_i + A(x_i)h(x_i) + B(x_i)\sqrt{h(x_i)}\zeta_i, \tag{2.6}$$

$$t_{i+1} = t_i + h(x_i). \tag{2.7}$$

From the previous experience of solving Eq. (2.1) [127,130,131], it appears that $h(x)$ should be chosen so that in the $x \to \infty$ limit it linearizes drift and diffusion terms:

$$A(x)h(x) \propto x^a, \;\; a \leq 1 \quad \text{and} \quad B(x)\sqrt{h(x)} \propto x^b, \;\; b \leq 1. \tag{2.8}$$

In case of Eq. (2.1) [127, 130, 131]:

$$h(x) = \kappa^2 x^{2-2\eta}, \tag{2.9}$$

where κ is a precision parameter which should be positive and at smaller than 1. Consequently difference equations solving Eq. (2.1) would take the following form:

$$x_{i+1} = x_i + \kappa^2 \left(\eta - \frac{\lambda}{2}\right) x_i + \kappa x_i \zeta_i, \tag{2.10}$$

$$t_{i+1} = t_i + \kappa^2 x^{2-2\eta}. \tag{2.11}$$

Note that for $\eta > 1$ in the limit of small x, $x \to 0$, $h(x)$ diverges to infinity. Thus, and as usually we need time series sampled at certain period T, it is natural to restrict $h(x)$ using min function:

$$h(x,t) = \min(\kappa^2 x^{2-2\eta}, jT - t), \quad \text{where } j = \min\{x : xT > t,\ x \in \mathbb{N}\}. \tag{2.12}$$

Another possible alternative is to use original $h(x)$ and interpolate to obtain the discretized time series. But this alternative is too tedious to implement, thus we stick with the simpler algorithm.

2.2 Power-law steady state PDF

Steady state PDF of x, generated by SDE (2.1), can be shown to follow power-law distribution. In most handbooks (e.g. [117–119]) for stochastic calculus one will find the following general formula:

$$p_{st}(x) = \frac{C}{B^2(x)} \exp\left[2 \int^x \frac{A(s)}{B^2(s)}\, \mathrm{d}\, s\right], \tag{2.13}$$

here $\int^x f(y)\, \mathrm{d}\, y = F(x)$ (where F is a primitive function of f), $A(x)$ is drift function and $B(x)$ is a diffusion function of the SDE for x. Note that the formula holds only if stationary PDF exists, if it does not exists the expression above will, most probably, still provide a result, yet it will be incorrect. E.g., standard Brownian motion, $A(x) = 0$ and $B(x) = 1$, has no stationary distribution, but the equation above provides us with the result $p_{st}(x) = 1$. So due caution should be exercised and analytical results should be carefully compared to basic intuition and numerical results.

By putting appropriate terms from Eq. (2.1) into it the following is obtained:

$$\begin{aligned} p_{st}(x) &= \frac{C}{x^{2\eta}} \exp\left[2\left(\eta - \frac{\lambda}{2}\right) \int^x \frac{\mathrm{d}\, s}{s}\right] = \\ &= \frac{C}{x^{2\eta}} \exp\left[(2\eta - \lambda) \ln(x)\right] = \frac{C}{x^{2\eta}} \exp\left[\ln(x^{2\eta-\lambda})\right] = C x^{-\lambda}. \end{aligned} \tag{2.14}$$

Thus stationary distribution of time series generated by SDE (2.1) is inverse power-law with the exponent λ. We compare this analytically obtained expression with numerical results further in Figure 2.2.

Note that the obtained PDF (2.14) contains normalization constant C. For $1 < \lambda$ it is impossible to obtain the exact expression for it as the normalization

integral is divergent. In numerical simulations it is clearly seen that solutions of SDE (2.1) tend to get stuck at $x = 0$. In other words $x = 0$ absorbs the trajectories. Thus one needs to introduce boundary conditions, limit the possible x values, to prevent this.

Even if we solve the normalization integral divergence problem by introducing reflective boundary from the side of small values, the n-th moments of the power-law distribution will still diverge for all n which satisfy $\lambda \leq 1 + n$. In order to have distribution with all finite moments we need to introduce reflective boundary condition from the side of large values as well. This boundary condition can be seen to arise from real-life considerations, in [141] it was shown that if noise is correlated on short time scales, then this restriction emerges as a side effect. The upper bound restriction is also necessary in order for drift and diffusion functions to be Lipshitz continuous [118, 147].

There are three simple ways to implement the restrictions: introduce boundary conditions, exponential cutoffs or "zero" fluctuations.

Let us start by discussing introduction of boundary conditions. For example, one may introduce reflective boundary conditions at some minimum value $x = x_{min}$ and at maximum value $x = x_{max}$. In this case stationary PDF will have the same form as given in Eq. (2.1), if $x \in [x_{min}, x_{max}]$, and will be equal to zero otherwise. Integration constant, in this case, will be given by:

$$C = \frac{1 - \lambda}{x_{max}^{1-\lambda} - x_{min}^{1-\lambda}}. \tag{2.15}$$

As mentioned introduction of exponential cutoffs is viable alternative to reflective boundary conditions. One of the ways to do it is to modify the drift function of SDE (2.1) in a following way:

$$A_x(x) = \sigma^2 \left[\eta - \frac{\lambda}{2} + \frac{m}{2} \left(\frac{x_{min}^m}{x^m} - \frac{x^m}{x_{max}^m} \right) \right] x^{2\eta - 1}, \tag{2.16}$$

here m sets the steepness of the cutoff (in general $m > 0$). In the modified case

stationary PDF has the following form, by using Eq. (2.13) and Eq. (2.14):

$$\begin{aligned} p_{st}(x) &= C x^{-2\eta} \exp\left[2\int^x \frac{\eta - \frac{\lambda}{2} + \frac{m}{2}\left(\frac{x_{min}^m}{s^m} - \frac{s^m}{x_{max}^m}\right)}{s}\,\mathrm{d}\,s\right] = \\ &= C x^{-\lambda} \exp\left[m\left(\int^x \frac{x_{min}^m}{s^{m-1}}\,\mathrm{d}\,s - \int^x \frac{s^{m-1}}{x_{max}^m}\,\mathrm{d}\,s\right)\right] = \\ &= C x^{-\lambda} \exp\left[-\frac{x_{min}^m}{x^m} - \frac{x^m}{x_{max}^m}\right]. \end{aligned} \tag{2.17}$$

With these restrictions probability to observe x outside of vicinity of $[x_{min}, x_{max}]$ decreases rapidly. Thus normalization integral no longer diverges and thus expression for C may be obtained:

$$C = \frac{m}{2}\left(x_{max}x_{min}\right)^{\frac{\lambda-1}{2}} K^{-1}_{\frac{1-\lambda}{m}}\left[2\left(\frac{x_{min}}{x_{max}}\right)^{\frac{m}{2}}\right], \tag{2.18}$$

where $K_n(z)$ is a modified Bessel function of the second kind [148].

Let us modify SDE (2.1) by introducing "zero" fluctuations. The modified SDE may take the following form:

$$\mathrm{d}\,x = \sigma^2\left(\eta - \frac{\lambda}{2}\right)\left(1 + x^2\right)^{\eta-1} x\,\mathrm{d}\,t + \sigma\left(1 + x^2\right)^{\frac{\eta}{2}}\mathrm{d}\,W. \tag{2.19}$$

The diffusion function of this SDE as $x \to 0$ approaches a certain fixed value, σ, and not zero as in SDE (2.1) case. Consequently in this case additive noise facilitates diffusion around $x = 0$. In this case stationary PDF has a form of a q-Gaussian [149], or alternatively Student's t [150], distribution:

$$p_{st}(x) = C\left(\frac{1}{1 + x^2}\right)^{\frac{\lambda}{2}} = C\exp_q\left(-\frac{\lambda x^2}{2}\right). \tag{2.20}$$

In this case normalization integral no longer diverges and expression for C may be obtained:

$$C = \frac{\Gamma\left(\frac{\lambda}{2}\right)}{\sqrt{\pi}\,\Gamma\left(\frac{\lambda-1}{2}\right)}. \tag{2.21}$$

This case is especially interesting as there is some agreement that distributions of some financial variables, e.g., absolute return, are well fitted by q-Gaussian distribution [135, 149].

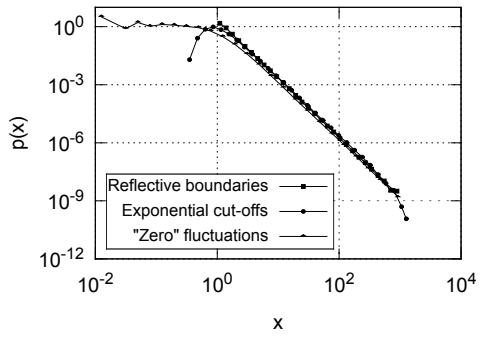

Figure 2.1: PDFs obtained by numerically solving SDE (2.1) with reflective boundaries, exponential cut-offs and "zero" fluctuations (reflective boundary placed at x_{max}). Parameters were set as follows: $\sigma^2 = 1$, $\eta = 2$, $\lambda = 3$, $x_{min} = 1$, $x_{max} = 10^3$. Time series were sampled with period $T = 10^{-5}$.

As you can see in Figure 2.2 reflective boundary conditions (squares) simply remove any probability to observed x outside $[x_{min}, x_{max}]$ range. Exponential cutoffs have a similar effect, with the probability to observe x decreasing exponentially fast outside the $[x_{min}, x_{max}]$ range. In case of "zero" fluctuations we have flat, instead of power-law, PDF for $x \ll 1$.

2.3 Power-law PSD

The PSD of the time series obtained by solving SDE (2.1) might be obtained by considering the approximate scaling properties of the signals [151]. The Wiener process, one-dimensional Brownian motion, is known to scale as

$$\mathrm{d}\, W_{at} \stackrel{\mathrm{d}}{=} a^{1/2}\, \mathrm{d}\, W_t. \tag{2.22}$$

Here $X \stackrel{\mathrm{d}}{=} Y$ implies that the random variables, or the processes, X and Y follow the same distribution.

This implies that scaling of the variable and scaling of time may be equivalent in statistical sense. Namely, when considering Eq. (2.1), two identical SDEs are obtained as a result of both transformations

$$x_s = ax, \quad \text{or} \quad t_s = a^{2\eta-2}t. \tag{2.23}$$

More generally this scaling relationship can be rewritten as identity for the transition probabilities (the conditional probability that at time t the process is in the state x' with the condition that at time $t = 0$ the was in the state x):

$$ap(ax', t|ax, 0) = p(x', a^{2\eta-2}t|x, 0). \tag{2.24}$$

This scaling property together with a general form of the steady state PDF, $p(x) \sim x^{-\lambda}$, leads to the PSD with power-law behavior [151]:

$$S(f) \sim \frac{1}{f^{\beta}}, \quad \beta = 1 + \frac{\lambda - 3}{2\eta - 2}. \tag{2.25}$$

The restrictions imposed on a diffusion of x, as discussed in Section 2.2, make relationship Eq. (2.24) only approximate. Consequently the obtained result, Eq. (2.25), is applicable only in a certain finite range of frequencies, $f_{min} \ll f \ll f_{max}$. Note that this result is rather natural as obtaining PSD with pure $1/f^{\beta}$ power-law behavior would indicate that time series contain a signal with infinite power which itself is physically impossible. The frequency ranges, for which Eq. (2.25) holds, where estimated for the reflective boundary conditions in mind [151]:

$$\sigma^2 x_{\min}^{2\eta-2} \ll 2\pi f \ll \sigma^2 x_{\max}^{2\eta-2}, \quad \text{for} \quad \eta > 1, \tag{2.26}$$

$$\sigma^2 x_{\max}^{2-2\eta} \ll 2\pi f \ll \sigma^2 x_{\min}^{2-2\eta}, \quad \text{for} \quad \eta < 1. \tag{2.27}$$

It should be evident that the width of the frequency range becomes broader with the increasing ratio between the maximum and the minimum reflective boundary positions,

$$w_{\beta} = \frac{f_{max}}{f_{min}} = \left(\frac{x_{max}}{x_{min}}\right)^{2\eta-2}, \quad \text{for} \quad \eta > 1, \tag{2.28}$$

$$w_{\beta} = \frac{f_{max}}{f_{min}} = \left(\frac{x_{min}}{x_{max}}\right)^{2-2\eta}, \quad \text{for} \quad \eta < 1, \tag{2.29}$$

as well as with increasing $|\eta - 1|$. If $\eta = 1$, then SDE (2.1) describes Geometric Brownian motion. PSD of Geometric Brownian motion is Brownian-like, $S(f) \sim 1/f^2$, thus, in this case, it is known that the width of frequency range in which Eq. (2.25) holds is zero.

Using Eq. (2.25) predictions we can see that a theoretically interesting case, $1/f$ noise, can be recovered with $\lambda = 3$ and $\eta \neq 1$. In Figure 2.2 we have demonstrated this using the three possible boundary conditions, considered in Section 2.2.

Also to show that Eq. (2.25) predictions work well for other possible β, we have selected three parameter sets to obtain power-law PSDs with distinct β. All parameters are kept the same except λ which is equal to 3, 3.6 and 4.2. Thus PSDs with $\beta = 1$, 1.3 and 1.6 can be observed in Figure 2.3.

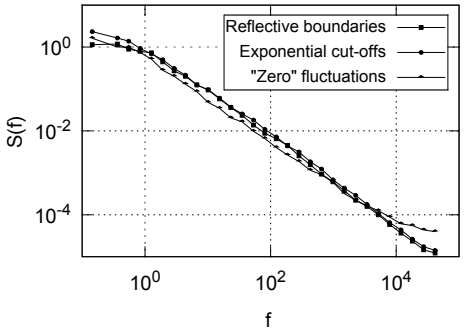

Figure 2.2: PSDs obtained by numerically solving SDE (2.1) with reflective boundaries, exponential cut-offs and "zero" fluctuations (reflective boundary placed at x_{max}). Parameters were set as follows: $\sigma^2 = 1$, $\eta = 2$, $\lambda = 3$, $x_{min} = 1$, $x_{max} = 10^3$. Time series were sampled with period $T = 10^{-5}$.

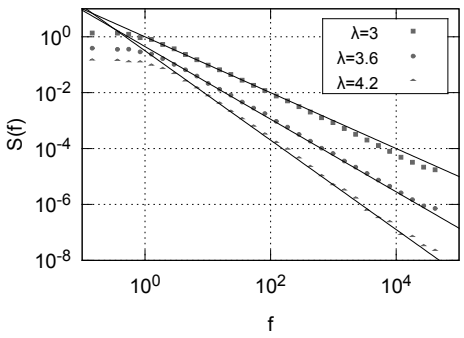

Figure 2.3: PSDs with different β obtained from time series generated by SDE (2.1) with reflective boundary conditions. Parameters were set as follows: $\lambda = 3$ (squares), 3.6 (circles) and 4.2 (triangles), $\sigma^2 = 1$, $\eta = 2$, $x_{min} = 1$, $x_{max} = 10^3$. Time series were sampled with period $T = 10^{-5}$. Black lines represent expected power-law fits: $1/f$ (black line behind the squares), $1/f^{1.3}$ (black line behind the circles) and $1/f^{1.6}$ (black line behind the triangles).

2.4 Double stochastic model for absolute return

The class of SDEs based on Eq. (2.1) is able to reproduce power-law PDF and power-law PSD, but the actual empirical PSD of high-frequency absolute return is fractured. Namely, the empirical PSD may be approximated by two power-law functions having different exponents, β. In a series of papers by Gontis and others [134, 135, 152] it was shown that both trading activity and absolute return can be modeled by considering a more sophisticated, in comparison with Eq. (2.1), SDE having two exponents of noise multiplicativity (two different η values).

It was proposed that absolute return may be modeled by solving the following SDE [135]

$$\begin{aligned} \mathrm{d}\, x = \sigma^2 \left[\eta - \frac{\lambda}{2} - \left(\frac{x}{x_{max}} \right)^2 \right] \frac{(1+x^2)^{\eta-1}}{\left(\epsilon \sqrt{1+x^2} + 1 \right)^2} x \,\mathrm{d}\, t + \\ + \sigma \frac{(1+x^2)^{\frac{\eta}{2}}}{\epsilon \sqrt{1+x^2} + 1} \,\mathrm{d}\, W. \end{aligned} \tag{2.30}$$

Here the parameter ϵ divides the diffusion area of absolute return, x, into two regions with different noise multiplicativity exponents. Note that if $x \gg 1/\epsilon$, then the effective exponent of noise multiplicativity is $\eta - 1$, while for $1 \ll x < 1/\epsilon$ the effective exponent of noise multiplicativity is just η. The existence of two diffusion regions with different noise multiplicativity creates PSD with fracture, i.e. one approximated by two power-law functions. As we are interested in absolute returns, defined for $x > 0$, the reflective boundary condition should be placed at $x = 0$.

Yet the problem with SDE (2.30) is a fact that the PSD exponents, β, are higher than empirical ones. To solve this problem it was proposed, in [135], to introduce a secondary stochastic process, q-Gaussian noise. Similarly trading activity model [134] uses Poisson noise as secondary stochastic process. The time series obtained by solving SDE (2.30), $x(t)$, is assumed to modulate the instantaneous q-Gaussian fluctuations, ζ_q. x is embed into r_0 parameter of a q-Gaussian distribution [135]:

$$r_T(t) = \zeta_q\{r_0(t,T), \lambda_2\}, \tag{2.31}$$

where T defines return window width. In general, the modulated parameter r_0 might be seen as measuring the instantaneous volatility of the high frequency return fluctuations. Through the analysis of empirical data, presented in [135], the following

relation to x was established:

$$r_0(t,T) = 1 + \frac{\bar{r}_0}{\sigma^2 T} \int_{\sigma^2 t}^{\sigma^2(t+T)} x(k)\mathrm{d}k, \tag{2.32}$$

here we have two empirically determined parameters: $\bar{r}_0$ might be seen as something similar to signal-to-noise ratio, while σ^2 allows to align physical time, t, and scaled model time, t_s. Both of the parameters are determined by comparing model and empirical PSDs. These numerical simulations demonstrate that secondary stochastic process may help to adjust the exponents of PDF and PSD.

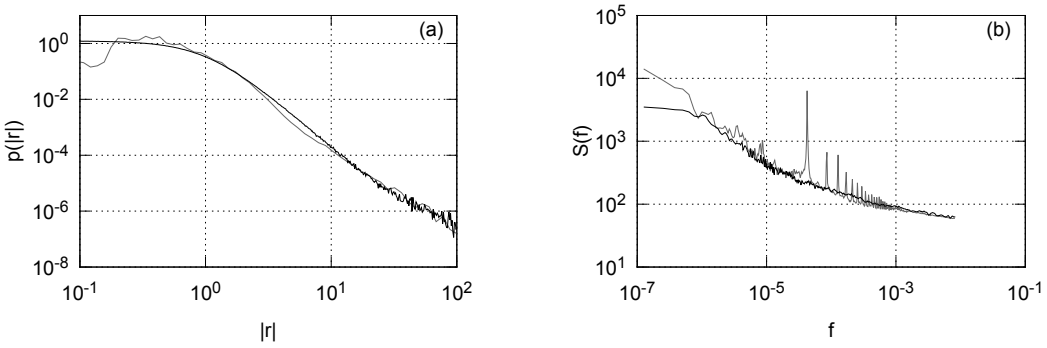

Figure 2.4: PDF (a) and PSD (b) of absolute return time series obtained from the double model (black curves) versus PDF (a) and PSD (b) of empirical one-minute absolute return time series (gray curves). Empirical PDF and PSD were obtained by averaging them over 26 stocks. The following model parameters were used: $\sigma^2 = 1/6 \cdot 10^{-5}\ \mathrm{s}^{-1}$, $\eta = 2.5$, $\lambda = 3.6$, $\epsilon = 0.017$, $x_{max} = 10^3$, $\tau = 60$ s, $\bar{r}_0 = 0.4$, $\lambda_2 = 5$.

2.5 Summary

In this chapter we have briefly discussed a general class of nonlinear SDEs proposed in earlier series of papers by Kaulakys, Ruseckas, Gontis and Alaburda [127–131]. Models built on this class of nonlinear SDEs generate time series exhibiting power-law PDF and PSD. Furthermore double stochastic model of absolute return generates time series exhibiting PDF and PSD similar to the empirical PDF and PSD of absolute return.

In this chapter we have also discussed some general analytical and numerical techniques which are used in the following chapters of this dissertation.

3 Power-law bursting behavior

In most econometric analysis the exponent of noise multiplicativity (corresponding to η in SDE (2.1)) is assumed to be slightly smaller than or equal to 1 [144]. This might be related to a general Lipshitz requirement applied to SDEs [118, 147] as well as other related econometric assumptions such as existence of the unique martingale measure [153]. Though there are noteable works which show that the financial market models with $\eta > 1$ perform better than those with $\eta \leq 1$ [134–136, 145]. The main reason behind this might be seen to be the natural tendency of the models with $\eta > 1$ to "explode" or burst [154]. These burst events might be compared to the flash-crashes observed in the real financial markets [132, 155, 156] and thus the comparison between the model, driven by SDE (2.1), bursting behavior and empirical bursting behavior would be relevant.

3.1 Definition of bursting behavior

We define a burst as a set of points belonging to the time series, $x(t)$, and lying above the fixed threshold, h_x. Adjacent points lying above the threshold are assumed to be a part of a single continuous burst. Similar logic applies to adjacent points lying bellow the threshold, they are assumed to be a part of a single continuous inter-burst period.

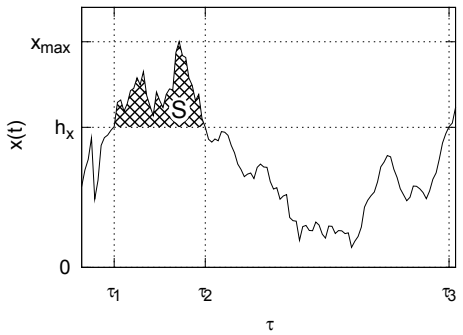

Figure 3.1: An example burst observed in a certain time series $x(t)$.

In Figure 3.1 we have plotted a simple example of a burst observed in certain time series, $x(t)$ (consequently the threshold is denoted as h_x). Three random threshold passage times, τ_1, τ_2 and τ_3, are shown. As you can see in the figure a single burst by itself may be described by its duration, $T = \tau_2 - \tau_1$, maximum value reached

during the burst, x_{max}, and so-called burst size, S, which is defined as the area above the threshold yet bellow the actual curve of the time series (area highlighted using x pattern in the Figure 3.1). One can also consider inter-burst, $\theta = \tau_3 - \tau_2$, (time interval in which no burst is observed) and waiting, $\tau = \tau_3 - \tau_1$, (time interval between the start times of two consecutive bursts) times to be able to fully cover as many statistical features, of bursty behavior, as possible.

3.2 Obtaining statistical properties of bursty behavior from empirical and numerical time series

In this chapter we consider bursty behavior of three different sources: a nonlinear SDE (2.1), a sophisticated double stochastic model, discussed in Section 2.4, and empirical data from NYSE.

The used empirical data set includes tick by tick data of 26 different stocks traded on NYSE since January, 2005 to March, 2007. Price time series were sampled from tick by tick data at one minute intervals. One-minute absolute return time series were obtained from the price time series. Absolute return time series were normalized in respect to the standard deviation of the return time series. Moving average filter, with window size of one hour, was used to remove instantaneous noise after the normalization procedure.

The nonlinear SDE time series were obtained by numerically solving SDE (2.1) with exponential cutoff from the small value side, $x_{min} = 1$. As the nonlinear SDE is not able to reproduce exact statistical features of the empirical absolute return time series we have set parameters values using the following logic. We have set $\lambda = 4$ as it is well known that empirical PDFs have power-law tail with exponent values scattered around 4. We have set $\eta = 2$ seeing it lying between $\eta = 2.5$ and 1.5 which are present in a more sophisticated double stochastic model (discussed in Section 2.4). We chosen σ^2 value to be the same as the one used in sophisticated double stochastic model (discussed in Section 2.4).

Double stochastic model time series were obtained as discussed in Section 2.4, by solving SDE (2.30) and applying q-Gaussian noise. To keep comparison with empirical data consistent we have used moving average filter in the same manner as

with empirical data.

3.3 Analytical treatment of the burst duration

First hitting (passage) time framework is well established mathematical framework used by mathematicians [144, 157] as well as physicists [119, 158]. This framework appears to be applicable to the problem of burst durations as first hitting time of the stochastic process starting on the threshold (infinitesimally above it) might be seen as being the same as burst duration. This is true by the definition as the first passage of threshold ends the burst.

Despite the fact that the framework is well established, models for which hitting times are explicitly known are few. Furthermore most of these models are relatively simple. Such models include, but are not limited to, Brownian motion, Geometric Brownian motion and Bessel process [144, 157]. As there are no general tools that could provide sufficient results related to the burst duration of SDE (2.1), the only way to solve the problem is to reduce it to the one with known result. It appears that after variable transformation SDE (2.1) can be transformed into Bessel process.

The Bessel process is a stochastic process describing time evolution of Euclidean norm of N-dimensional Brownian particle,

$$R(t) = \left\| \vec{W}(t)^{(N)} \right\| = \sqrt{\sum_{i=1}^{N} W_i^2(t)}. \tag{3.1}$$

The same process may be modeled using the following SDE:

$$\mathrm{d}R = \frac{N-1}{2}\frac{\mathrm{d}t}{R} + \mathrm{d}W = \left[\nu + \frac{1}{2}\right]\frac{\mathrm{d}t}{R} + \mathrm{d}W. \tag{3.2}$$

In the above ν is the so-called index of the Bessel process which relates to the number of dimensions as

$$\nu = \frac{N}{2} - 1. \tag{3.3}$$

SDE (2.1) may be reduced to the Bessel process by using appropriate Lamperti transformation. Namely, we require that after changing the current variable x to a new variable y, $\ell : x \mapsto y(x)$, the diffusion function in the newly obtained SDE

should not depend on the new variable. Using the Ito variable substitution formula [119] we obtain the following ODE

$$x^{\eta}\frac{\mathrm{d}}{\mathrm{d}\,x}y_{\pm}(x) = \pm 1. \tag{3.4}$$

Note that here we used both plus and minus signs as $\mathrm{d}\,W$ and $-\mathrm{d}\,W$ are statistically equivalent.

It should be evident that the solution of Eq. (3.4) is given by:

$$y_{\pm}(x) = \mp\frac{1}{(\eta-1)x^{\eta-1}}. \tag{3.5}$$

As we are interested in $\eta > 1$, the only solution with actual physical meaning is y_{-}. Consequently the Lamperti transformation, in our case, should have the following form

$$\ell : x \mapsto y(x) = \frac{1}{(\eta-1)x^{\eta-1}}. \tag{3.6}$$

Applying the obtained transformation to the drift function of SDE (2.1) results in:

$$A_y = A_x\frac{\mathrm{d}\,y(x)}{\mathrm{d}\,x} + \frac{1}{2}B_x^2\frac{\mathrm{d}^2\,y(x)}{\mathrm{d}\,x^2} = \frac{\lambda-\eta}{2}x^{\eta-1} = \frac{\lambda-\eta}{2\eta-2}\frac{1}{y}. \tag{3.7}$$

As diffusion function should be definitely equal to -1 (implied by Eq. (3.4)) and the minus sign might be "absorbed" into $\mathrm{d}\,W$ (due to statistical equivalence), the simple SDE (2.1) is reduced to the Bessel process,

$$\mathrm{d}\,y = \left(\nu + \frac{1}{2}\right)\frac{\mathrm{d}\,t}{y} + \mathrm{d}\,W, \tag{3.8}$$

with index $\nu = \frac{\lambda-2\eta+1}{2(\eta-1)}$. The corresponding dimension of this Bessel process is given by $N = \frac{\lambda-1}{\eta-1}$.

So the stochastic process described by SDE (2.1) can be reduced to the Bessel process, thus we can move forward by expecting to use some known results related to the Bessel process. Any burst should have some starting time t_0. By definition at this very moment the stochastic process should just have crossed the threshold and is slightly above it, $x(t_0) > h_x$. The burst will last until at some time t the process will cross back the threshold h_x from the above. In terms of Bessel process dynamics are inverted: the burst will start with y being infinitesimally bellow h_y

(whete $h_y := \ell(h_x)$) and end when y will cross h_y from bellow. So the burst duration T is defined as a first passage time of stochastic process starting above threshold h_y:

$$T = \tau^{(\nu)}_{y_0,h_y} = \inf_{t>t_0}\left\{t - t_0,\ y(t) \geq h_y\right\}, \quad 0 < h_y - y_0 \ll 1. \tag{3.9}$$

As given in [157], the following holds for $0 < y_0 < h_y$:

$$\rho^{(\nu)}_{y_0,h_y}(T) = \frac{h_y^{\nu-2}}{y_0^{\nu}} \sum_{k=1}^{\infty} \frac{j_{\nu,k} J_\nu\left(\frac{y_0}{h_y} j_{\nu,k}\right)}{J_{\nu+1}(j_{\nu,k})} \exp\left(-\frac{j^2_{\nu,k}}{2h_y^2} T\right), \tag{3.10}$$

here $\rho^{(\nu)}_{y_0,h_y}(T)$ is a PDF of the first passage time at level h_y of Bessel process with index ν starting from y_0, J_ν is a Bessel function of the first kind (the properties of this function is discussed in [159, 160]) of order ν and $j_{\nu,k}$ is a k-th zero of J_ν (the concept of Bessel function zeros is discussed in [159, 161]).

Note that if $y_0 \to h_y$, then $\rho^{(\nu)}_{y_0,h_y}(T) \to 0$. This result might be expected as stochastic process placed on the threshold crosses it instantaneously. In order to avoid this trivial convergence. Let us assume that the burst duration PDF is the following limit of $\rho^{(\nu)}_{y_0,h_y}(T)$:

$$p^{(\nu)}_{h_y}(T) = \lim_{y_0 \to h_y} \frac{\rho^{(\nu)}_{y_0,h_y}(T)}{h_y - y_0}. \tag{3.11}$$

To evaluate this limit we expand Bessel function, $J_\nu\left(\frac{y_0}{h_y} j_{\nu,k}\right)$, around $\frac{y_0}{h_y} = 1$. We use Taylor series dropping all terms above the second order terms:

$$\begin{aligned} J_\nu\left(\frac{y_0}{h_y} j_{\nu,k}\right) &\approx J_\nu(j_{\nu,k}) - \left(1 - \frac{y_0}{h_y}\right)\left[\nu J_\nu(j_{\nu,k}) - j_{\nu,k} J_{\nu+1}(j_{\nu,k})\right] = \\ &= \left(1 - \frac{y_0}{h_y}\right) j_{\nu,k} J_{\nu+1}(j_{\nu,k}). \end{aligned} \tag{3.12}$$

Note that some terms were also dropped as by definition $J_\nu(j_{\nu,k}) = 0$ for all integer k.

By putting this expansion into Eq. (3.11), the form of burst duration PDF becomes noticeably simpler:

$$p^{(\nu)}_{h_y}(T) = C_1 \sum_{k=1}^{\infty} j^2_{\nu,k} \exp\left(-\frac{j^2_{\nu,k}}{2h_y^2} T\right), \tag{3.13}$$

here C_1 is a normalization constant. Yet this expression can still be further simplified by taking a note that Bessel zeros, $j_{\nu,k}$, are almost equally spaced [159, 161]. This simple notion allows us to roughly approximate the infinite sum by integration

$$p^{(\nu)}_{h_y}(T) \approx C_2 \int_{j_{\nu,1}}^{\infty} x^2 \exp\left(-\frac{x^2 T}{2h_y^2}\right) \mathrm{d}\, x = \\ = C_2 \left[\frac{h_y^2 j_{\nu,1} \exp\left(-\frac{j_{\nu,1}^2 T}{2h_y^2}\right)}{T} + \sqrt{\frac{\pi}{2}} \frac{h_y^3 \operatorname{erfc}\left(\frac{j_{\nu,1}\sqrt{T}}{\sqrt{2}h_y}\right)}{T^{3/2}} \right]. \tag{3.14}$$

Note that the asymptotic behavior of the obtained PDF as $T \to 0$ is divergent, thus normalization constant cannot be defined unless some minimum value of T is set. Time domain accuracy of the numerical simulation or some minimum inter-trade time (time tick size) might be considered as a viable choices. Asymptotic behavior of the burst duration PDF is rather clear for other values of T:

$$p^{(\nu)}_{h_y}(T) \sim T^{-3/2}, \quad \text{when} \quad 0 < T \ll \frac{2h_y^2}{j_{\nu,1}^2}, \tag{3.15}$$

$$p^{(\nu)}_{h_y}(T) \sim \frac{\exp\left(-\frac{j_{\nu,1}^2 T}{2h_y^2}\right)}{T}, \quad \text{when} \quad T \gg \frac{2h_y^2}{j_{\nu,1}^2} \tag{3.16}$$

The obtained result is in agreement with a general property of the diffusion processes discussed in [158]. Namely, the asymptotic behavior of first hitting times is expected to be power-law $T^{-3/2}$ for all one dimensional stochastic processes. Note that using Ito variable transformation formula we can transform SDE (2.1) into CIR process, for which hitting times are also well known [162].

The exponential cutoff may be explained as a result of the positive drift term of the Bessel process when $N > 1$ ($\nu > -0.5$). The Bessel process is known to be transient for $N \geq 2$ ($\nu \geq 0$), namely, there is non-zero probability that the process will not visit the same state again. This is easily understood from the physical interpretation of the Bessel process: the higher dimensionality of Brownian particle, the higher the probability that it will randomly move away from the origin.

As it is shown in Figure 3.2 the numerical results, obtained by solving Eq. (2.1) with exponential cut-off from small value side, confirm that the burst duration PDF is well approximated by Eq. (3.14). We have neglected the exponential cut-off in the analytical derivations above, but it does not play a major role as long as $x_{min} < h_x$.

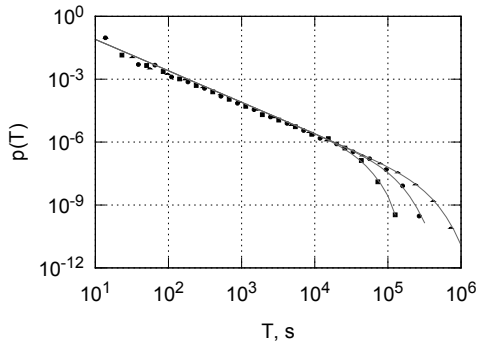

Figure 3.2: Burst duration PDF of a nonlinear SDE time series (squares, circles and triangles) compared to analytical predictions for respective parameter sets (gray curves). The model parameters were set as follows: $\sigma^2 = 1/6 \cdot 10^{-5}\mathrm{s}^{-1}$, $\lambda = 4$, $\eta = 2.5$ (squares; corresponds to $\nu = 0$), $\eta = 2$ (circles; $\nu = 0.5$) and $\eta = 1.5$ (triangles; $\nu = 2$). The threshold was set as follows: $h_x = 2$.

Empirical burst duration PDF, Figure 3.3, shows a bit more sophisticated behavior, note the cusp between 10^3 s and 10^4 s. This is the only essential discrepancy which may be explained by the fact that we have used moving average filter, while preparing the time series for the analysis. This assumption is confirmed by the fact that time series obtained from the double model, which were also affected by the moving average filter, exhibit the same PDF of burst duration. Interestingly enough, a double model without either q-Gaussian or moving average filter is not enough to reproduce empirical burst duration PDF.

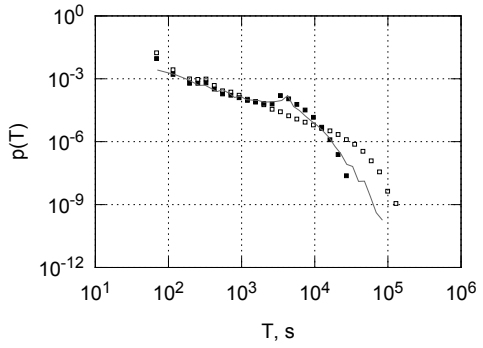

Figure 3.3: Empirical burst duration PDF (gray curve) compared to a double model burst duration PDF when q-Gaussian noise and moving average filter are not applied (empty squares) and when q-Gaussian noise and moving average filter are applied (filled squares). The double model parameters were set as follows: $\sigma^2 = 1/6 \cdot 10^{-5}\mathrm{s}^{-1}$, $\lambda = 3.6$, $\eta = 2.5$, $\epsilon = 0.017$, $x_{max} = 10^3$, $\bar{r}_0 = 0.4$, $\lambda_2 = 5$. The threshold was set as follows: $h_x = 2$.

3.4 Power-law scaling in geometric properties of bursts

As bursting behavior is caused by large fluctuations, which follow power-law distribution, it is natural to expect that the geometrical properties of the bursts should scale as power-law. Analysis of empirical data and time series generated by solving Eq. (2.1) confirms this fact. It appears that the three variables describing single burst, burst duration, peak value and burst size, are interdependent and their interdependence is of power-law nature. Namely, $x_{max} \propto T^{\frac{2}{3}}$ (see Figure 3.4), $S \propto T^{\frac{5}{3}}$ (see Figure 3.5) and consequently $S \propto \left(x_{max}^{\frac{3}{2}}\right)^{\frac{5}{3}} \propto x_{max}^{\frac{5}{2}}$ (see Figure 3.6).

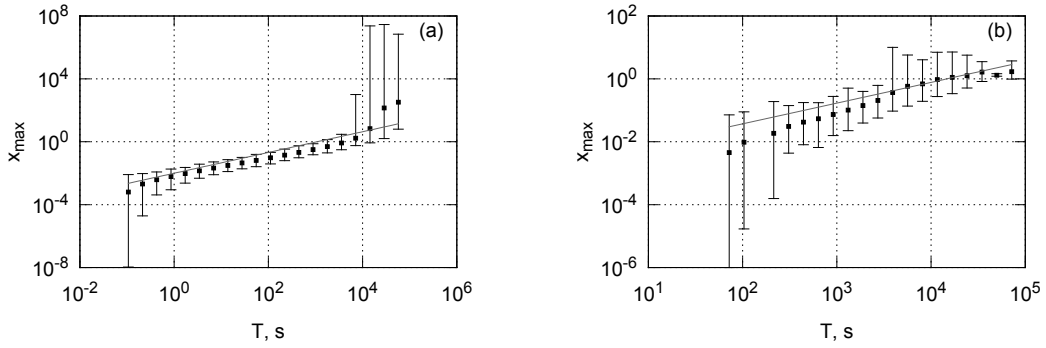

Figure 3.4: The scatter plot of the SDE (2.1) (a) and empirical (b) burst peak values, x_{max}, vs burst durations, T. In both sub-figures filled squares represent median values, while error bars indicate minimum and maximum values, in the vicinity of a given point. Grey curves provide power-law fits with $\alpha = \frac{2}{3}$. The parameters of SDE (2.1) were the same as in Figure 3.2. The threshold was set as follows: $h_x = 2$.

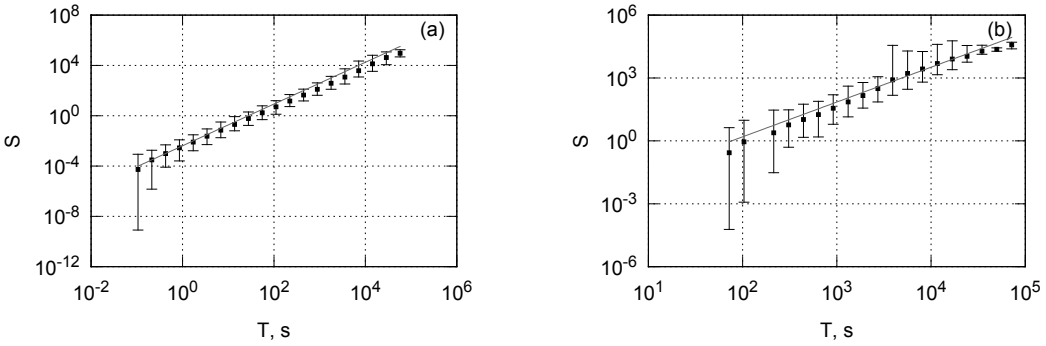

Figure 3.5: The scatter plot of the SDE (2.1) (a) and empirical (b) burst size, S, vs burst durations, T. In both sub-figures filled squares represent median values, while error bars indicate minimum and maximum values, in the vicinity of a given point. Grey curves provide power-law fits with $\alpha = \frac{5}{3}$. The parameters of SDE (2.1) were the same as in Figure 3.2. The threshold was set as follows: $h_x = 2$.

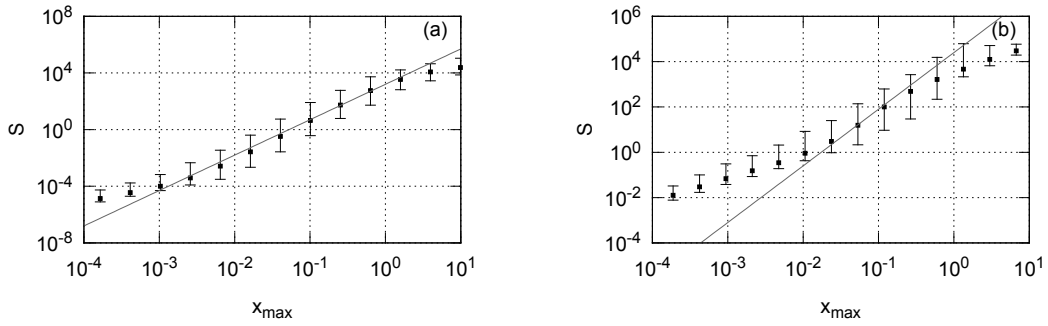

Figure 3.6: The scatter plot of the SDE (2.1) (a) and empirical (b) burst size, S, vs burst peak values, x_{max}. In both sub-figures filled squares represent median values, while error bars indicate minimum and maximum values, in the vicinity of a given point. Grey curves provide power-law fits with $\alpha = \frac{5}{2}$. The parameters of SDE (2.1) were the same as in Figure 3.2. The threshold was set as follows: $h_x = 2$.

Note that power-law interdependencies hold well for broader ranges in the non-linear SDE time series than in the empirical data. This may happen because the empirical data is distorted by instantaneous fluctuations and tick sizes (time, price and thus return). Power-law interdependency is weakest for the (S, x_{max}) pair.

3.5 Summary

In this chapter we have compared bursting behavior of absolute return observed in empirical data of 26 NYSE stocks with bursting behavior observed in time series generated by the stochastic models discussed in Chapter 2. Besides the demonstrated similarity between burst duration PDFs, the most important highlight of this chapter is the obtained analytical approximation of burst duration PDF. This approximation was derived from the SDE (2.1), but works reasonably well as a fit for the burst duration PDF observed in empirical data and time series obtained by evaluating double stochastic model.

Furthermore we have found that power-law scaling behavior between the three main variables related to burst geometry. Similar power-law scaling behavior was observed both in empirical absolute return time series as well as in time series obtained by solving SDE (2.1).

4 Nonlinear GARCH(1,1) process exhibiting power-law statistics

Slightly more than 50 years ago mathematician Benoit B. Mandelbrot, economist Eugene F. Fama as well as other contemporaries proposed a novel idea that market volatility fluctuations might be responsible for the intermittent nature of the observed market dynamics [163–165]. In more recent works intermittency is related to volatility clustering phenomena [166–168]. It is believed that modeling evolution of the second-order moment, referred to as heteroskedasticity [169–172], of the financial observables may replicate the same intermittent nature and thus enable the improvement of performance of option-price, and related, models [19, 173–175].

ARCH family models [19, 169–175] are widely used by the practitioners to provide future forecasts based on the recent historical data. Namely, these models are special as their parameters are usually estimated directly from the data itself. This is rather sophisticated process as ARCH family models have explicitly built-in memory the next state of the system may depend not only on the current state, but also on previous states. SDEs, on the other hand, are much simpler as there is no explicitly built-in memory – the next state of the system is assumed to depend only on the current state. Nevertheless the general form of the iterative equations used to numerically implement ARCH family models as well as numerically solve SDEs, Eq. (2.4), are somewhat similar. This similarity allows to propose certain transformations of ARCH process which reproduce power-law behavior similar as in the case with SDE (2.1).

In numerous previous works it was demonstrated that the built-in memory of ARCH family models (such as FIGARCH) enables reproduction of power-law autocorrelations [66, 176–180]. Unlike these works here we will consider only memoryless, dependent only on the current state (or alternatively Markovian), GARCH processes.

4.1 Linear GARCH

In a seminal articles [169–171] economists Robert F. Engle and Tim Bollerslev proposed an idea that certain heteroskedastic economic variables (e.g., return and

trading activity in the financial markets) maybe modeled as a multiplicative product of stochastic part, ω_t and time dependent standard deviation (i.e. volatility), σ_t:

$$z_t = \sigma_t \omega_t. \tag{4.1}$$

Here, in general, ω_t might follow any distribution, but most commonly it is assumed to follow Gaussian distribution, though other alternatives are also possible [181–184]. Here we will assume that ω_t follows Gaussian distribution with zero mean $\langle \omega_t \rangle = 0$ and unit variance $\langle \omega_t^2 \rangle = 1$.

In general, temporal evolution of the standard deviation in GARCH family models is described using the following iterative equation [170]:

$$\sigma_t^2 = a + \sum_{i=1}^{p} b_i \sigma_{t-i}^2 \omega_{t-i}^2 + \sum_{i=1}^{q} c_i \sigma_{t-i}^2, \tag{4.2}$$

where a, b_i and c_i are model parameters (it is required that $a > 0$, $b \geq 0$ and $c \geq 0$): a represents persisting fluctuations, b_i represents strength of feedback loops based on external observable, c_i represents strength of feedback loops based on internal state.

Originally Engle and Bollerslev proposed a model with feedback based only on the external observable, defined by Eq. (4.1), [169] (this model is referred to ARCH(p)). But a few years latter in [170] they generalized original ARCH model by adding feedback based on the volatility itself (this model is referred to GARCH(p,q)). Note that if either $p > 1$ or $q > 1$, then the newly generated state of the model depends on the prior evolution of the model (namely, the model posses memory). Consequently if both $p = 1$ and $q = 1$, then the volatility time series should posses no memory effects as in such case the newly generated state depends only on the current state:

$$\sigma_t^2 = a + b \sigma_{t-1}^2 \omega_{t-1}^2 + c \sigma_{t-1}^2. \tag{4.3}$$

As now we consider only $p = q = 1$ case, we drop the subscripts which were present in Eq. (4.2).

The iterative equation (4.3) might be approximated using stochastic calculus, namely, by the SDE. There are two main approaches to take the diffusion limit of the GARCH(1,1) process - one by Nelson and the other by Kluppelberg *et al.* [185–188]. Nelson's approach is the simpler of the two, but has a drawback – the resulting COGARCH(1,1) process is driven by two stochastic processes, while

the initial GARCH(1,1) is driven by single stochastic process, ω_t. Kluppelberg's approach doesn't have this drawback and thus usually is preffered to Nelson's approach [187, 188]. But the drawback is irrelevant to us, as we are interested only in approximating volatility process of GARCH(1,1). Thus further we follow ideas from Nelson's paper [185].

As per usual the parameters of the GARCH process are obtained by retrofitting empirical time series sampled at fixed discretization period, h. Consequently the obtained values of the parameters a, b and c are directly dependent on h. To highlight the dependence on the selected time scale subscript h is added where it is appropriate:

$$\begin{aligned}\sigma^2_{kh,h} &= a_h + b_h\sigma^2_{(k-1)h,h}\omega^2_{(k-1)h,h} + c_h\sigma^2_{(k-1)h,h} = \sigma^2_{(k-1)h,h} + \\ &+ a_h - (1 - b_h - c_h)\sigma^2_{(k-1)h,h} + b_h\sigma^2_{(k-1)h,h}\left(\omega^2_{(k-1)h,h} - 1\right).\end{aligned} \tag{4.4}$$

Consequently subscript representing time, t, was changed to kh (where $k \in \mathbb{N}$).

As process described by Eq. (4.4) is clearly Markovian, we can easily obtain mean drift and the second moment of σ^2 per unit of time. But first let us note that random variable $\omega^2 - 1$ has the following properties:

$$\langle\omega^2 - 1\rangle = \langle\omega^2\rangle - 1 = 0, \tag{4.5}$$

$$\langle(\omega^2 - 1)^2\rangle = \langle\omega^4\rangle - 2\langle\omega^2\rangle + 1 = \langle\omega^4\rangle - 1 = 3(\langle\omega^2\rangle)^2 - 1 = 2. \tag{4.6}$$

Then the mean drift per unit of time of σ^2 equals:

$$\lim_{h\to 0}\left\langle\frac{\sigma^2_{(k+1)h,h} - \sigma^2_{kh,h}}{h}\right\rangle = \lim_{h\to 0}\left[\frac{a_h}{h} - \frac{1 - b_h - c_h}{h}\sigma^2_{kh,h}\right] = A - C\sigma^2_t, \tag{4.7}$$

and in the similar manner the second moment per unit of time equals:

$$\begin{aligned}\lim_{h\to 0}\left\langle h^{-1}\left(\sigma^2_{(k+1)h,h} - \sigma^2_{kh,h}\right)^2\right\rangle &= \lim_{h\to 0} h^{-1}\left[\left(a_h - (1 - b_h - c_h)\sigma^2_{(k-1)h,h}\right)^2 + \right. \\ &\left. + b_h^2\sigma^4_{(k-1)h,h}\left\langle\left(\omega^2_{(k-1)h,h} - 1\right)^2\right\rangle + 0\right] = \\ &= B^2\sigma^4_t.\end{aligned} \tag{4.8}$$

In the above A, B and C are continuous time parameters (we require that $A > 0$, $B > 0$) obtained by expanding implicit dependence of a_h, b_h and c_h on h using

Taylor expansion at $h \to 0$:

$$a_h = Ah, \quad 1 - b_h - c_h = Ch, \quad 2b_h^2 = B^2 h. \tag{4.9}$$

Using the expressions obtained in Eqs. (4.7) and (4.8) we can write the following SDE for $y_t = \sigma_t^2$ [185]:

$$\begin{aligned} \mathrm{d}\, y &= (A - Cy)\,\mathrm{d}\, t + By\,\mathrm{d}\, W_t = \\ &= B^2 \left(1 - \frac{\lambda}{2} + \frac{1}{2}\frac{y_{\min}}{y}\right) y\,\mathrm{d}\, t + By\,\mathrm{d}\, W_t, \end{aligned} \tag{4.10}$$

which approximates volatility process of GARCH(1,1). In the above:

$$\lambda = 2 + \frac{2C}{B^2} = 2 + \frac{1 - b_h - c_h}{b_h^2}, \tag{4.11}$$

$$y_{\min} = \frac{2A}{B^2} = \frac{a_h}{b_h^2}. \tag{4.12}$$

Note that these relations were derived and thus hold in the diffusion limit, $h \to 0$. The dependence on a_h, b_h and c_h might be different if they are obtained from empirical data with larger h. The approximation holds as long as b_h is small.

Observe that by setting $\eta = 1$ in SDE (2.1) we obtain a Geometric Brownian motion process similar to SDE (4.10). As discussed in Section 2.2 the PDF of y should have a power-law tail with the exponent λ. The analytical predictions for the PSD, Eq. (2.25), do not work in this case as they diverge in the limit $\eta \to 1$, but from the general properties of Geometric Brownian motion it well known that PSD of such process should have the $S(f) \sim 1/f^2$ form.

4.2 Nonlinear modifications of GARCH(1,1) volatility process

As SDE (4.10) is a special case of SDE (2.1) with $\eta = 1$, it would prove usefull to generalize mathematical form of GARCH(1,1) so that SDE obtained in the diffusion limit would have $\eta \neq 1$. Furthermore Eq. (2.25) suggests that in such case we would be able to reproduce larger variety of power-law PSDs. In the previous works by Gontis and others it was shown that $\eta > 1$ case works well for reproduction of essential statistical properties observed in high-frequency trading activity and abso-

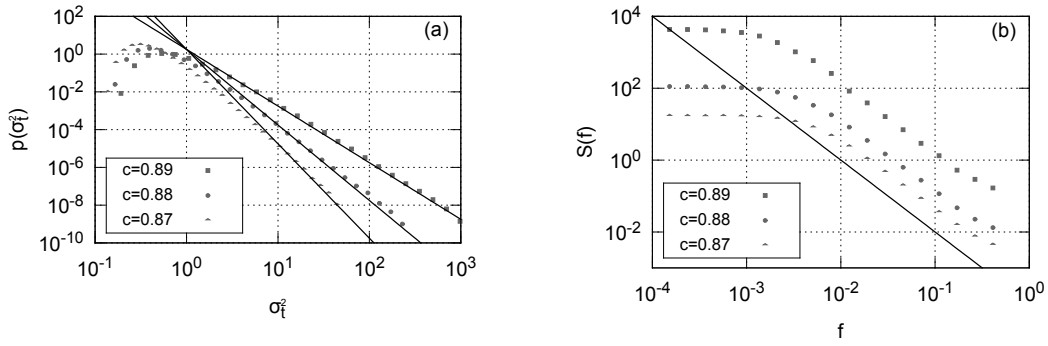

Figure 4.1: Statistical properties of σ_t^2 time series obtained by numerically solving Eq. (4.3): stationary PDF (a) and PSD (b). The following parameter values were used: $a = 0.015$, $b = 0.1$, $c = 0.89$ (squares), 0.88 (circles), 0.87 (triangles). Black lines represent expected power-law fits: (a) $p(\sigma_t^2) \sim (\sigma_t^2)^{-3}$ (black line behind the squares), $(\sigma_t^2)^{-4}$ (black line behind the circles) and $(\sigma_t^2)^{-5}$ (black line behind the triangles), (b) $S(f) \sim f^{-2}$ (black line).

lute return time series [134–136], although theoretically it was shown that $\eta < 1$ case might be also considered [189].

We consider the following two nonlinear modifications, allowing for $\eta > 1$, of GARCH(1,1) volatility process:

$$\sigma_t^2 = a + b\sigma_{t-1}^{\mu}\omega_{t-1}^{\mu} + c\sigma_{t-1}^2, \tag{4.13}$$

here $\mu > 2$ is required to be an odd integer, and

$$\sigma_t^2 = a + b\sigma_{t-1}^{\mu}|\omega_{t-1}|^{\mu} + \sigma_{t-1}^2 - c\sigma_{t-1}^{\mu}, \tag{4.14}$$

while in the second case μ may be any real number. Note that in contrast to GARCH(1,1) process, Eq. (4.3), Eqs. (4.13) and (4.14) do not ensure that σ_t^2 remains positive. In order to avoid transitions to negative values we put a reflective boundary at zero, $\sigma_t^2 = 0$.

A similar nonlinear form of the GARCH model was already considered by Engle and Bollerslev in [171]. The nonlinear GARCH model considered in the paper had a form similar to both Eq. (4.13) and Eq. (4.14). The difference in comparison with Eq. (4.13) was that Engle and Bollerslev took a modulus of ω_{t-1} was taken prior to raising it to a generalized power μ (change ω_{t-1}^{μ} to $|\omega_{t-1}|^{\mu}$). The difference in comparison with Eq. (4.14) was the lack of σ_{t-1}^{μ} term. By fitting the nonlinear GARCH model to empirical data Engle and Bollerslev found that for the most considered time series $\mu \lessapprox 2$ and thus concluded that linear GARCH models are sufficient for the most cases.

Another attempt at studying the properties of nonlinear GARCH models was done by Higgins and Bera in [190]. Their approach is different in a sense that they considered evolution of higher order moment, σ_t^{μ}, and not variance, σ_t^2.

Some other GARCH models propose to include different functions dependent on past variances, σ_{t-1}^2, or observables, z_{t-1}, [175]. In this context it is worthwhile to note that the last two terms of Eq. (4.14) can be seen as a Taylor series expansion of a function, $f(\sigma_{t-1})$.

4.2.1 The diffusion limit of Eq. (4.13)

Lets proceed in a similar fashion as in Section 4.1. As before the time series sampling may be taken into account by rewriting the iterative equation (4.13) as follows:

$$\sigma_{kh,h}^2 = \sigma_{(k-1)h,h}^2 + a_h - (1-c_h)\sigma_{(k-1)h,h}^2 + b_h \sigma_{(k-1)h,h}^{\mu} \omega_{(k-1)h,h}^{\mu}. \tag{4.15}$$

Recall that here μ is odd integer larger than 2. Thus we have $\langle \omega^{\mu} \rangle = 0$ and let us choose the following notation $\hat{\omega}_{\mu} = \langle \omega^{2\mu} \rangle$.

In this case the mean drift per unit of time of σ^2 equals:

$$\lim_{h\to 0} \left\langle \frac{\sigma_{(k+1)h,h}^2 - \sigma_{kh,h}^2}{h} \right\rangle = \lim_{h\to 0} \left[\frac{a_h}{h} - \frac{1-c_h}{h} \sigma_{kh,h}^2 \right] = A - C\sigma_t^2, \tag{4.16}$$

and in the similar manner the second moment per unit of time equals:

$$\begin{aligned} \lim_{h\to 0} \left\langle h^{-1} \left(\sigma_{(k+1)h,h}^2 - \sigma_{kh,h}^2 \right)^2 \right\rangle = \lim_{h\to 0} h^{-1} \Big[& \left(a_h - (1-c_h)\sigma_{kh,h}^2 \right)^2 + \\ & + b_h^2 \sigma_{kh,h}^{2\mu} \hat{\omega}_{\mu} + 0 \Big] = \\ & = B^2 \sigma_t^{2\mu}. \end{aligned} \tag{4.17}$$

In the above A, B and C are continuous time parameters (we require that $A > 0$ and $B > 0$) obtained by expanding implicit dependence of a_h, b_h and c_h on h using Taylor expansion at $h \to 0$:

$$a_h = Ah, \quad 1 - c_h = Ch, \quad \hat{\omega}_{\mu} b_h^2 = B^2 h. \tag{4.18}$$

Expressions obtained in Eqs. (4.16) and (4.17) allow us to write the following

SDE for $y_t = \sigma_t^2$:

$$\begin{aligned} \mathrm{d}\, y &= \left(\frac{A}{y^{\mu-1}} - \frac{C}{y^{\mu-2}}\right) y^{\mu-1}\,\mathrm{d}\, t + B y^{\frac{\mu}{2}}\,\mathrm{d}\, W_t = \\ &= B^2\left[\frac{1}{2}(\mu-1)\left(\frac{y^{(1)}}{y}\right)^{\mu-1} - \frac{1}{2}(\mu-2)\left(\frac{y^{(2)}}{y}\right)^{\mu-2}\right] y^{\mu-1}\,\mathrm{d}\, t + \\ &+ B y^{\frac{\mu}{2}}\,\mathrm{d}\, W_t, \end{aligned} \tag{4.19}$$

which approximates the volatility process defined by Eq. (4.13). In the above:

$$y^{(1)} = \left(\frac{2A}{(\mu-1)B^2}\right)^{\frac{1}{\mu-1}}, \tag{4.20}$$

$$y^{(2)} = \left(\frac{2C}{(\mu-2)B^2}\right)^{\frac{1}{\mu-2}}. \tag{4.21}$$

SDE (4.19) has a form similar to SDE (2.1) with the parameters in the equations related as $\lambda = \mu$ and $\eta = \mu/2$.

Using Eq. (2.13), as well as the comparison with SDE (2.1), it is straightforward to see that PDF of y has a region in which the probabilities scale as power-law function with the exponent $\lambda = \mu$. While $y^{(1)}$ and $y^{(2)}$ shape the exponential cut-offs:

$$p(y) \sim \frac{1}{y^{\mu}} \exp\left[-\left(\frac{y^{(1)}}{y}\right)^{\mu-1} + \left(\frac{y^{(2)}}{y}\right)^{\mu-2}\right]. \tag{4.22}$$

As SDE (4.19) is a special case of (2.1) with $2\eta = \mu$ and $\lambda = \mu$, the PSD of y time series should have a frequency range with the power-law behavior (due to Eq. (2.25)):

$$S(f) \sim \frac{1}{f^{\beta}}, \quad \beta = 1 + \frac{\mu-3}{\mu-2}. \tag{4.23}$$

Note, that we get $1/f$ PSD which is an interesting case related to so-called long-range memory phenomenon, when $\mu = 3$.

The statistical properties, PDF and PSD, of the time series of y obtained by numerically solving Eq. (4.13) with $\mu = 3$ are shown in Figure 4.2. The reflective boundary was used and it was placed at zero, $\sigma_t = 0$. As you can see in the figure analytical predictions of power-law exponents work well, PDF has a power-law tail with $\lambda = 3$ and over 4 decades of PSD $1/f$ dependency is observed.

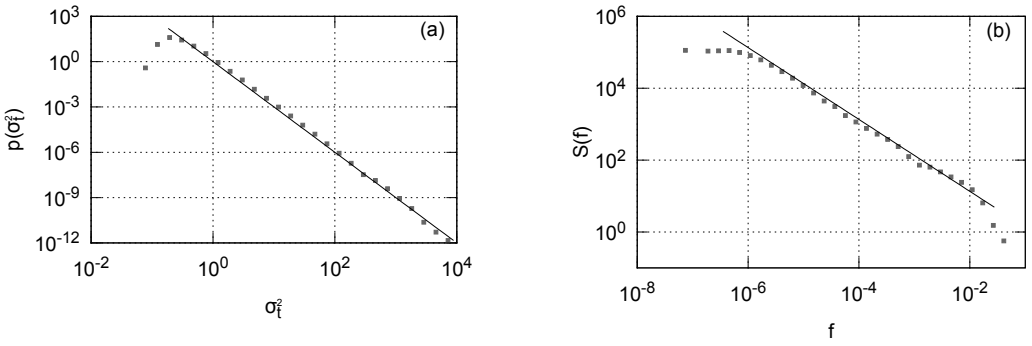

Figure 4.2: Statistical properties of σ_t^2 time series obtained by numerically solving Eq. (4.13) with $\mu = 3$: stationary PDF (a) and PSD (b). The following parameter values were used: $a = 10^{-6}$, $b = 10^{-3}$, $c = 1$. Black lines represent the expected power-law fits: (a) $p(\sigma_t^2) \sim (\sigma_t^2)^{-3}$ and (b) $S(f) \sim 1/f$ for the PSD.

4.2.2 The diffusion limit of Eq. (4.14)

Lets repeat the same steps with Eq. (4.14). First the time series sampling should be taken into account:

$$\sigma^2_{kh,h} = \sigma^2_{(k-1)h,h} + a_h - c_h\sigma^\mu_{(k-1)h,h} + b_h\sigma^\mu_{(k-1)h,h}|\omega_{(k-1)h,h}|^\mu. \tag{4.24}$$

Recall that here μ maybe any real number larger than 2. Let us choose the following notation – $\bar{\omega}_\mu = \langle|\omega|^\mu\rangle$.

In this case the mean drift per unit of time of σ^2 equals:

$$\begin{aligned}\lim_{h\to 0}\left\langle\frac{\sigma^2_{(k+1)h,h} - \sigma^2_{kh,h}}{h}\right\rangle &= \lim_{h\to 0}\left[\frac{a_h}{h} - \frac{c_h}{h}\sigma^\mu_{kh,h} + \frac{b_h}{h}\sigma^\mu_{kh,h}\bar{\omega}_\mu\right] = \\ &= A + C\sigma_t^\mu,\end{aligned} \tag{4.25}$$

and in the similar manner the second moment per unit of time equals:

$$\begin{aligned}\lim_{h\to 0}\left\langle h^{-1}\left(\sigma^2_{(k+1)h,h} - \sigma^2_{kh,h}\right)^2\right\rangle = \lim_{h\to 0} h^{-1}\Big[&\left(a_h - c_h\sigma^\mu_{kh,h}\right)^2 + \\ &+ b_h^2\sigma^{2\mu}_{kh,h}\bar{\omega}_{2\mu} + \\ &+ 2\left(a_h - c_h\sigma^\mu\right)b_h^2\sigma^{2\mu}_{kh,h}\bar{\omega}_\mu\Big] = B^2\sigma_t^{2\mu}.\end{aligned} \tag{4.26}$$

In the above A, B and C are continuous time parameters obtained (we require that $A > 0$ and $B > 0$) by expanding implicit dependence of a_h, b_h and c_h on h using Taylor expansion at $h \to 0$:

$$a_h = Ah, \quad b_h\bar{\omega}_\mu - c_h = Ch, \quad \bar{\omega}_{2\mu}b_h^2 = B^2h. \tag{4.27}$$

Expressions obtained in Eqs. (4.25) and (4.26) allow us to write the following SDE for $y_t = \sigma_t^2$:

$$\begin{aligned} \mathrm{d}\, y &= \left(\frac{A}{y^{\mu-1}} + \frac{C}{y^{\frac{\mu}{2}-1}}\right) y^{\mu-1}\,\mathrm{d}\, t + B y^{\frac{\mu}{2}}\,\mathrm{d}\, W_t = \\ &= B^2\left[\frac{1}{2}(\mu-1)\left(\frac{y^{(1)}}{y}\right)^{\mu-1} + \right. \\ &\left. + \frac{1}{2}\mathrm{sign}(C)\left(\frac{\mu}{2}-1\right)\left(\frac{y^{(3)}}{y}\right)^{\frac{\mu}{2}-1}\right] y^{\mu-1}\,\mathrm{d}\, t + B y^{\frac{\mu}{2}}\,\mathrm{d}\, W_t, \end{aligned} \tag{4.28}$$

$$y^{(1)} = \left(\frac{2A}{(\mu-1)B^2}\right)^{\frac{1}{\mu-1}}, \tag{4.29}$$

$$y^{(3)} = \left(\frac{4|C|}{(\mu-2)\,B^2}\right)^{\frac{2}{\mu-2}}. \tag{4.30}$$

Using Eq. (2.13), as well as the comparison with SDE (2.1), it is straightforward to see that PDF of y has a region in which the probabilities scale as power-law function with the exponent $\lambda = \mu$. While $y^{(1)}$ and $y^{(3)}$ shape the exponential cut-offs:

$$p(y) \sim \frac{1}{y^{\mu}} \exp\left[-\left(\frac{y^{(1)}}{y}\right)^{\mu-1} - \mathrm{sign}(C)\left(\frac{y^{(3)}}{y}\right)^{\mu-2}\right]. \tag{4.31}$$

As SDE (4.28) is a special case of (2.1) with $2\eta = \mu$ and $\lambda = \mu$ (similarly to SDE (4.19)), the PSD of y_t time series should also have a frequency range where Eq. (4.23) holds.

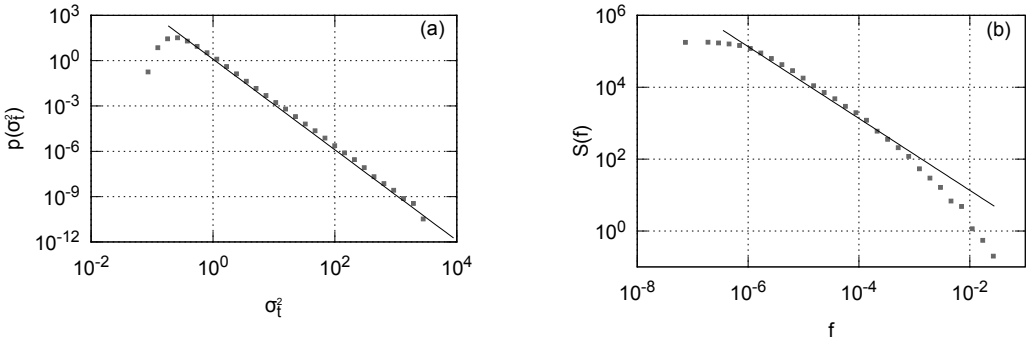

Figure 4.3: Statistical properties of σ_t^2 time series obtained by numerically solving Eq. (4.14) with $\mu = 3$: stationary PDF (a) and PSD (b). The following parameter values were used: $a = 10^{-6}$, $b = 10^{-3}$, $c = 2\sqrt{\frac{2}{\pi}} \cdot 10^{-3} \approx 1.595769 \cdot 10^{-3}$. Black lines represent the expected power-law fits: (a) $p(\sigma_t^2) \sim (\sigma_t^2)^{-3}$ and (b) $S(f) \sim 1/f$ for the PSD.

The statistical properties, PDF and PSD, of the time series of y obtained by

numerically solving Eq. (4.14) with $\mu = 3$ are shown in Figure 4.2. The reflective boundary was used and it was placed at zero, $\sigma_t = 0$. As you can see in the figure analytical predictions of power-law exponents work well, PDF has a power-law tail with $\lambda = 3$ and over 3 decades of PSD $1/f$ dependency is observed.

4.2.3 A remark on the power-law behavior and parameter C

It is worthwhile to note that in all cases with nonlinear GARCH model we have selected parameters as to set $C = 0$. This is necessary as C (and consequently c) might be seen as determining the "prominence" of exponential cut-off. Namely, the larger deviation of C from zero the more prominent exponential "bump" becomes and power-law dependency becomes significantly less apparent. As you can see in Figure 4.4, the PDF is very sensitive to the changes of C (even smallest deviation from zero makes it nearly impossible to observe power-law tail of the PDF). As $1/f$ PSD is closely related to the large deviations of the observable, it would be also severely affected by the non-zero C.

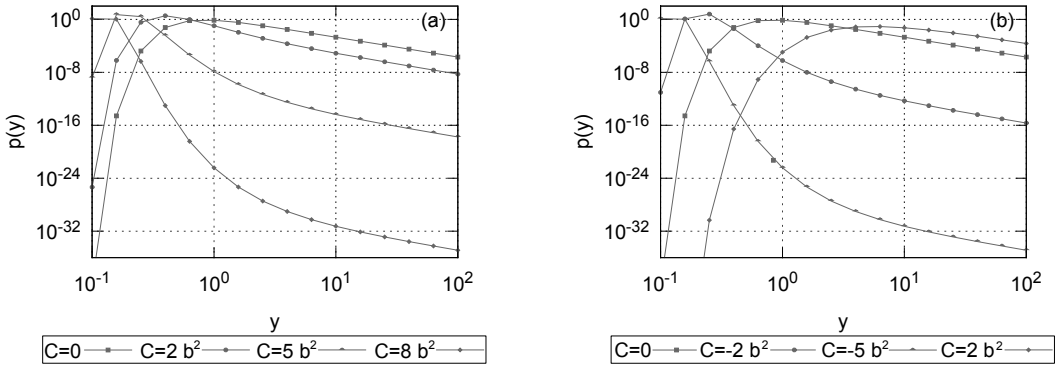

Figure 4.4: Analytical PDFs, Eqs. (4.22) and (4.31), for different values of C (see figure legends). Other parameters were set as follows: $\mu = 3$, $a = 10^{-6}$, $b = 10^{-3}$.

4.3 Summary

In this chapter we have compared ARCH models and general class of SDEs discussed in Chapter 2. We consider GARCH(1,1) volatility process as it has a form of iterative equation which is reminiscent to the iterative equations used to numerically solve SDEs. Thus in the diffusion limit we can rewrite GARCH(1,1) volatility process as SDE. We have compared SDE resulting from the original GARCH(1,1)

volatility process to SDE (2.1) and determined that it is able to produce power-law PDF, but only a Brownian-like PSD, $S(f) \sim 1/f^2$.

Thus we have proposed a two nonlinear modifications of GARCH(1,1) volatility process. Using the modified volatility process we were to recover volatility time series exhibiting $1/f$ PSD. SDEs obtained from nonlinear modifications of GARCH(1,1) volatility process belong to a general class of SDEs described by Eq. (2.1). The similarity suggests that using nonlinear modifications of GARCH(1,1) volatility process should allow reproduction of PSD with different exponents, $S(f) \sim 1/f^{\beta}$ ($0 < \beta < 2$). Formulas predicting PSD exponent, β, were also given in this chapter.

Introducing nonlinearity into GARCH(1,1) volatility process has interesting side-effect, in both cases parameter controlling internal state feedback, c, needs to be set almost precisely so that the corresponding parameter in the diffusion limit, C, equals to zero. Otherwise power-law behavior of the PDF is lost as well as ability to reproduce PSD with varying exponent, β, values (PSD becomes Brownian-like).

5 Modeling of the two-state system with herding interactions

In previous chapters we have considered the SDE (2.1) and other stochastic models built on it. The stochastic models appear to do great at reproducing empirical statistical features, but they do not do as well in explaining them. Agent-based framework enables the study of the actual reasons, based on human, firm or other entity, behind the market dynamics. There are already some great simpler [125, 126, 191–193] and more nuanced [80–82, 93] ABMs for the financial markets, but most of the well known models are able to reproduce only generalized empirical statistical facts, not the exact empirical statistical features. Which is why building bridges between the macroscopic (stochastic) and microscopic (agent-based) modeling has become an active topic [72–75, 83, 121, 122, 194, 195].

Starting from the stochastic models and moving towards ABM, the top-down bridging approach, is a rather formidable task, as a macroscopic dynamics of a complex system can not be understood as a simple superposition of interacting agents. It is also rather problematic to start from sophisticated ABMs and directly figure out their macroscopic description in terms of stochastic calculus. Though there is a notable case of [83], in which financial market ABM based on Ising model [80] was translated into SDE. But there is a simpler path: start from a simple ABM and build up its complexity as it becomes necessary.

5.1 Kirman's ABM of herding behavior

In the original paper [96] French economist Alan Kirman noted that entomologists and economists observe similar behavioral patterns in behavior of social insects (e.g., ants) [5, 6] and humans [4]. Based on these observations he proposed a simple mathematical model for herding behavior.

Namely, Kirman, in [96], cites a couple of works [5, 6] by a group of entomologists led by Pasteels, who have observed asymmetric ant behavior in a symmetric setup. Entomologists allowed ants to reach a food source using either of the two identical paths (a nice photo of the experimental setup may be found in a more recent paper [7]). Yet ants exploited only one on the available paths at any given moment.

Interestingly enough, from time to time, switches between the chosen paths occured.

For a schematic representation of the entomological experiment, as well as Kirman's model, see Figure 5.1. In this scheme circles represent ants (or agents) which choose one of the two identical paths (indicated by gray lines) connecting two points (e.g., colony and food source). Filled circles represent ants (or agents) who choose the upper path, while empty circles represent those who choose the bottom path. Two possible "interactions" are showcased in dashed boxes: ants (or agents, governed by the parameter σ in the transition equations) may switch independently of the others (single "particle interactions" on the left) or due to the influence of the others (two "particle interactions" on the right, governed by the parameter h in the transition equations).

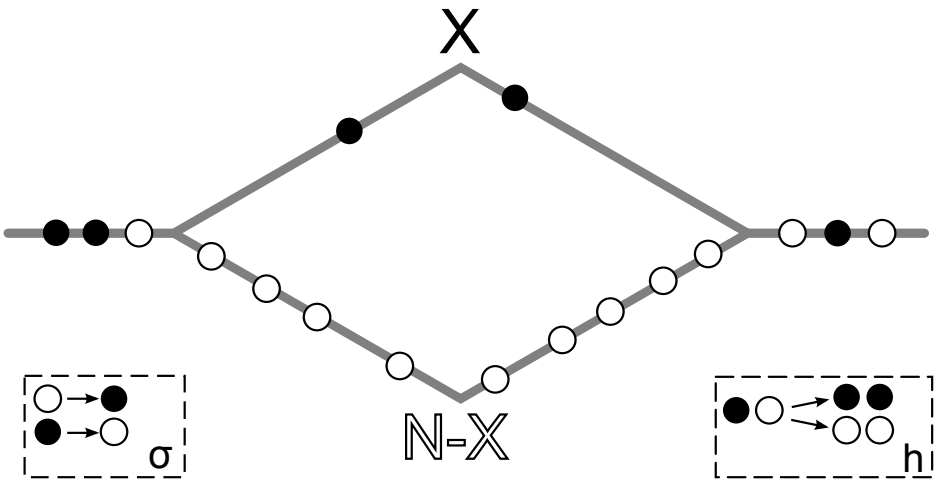

Figure 5.1: A general scheme illustrating experimental setup by Pasteels et al. [5–7] as well as ABM proposed by Kirman [96].

So, initially, Kirman proposed that a single ant (further, in order to generalize, we will refer to them as agents) gets to make a switch at any given point of time. Thus the system state which may be defined as a number of agents using selected path (or, in order to generalize, occupying selected state), X, at any given point of time might change by one:

$$p(X \to X + 1) = (N - X)\mu_{21}(X, N)\Delta t, \tag{5.1}$$

$$p(X \to X - 1) = X\mu_{12}(X, N)\Delta t. \tag{5.2}$$

In the above N is a total number of agents in colony, Δt is a small time step during which only one transition is probable, while μ_{ij} are functions describing individual agent decision making process when switching from state i to state j. For a physicist

it should be straightforward to see that μ_{ij} are actually transition rates between the two-states. Here we have assumed that state 1 represents the system state (namely, $X_1 = X$) and state 2 is the other state (namely, $X_2 = N - X$).

From the above we know that time step, Δt, should be small enough for only one transition being possible,

$$p(X \to X + 1) + p(X \to X - 1) \ll 1. \tag{5.3}$$

Though there are alternative interpretations which allow multiple agents to make choice simultaneously [196–199]. This does not add anything significant dynamics and in the large system, $N \to \infty$, and small time step, $\Delta t \to 0$, limit [198, 199]. But if the time step is comparatively large, then such interpretation seems to introduce information processing lag [199]. The requirement set by Eq. (5.3) is rather general and maybe implemented in various ways, we choose to rewrite it as:

$$\Delta t = \frac{\kappa}{(N - X)\mu_{21}(X, N) + X\mu_{12}(X, N)}, \quad 0 < \kappa \ll 1, \tag{5.4}$$

where κ is a numerical precision parameter. In our numerical simulations we found that $\kappa = 0.1$ is good value to use as it provides good results in reasonable time.

5.1.1 Symmetry in Kirman's ABM

In general $\mu_{ij}(X, N)$ may take many different forms [200], but in case of the Kirman's ABM we have simple:

$$\mu_{21}(X, N) = \sigma + hX, \quad \mu_{12}(X, N) = \sigma + h(N - X), \tag{5.5}$$

where σ describes idiosyncratic switching rate (intensity of transition in a "single-particle interactions"), while h describes switching rate due to influence of the other agents (intensity of transitions in a "two-particle interactions"). Though, there is also alternative interpretation of the original article which rewrites $\mu_{ij}(X, N)$ as [123, 124]:

$$\mu_{21}(X, N) = \sigma + \frac{hX}{N}, \quad \mu_{12}(X, N) = \sigma + \frac{h(N - X)}{N}. \tag{5.6}$$

This interpretation is frequently referred to as local interaction interpretation [123, 124]. In Section 5.3 we will consider the differences and similarities between these interpretations, but for now let us stick with Eq. (5.5) which is correspondingly

referred to as global interaction interpretation [123, 124]. Probabilities of a similar form are present in the long-range memory model proposed by [201]. The main difference is that the probabilities in the model proposed by Diebold are dependent on sample size, instead of number agents.

In case of Eq. (5.5) general expression for the time step, Eq. (5.4), might be simplified as follows

$$\Delta t = \frac{2\kappa}{N(2\sigma + hN)}, \quad 0 < \kappa \ll 1. \tag{5.7}$$

To obtain the above we have used the fact that model is symmetric in respect to idiosyncratic switching rates and thus denominator maximizes itself when $X = N/2$.

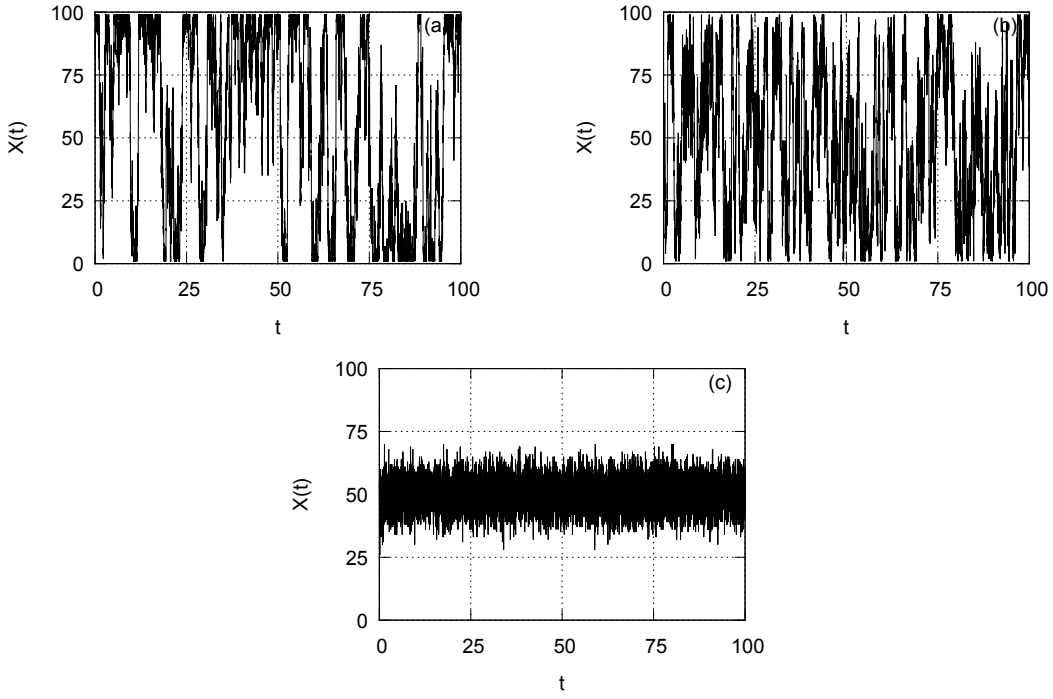

Figure 5.2: Three different behavioral regimes observed in Kirman's model: (a) prevalent herding behavior ($\sigma = 0.01$), (b) balanced behavior ($\sigma = 1$) and (c) prevalent individualistic behavior ($\sigma = 100$). Other model parameters were set as follows: $h = 1$, $N = 100$.

Time series shown in Figure 5.2 showcase three different behavioral regimes. The observed behavioral regime clearly depends on $\frac{\sigma}{h}$ ratio. Let us further denote this ratio as ε. If $\varepsilon < 1$, then herding behavior prevails: most of the time majority of agents occupy the same state as everybody else (the agents agree). If $\varepsilon > 1$, then individualistic behavior prevails: agents select their state randomly (the agents disagree). While in the region around $\varepsilon = 1$ balanced behavior is observed: a conflict

between individualistic behavior and herd following causes seemingly unstable system dynamics. These insights are confirmed by the stationary PDF of the time series generated using same parameter sets (see Figure 5.3).

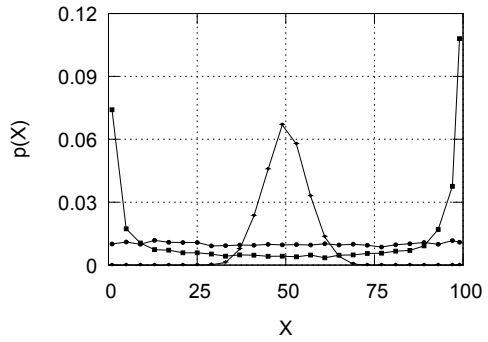

Figure 5.3: Stationary PDFs of X in the three different behavioral regimes observed in Kirman's model: prevalent herding behavior (squares; $\sigma = 0.01$), balanced behavior (circles; $\sigma = 1$) and prevalent individualistic behavior (triangles, $\sigma = 100$). Other model parameters were set as follows: $h = 1$, $N = 100$.

So as ε might be seen as parameter allowing to switch between the behavioral regimes, h might be seen as influencing fluctuation rates. Simple mathematics, $t_s = ht$, gives us the following:

$$p(X \to X + 1) = (N - X)\,(\varepsilon + X)\,\Delta t_s, \tag{5.8}$$

$$p(X \to X - 1) = X\,(\varepsilon + [N - X])\,\Delta t_s. \tag{5.9}$$

5.1.2 Asymmetry in Kirman's ABM

The model can be simply generalized by assuming that states are not equivalent to each other. Entomologists have observed ants in asymmetric setups and found that ants do not neglect the path which is worse (e.g., longer) than its alternative [5–7].

As we have seen previously h is related to the event time scale. Thus one might argue that h is specific to the transitions between two considered states and is not a property of any of the two-states (though alternative interpretations are possible [202,203]). Consequently only ε is open to be related to the "attractiveness" (perceived fitness) of each state. Having this in mind we can rewrite the transition

probabilities as follows:

$$p(X \to X+1) = (N-X)(\varepsilon_1 + X)\Delta t_s, \tag{5.10}$$

$$p(X \to X-1) = X\,(\varepsilon_2 + [N-X])\,\Delta t_s. \tag{5.11}$$

In the above ε_1 can be seen as attractiveness of the system state, while ε_2 can be seen as attractiveness of the other state.

Appropriate Δt values are chosen following the same logic as previously. Indeed, if ε_i are not very different, then one can simply use Eq. (5.7) as inspiration:

$$\Delta t_s = \frac{2\kappa}{N(\varepsilon_1 + \varepsilon_2 + N)}. \tag{5.12}$$

Looking for a better precision one might add correction term:

$$\Delta t_s = \frac{2\kappa}{N(\varepsilon_1 + \varepsilon_2 + N) + \left(\frac{\varepsilon_1 - \varepsilon_2}{2}\right)^2}. \tag{5.13}$$

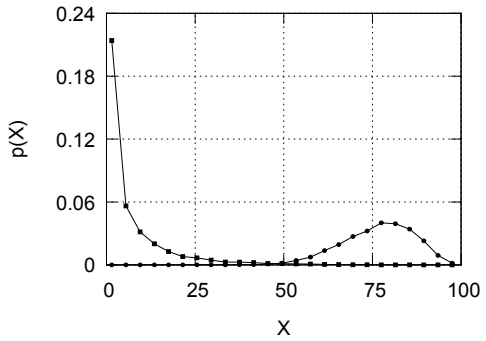

Figure 5.4: Influence of asymmetric individual behavior on the stationary PDF. Parameters were set as follows: $\varepsilon_1 = 0.2$ (squares) and 16 (circles), $\varepsilon_2 = 5$, $h = 1$, $N = 100$.

As it should be expected slightest difference in σ_i value cause movement of the PDF maxima (see Figure 5.4). The maxima moves towards the more attractive state side. Namely, agents try to occupy the more attractive state more frequently than its alternative, though the alternative is not be completely neglected.

5.2 Analytical treatment of Kirman's ABM

It should be evident that by definition such ABM lacks memory as agent transition probabilities depend only on the current system state. This lack of memory

suggest that it should be possible to formalize the ABM as SDE. There are couple of different ways how to approach derivation of SDE describing the same dynamics as Kirman's ABM. One is based on the notion of probability fluxes [123], while the other is based on the expansion of one step operators [124].

5.2.1 Macroscopic description using birth-death process formalism

As stochastic calculus normally operates with continuous variables as well as continuous time, we need to assume that number of agents, N, in the system is large enough for $x = X/N$ to be continuous. Though it is more convenient just to take infinity limit, $N \to \infty$. Let x describe the system state, then the transition probabilities per unit of time take the following form:

$$\pi^{+}(x) = (1 - x)\left(\frac{\varepsilon_1}{N} + x\right), \tag{5.14}$$

$$\pi^{-}(x) = x\left(\frac{\varepsilon_2}{N} + \{1 - x\}\right). \tag{5.15}$$

The relation between the discrete one-step transition probabilities, $p(X \to X \pm 1)$, and continuous transition rates, $\pi^{\pm}$, is rather straightforward:

$$p(X \to X \pm 1) = N^2 \pi^{\pm}(x)\Delta t_s. \tag{5.16}$$

Now by using one-step operators, $\mathbf{E}$ and $\mathbf{E}^{-1}$, we can write down the master equation:

$$\frac{\partial}{\partial t}p(x,t) = N^2\left\{(\mathbf{E} - 1)[\pi^{-}(x)\omega(x,t)] + (\mathbf{E}^{-1} - 1)[\pi^{+}(x)\omega(x,t)]\right\}. \tag{5.17}$$

Let us recall the definition of one step operators, $\mathbf{E}$ and $\mathbf{E}^{-1}$, [204] and expand them in small step limit (up to the second term):

$$\mathbf{E}[f(x)] = f(x + \Delta x) \approx f(x) + \Delta x \frac{\mathrm{d}}{\mathrm{d}\,x} f(x) + \frac{\Delta x^2}{2}\frac{\mathrm{d}^2}{\mathrm{d}\,x^2} f(x), \tag{5.18}$$

$$\mathbf{E}^{-1}[f(x)] = f(x - \Delta x) \approx f(x) - \Delta x \frac{\mathrm{d}}{\mathrm{d}\,x} f(x) + \frac{\Delta x^2}{2}\frac{\mathrm{d}^2}{\mathrm{d}\,x^2} f(x). \tag{5.19}$$

Putting these Taylor expansions into the master equation results in the follow-

ing Fokker–Plank equation:

$$\frac{\partial}{\partial t}p(x,t) = -N\frac{\partial}{\partial x}[\{\pi^+(x) - \pi^-(x)\}p(x,t)] + \\ + \frac{1}{2}\frac{\partial^2}{\partial x^2}[\{\pi^+(x) + \pi^-(x)\}p(x,t)]. \tag{5.20}$$

By introducing custom drift, $A(x)$, and diffusion, $B(x)$, functions:

$$A(x) = N\{\pi^+(x) - \pi^-(x)\} = \varepsilon_1(1-x) - \varepsilon_2 x, \tag{5.21}$$

$$B(x) = \pi^+(x) + \pi^-(x) = 2x(1-x) + \frac{\varepsilon_1}{N}(1-x) + \frac{\varepsilon_2}{N}x \approx \\ \approx 2x(1-x), \tag{5.22}$$

one can rewrite the Fokker–Planck equation as SDE in Ito sense:

$$\mathrm{d}x = A(x)\mathrm{d}t_s + \sqrt{B(x)}\mathrm{d}W_s = \\ = [\varepsilon_1(1-x) - \varepsilon_2 x]\mathrm{d}t_s + \sqrt{2x(1-x)}\mathrm{d}W_s. \tag{5.23}$$

In Figure 5.5 we have shown that this SDE approximates the dynamics of ABM rather well, even with not a large number of agents, $N = 100$.

Steady state PDF of x, in merit of Eq. (2.13), is given by:

$$p(x) = Cx^{\varepsilon_1 - 1}(1-x)^{\varepsilon_2 - 1}, \tag{5.24}$$

where C is a normalization constant which is given by:

$$C = \frac{1}{\int_0^1 x^{\varepsilon_1-1}(1-x)^{\varepsilon_2-1}\,\mathrm{d}\,x} = \frac{\Gamma(\varepsilon_1+\varepsilon_2)}{\Gamma(\varepsilon_1)\Gamma(\varepsilon_2)} = \frac{1}{B(\varepsilon_1,\varepsilon_2)}. \tag{5.25}$$

Its mathematical form is identical to the so-called Beta distribution [159] and, as shown in Section 5.3, can be transformed to have a mathematical form identical to the q-Gaussian distribution.

It is worth noting that derivation of Eq. (5.23) does not significantly depend on actual forms of $\pi^{\pm}(x)$. The only requirement is that $\pi^{\pm}(x)$ should stay bounded as long as $N \to \infty$. As derivation is rather universal, it is open to possible generalizations. These generalizations will be further elaborated in the following chapters of this dissertation.

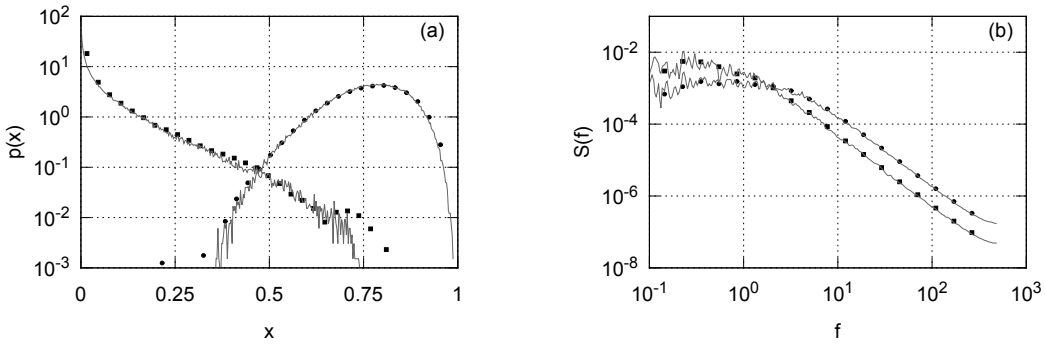

Figure 5.5: Comparison of statistical properties, (a) PDF and (b) PSD, obtained from ABM (squares and circles) and its macroscopic approximation by SDE (gray curves behind squares and circles). Model parameters were set as follows: $\varepsilon_1 = 0.2$ (squares, gray curve behind the squares) and 16 (circles, gray curve behind the circles), $\varepsilon_2 = 5$, $h = 1$, $N = 100$ (squares and circles).

5.2.2 Bass Diffusion model as a special case of Kirman's ABM

Bass Diffusion model, proposed by F. M. Bass in [205], is a prominent model in the Marketing theory [206–209]. This model is a basic model offering forecast of the adoption rate of a new product or technology. Mathematically it is formulated as ODE with a boundary condition:

$$\frac{\mathrm{d}}{\mathrm{d}t}X(t) = [N - X(t)]\left[p + \frac{q}{N}X(t)\right], \tag{5.26}$$

$$X(0) = 0. \tag{5.27}$$

In the above $X(t)$ gives a number of current consumers, of the product or technology entering the market, at time t, N is market potential (total number of agents possibly interested in the new product), p is the so-called coefficient of innovation (the likelihood for individual to adopt new product based on individual decision, due to influence of commercials or similar external factors) and q is the so-called coefficient of imitation (a measure of likelihood for individual to adopt new product based on peer pressure, knowing that other individuals own it). This nonlinear ODE serves as a macroscopic description of new product adoption by consumers widely used in business planning [206].

It is straightforward to note that Bass Diffusion model operates using the same concepts as Kirman's model [96]. Though there are two essential differences, the first is that Bass Diffusion model assumes that products are durable. This means

that current consumers never switch back to being potential consumers. Second important difference is that agents in the market are assumed to interact only locally, namely, with their friends and colleagues (small number of people compared to the whole system). Mathematically this translates into the following per agent per unit of time transition rates:

$$\pi^{+}(x) = (1 - x)\left(\frac{\sigma}{N} + \frac{h}{N}x\right), \tag{5.28}$$

$$\pi^{-}(x) = 0. \tag{5.29}$$

We use Eq. (5.16) to recover the corresponding transition probabilities for the ABM.

The obtained unidirectional ABM in essence is very similar to the Linear and GLM models discussed in [197], with the essential difference being that the models in [197] are defined in terms of probability that a single agent will take opinion of other single agent into account. In our case, in Kirman's model, σ and h are assumed to reflect aggregate behavior, namely, σ and h values represent the collective influence of all agents on any single agent. Despite the essential difference, in the small step limit, $\Delta t \to 0$, all models provide the same mathematical expressions.

In case of the transition rates (5.28) and (5.29) the macroscopic description functions, namely, drift, $A(x)$, (check with Eq. (5.21)) and diffusion, $B(x)$, (check with Eq. (5.22)) become

$$A(x) = N\pi^{+}(x) = (1 - x)\left(\sigma + hx\right), \tag{5.30}$$

$$B(x) = \pi^{+}(x) = \frac{(1 - x)}{N}\left(\sigma + hx\right). \tag{5.31}$$

If total number of agents is extremely large, then one can neglect $B(x)$. This leaves us with ODE identical to the Bass Diffusion model ODE, Eq. (5.26), with $\sigma = q$ and $p = h$. This serves as a direct proof that Bass Diffusion model is an unidirectional case of Kirman's herding model.

In Figure 5.6 we demonstrate the similarity of results obtained from the macroscopic Bass Diffusion model, Eq. (5.26), and microscopic unidirectional Kirman's ABM. The agreement of the results is achieved as long as market potential grows larger, as well as with the increasing observation time interval, τ.

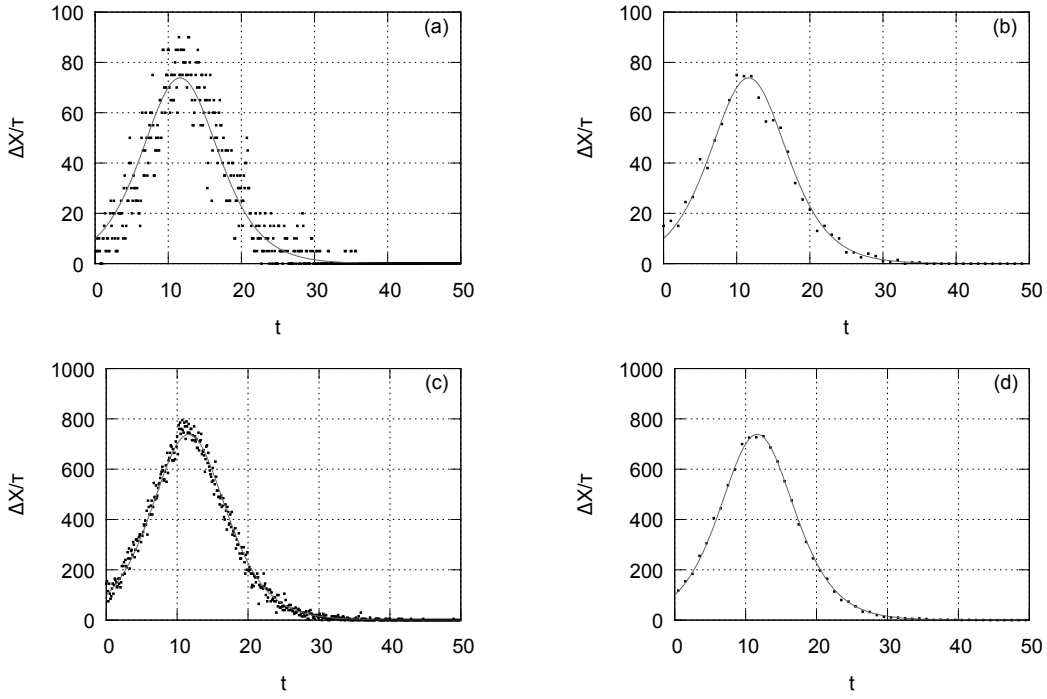

Figure 5.6: Comparison of the time series obtained from the macroscopic Bass Diffusion model (gray curves) and the unidirectional Kirman's ABM (black dots). Different sub-figures showcase differing market potentials ((a), (b) $N = 1000$; (c), (d) $N = 10000$) and differing observation time intervals ((a), (c) $\tau = 0.1$; (b), (d) $\tau = 1$). Other model parameters were set as follows: $\sigma = 0.01$, $h = 0.275$.

5.3 Implications of interaction topology

In Section 5.2 we have seen that in the $N \to \infty$ limit we may obtain either SDE or ODE as a macroscopic description of Kirman's ABM. This depends on the scale of agent interactions. If any agent may interact with any other agent, namely, the agents interact globally, then SDE is obtained. Alternatively, if agent may interact only in its small (compared to N) neighborhood, namely, the agents interact locally, then ODE is obtained. For large but finite, $N \gg 1$, agent-based simulations similar results were obtained [210, 211]. Namely, if agents interact globally, then power-law PDF is observed for many different N. Yet if agents interact locally, then power-law PDF quickly transitions to Gaussian-like PDF with growing N. The same observations were made by Traulsen et al., who have obtained similar macroscopic SDE from slightly different assumptions originating from the game theory, [212–214]. This dependence suggests that it might be interesting to define Kirman's model to be executed on some definite topology (network) with variable scale of agent interactions.

5.3.1 Network formation algorithm generating variable scale of interactions

In [210] Kirman's ABM was tested on three network topologies: random network, small world network and scale-free network. Here we propose a new network formation algorithm which is able to generate networks with variable of agent interactions using a single parameter. Thus depending on the parameter generated topologies may describe either local or global interactions, furthermore intermediate, or "hybrid", interactions topologies may be obtained as well. Networks generated using the proposed algorithm exhibit sub-linear increase of the mean degree, $\langle d \rangle$, with the increasing number of nodes, N, in the network,

$$\langle d \rangle \propto N^{\alpha}, \quad 0 \leq \alpha \leq 1, \tag{5.32}$$

where α is the mean degree scaling exponent. Namely, the generated network exhibits network densification observed in different real-life social systems [110–114].

As a base model for the proposed network formation algorithm we have chosen a Barabasi–Albert model [109] which we further extend by adding an additional step. The work flow of the modified algorithm is implemented as described bellow:

1. Form a network with two nodes and link between them.

2. Add a new node to the network.

3. Form a link between the new node and chosen old node. The old node should be chosen as per-usual in Barabasi–Albert model, using the linear "rich gets richer" scheme,

$$p_i \propto d_i, \tag{5.33}$$

where i is the index of the old node.

4. Form additional links to the neighbors of the chosen old node with the probability

$$p = p_0 d^{-\gamma}, \tag{5.34}$$

here p_0 is a probability that link will be formed when $\gamma = 0$, d is a degree of the old node chosen during the step 3, while γ is scaling exponent.

5. Repeat from Step 2 to Step 4 until number of nodes in the network reaches N.

See Figure 5.7 for an example illustrating this algorithm. Previously two nodes (3 and 4) were added to the network. During another iteration of the algorithm, step 2, Node 5 was added. Using the linear "rich gets richer" scheme (step 3) it was linked to Node 2 (dashed line without arrow). During the additional step (step 4) Node 5 may form links to Node 1 and Node 3 (as they are neighbors of Node 2), but not Node 4 (as it is not a direct neighbor of Node 2), with probability given by Eq. (5.34) (with $d_i = 2$).

Procedure performed in Step 4 was inspired by a similar techniques used in other network formation algorithms which exhibit sub-linear mean degree scaling: the triad formation [110, 114], friends of friends [111] and forest fire [112] network formation algorithms. Our approach is similar to the ones discussed in [110, 111, 114] in a sense that the additional links are formed only with the direct neighbors of the chosen node. We differ from [111] in our choice of base model, we have chosen Barabasi–Albert model and not random network model. Furthermore, in comparison with [110, 111, 114], we add a random amount of links instead of fixed amount of links. The forest fire algorithm [112] also adds random amount of links, but it

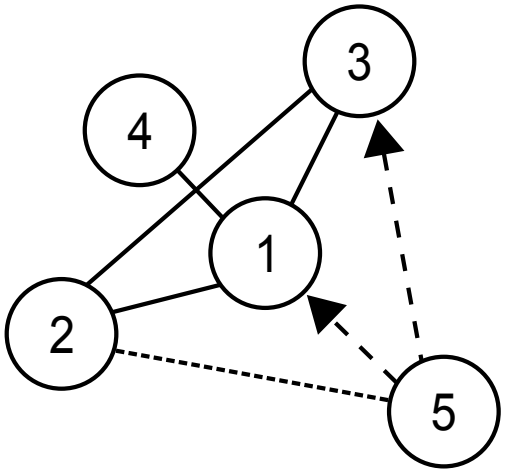

Figure 5.7: An example iteration of network formation algorithm. Node 5 has just joined the network and formed a link with Node 2. It may further form links, according to Eq. (5.34), with Nodes 1 and 3.

considers only $\gamma = 0$ case. In [112] sub-linear mean degree scaling is achieved simply by repeating the linking with new neighbors of neighbors (friends of friends) until no new links are formed. It is worth noting that there are more network formation models which exhibit the desired scaling of the mean degree, but most of them are too general and consequently lack any direct connections to the actual processes happening in the socio-economic systems [215–217].

In Figure 5.8 you can see how the mean degree scaling depends on parameters γ. These, as well as other, simulations indicated that for $\gamma \in [0, 1)$ the following relation to the mean degree scaling exponent holds:

$$\alpha \approx (1 - \gamma)^2. \tag{5.35}$$

For $\gamma > 1$, α rapidly saturates at $\alpha = 0$.

In Figure 5.9 we have shown that the proposed network formation algorithm is able to produce topologies comparable with random network model as well as scale-free network model. With small γ the network topology looks like completely random structure, while Gaussian-like degree PDF is observed. While the opposite result is observed with γ approaching 1 and becoming larger, nodes align into scale-free structure. For intermediate values of γ random links are observable as well as characteristic features of scale-free topology (such as hubs). Mean degree scaling is the same as was shown in Figure 5.8.

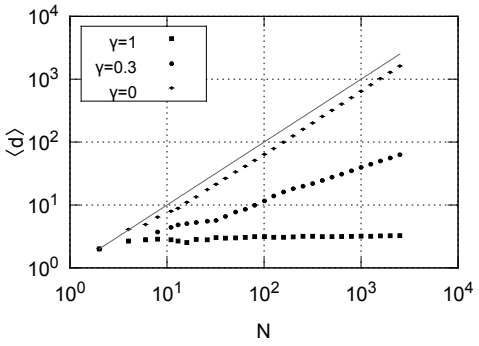

Figure 5.8: Mean degree with the increasing number of N for different values of probability scaling exponent γ. Gray curve shows the mean degree scaling in completely connected network. p_0 parameter was assigned a value of 0.3.

5.3.2 Two-state ABM based on herding behavior executed on the generated interaction topologies

In general per-agent transition rates of a symmetric Kirman's ABM are now different for each agent:

$$\mu^{(i)}\left(S \to S'\right) = \sigma + h n_i\left(S'\right). \tag{5.36}$$

here i is an index representing agent, S is state agent i is currently in, S' is state the agent may switch to, $n_i(S')$ is a function which gives us a number of agent's i neighbors which are in the state S'.

Although in numerical simulations we will have to use Eq. (5.36), in order to obtain analytical insights we may still use mean-field approach. Taking average of a per-agent transition rate over all agents in state S yields the following,

$$\langle \mu^{(i)}(S \to S') \rangle = \sigma + h\langle d \rangle \frac{N_{S'}}{N}, \tag{5.37}$$

where $N_{S'}$ is a total number of agents in the state S'. These averages are exactly the same as corresponding system-wide transition rates discussed in Section 5.1,

$$\mu_{21} = \langle \mu^{(i)}(2 \to 1) \rangle, \quad \mu_{12} = \langle \mu^{(i)}(1 \to 2) \rangle. \tag{5.38}$$

5.3.3 Mean-field approximation

In merit of discussion in Section 5.2, we may hope that the following SDE describes the macroscopic dynamics of the generalized Kirman's ABM

$$\mathrm{d}\, x = \sigma(1 - 2x)\,\mathrm{d}\, t + \sqrt{\frac{2h\langle d \rangle x(1-x) + \sigma}{N}}\,\mathrm{d}\, W_t. \tag{5.39}$$

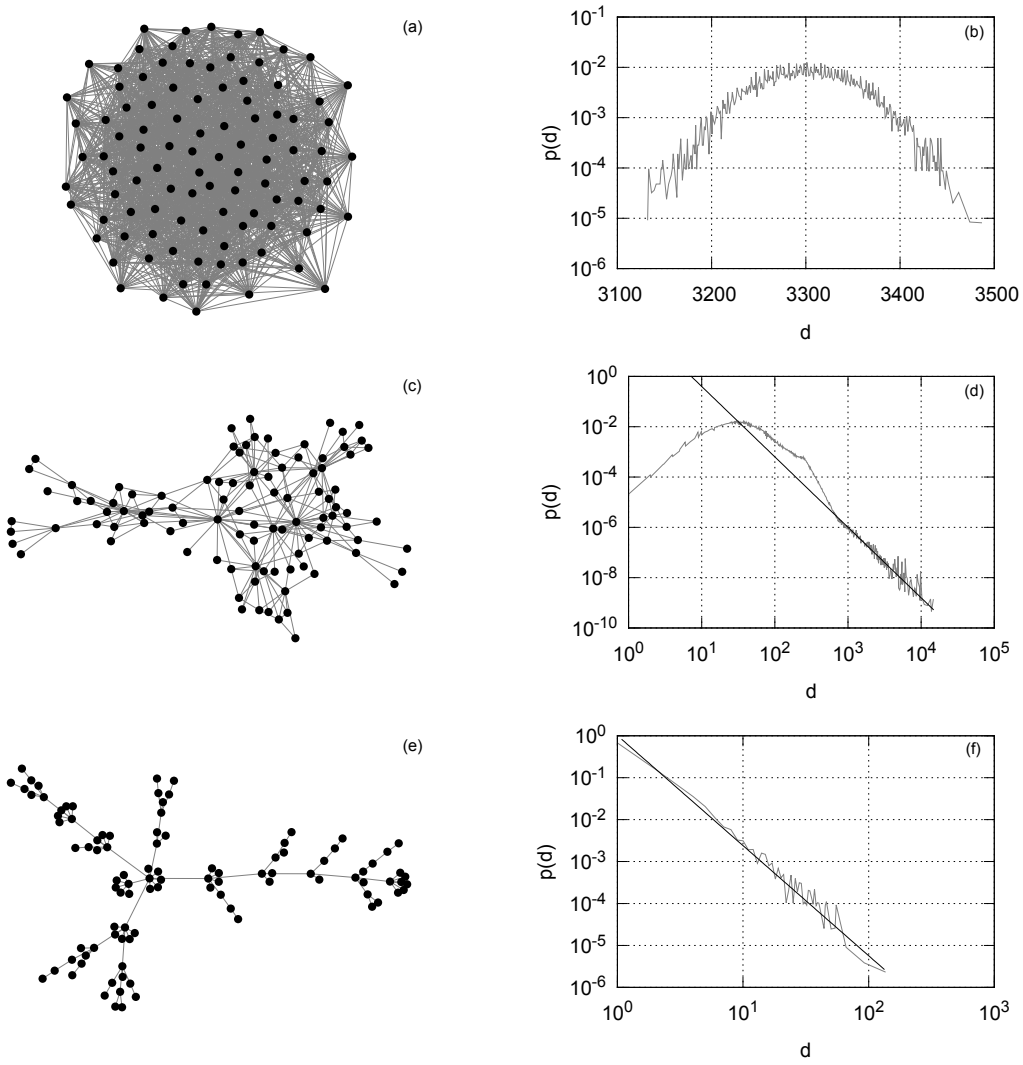

Figure 5.9: Different network topologies generated using the proposed network formation algorithm: random network ((a) topology and (b) degree PDF), scale-free network ((e) topology and (f) degree PDF) and "hybrid" network ((c) topology and (d) degree PDF). Network topology snapshots ((a), (c) and (e)) were taken at $N = 100$. While degree PDFs were obtained from networks with $N = 10^4$ (for random network topology) and with $N = 3 \cdot 10^4$ ("hybrid" and scale-free topologies) nodes. Black lines in (d) and (f) provide power-law fit (with exponent $\lambda = 3$) for the tail of the PDF. Following parameter values were used: $p_0 = 0.3$, $\gamma = 0$ (random network), 0.3 ("hybrid" network), 1 (scale-free network).

This SDE should applicable to any interaction topology provided N is large enough. In previous section we have proposed a network formation algorithm in which mean degree scales as a power of number of nodes,

$$\langle d \rangle = d_0 N^{\alpha}, \tag{5.40}$$

$$\mathrm{d}\, x = \varepsilon(1-2x)\,\mathrm{d}\, t_s + \sqrt{\frac{2N^{\alpha}x(1-x)+\varepsilon}{N}}\,\mathrm{d}\, W_s, \tag{5.41}$$

$$\varepsilon = \frac{\sigma}{h d_0}, \quad t_s = h d_0 t. \tag{5.42}$$

The steady state PDF of x driven by SDE (5.41) according to Eq. (2.13) is given by

$$p(x) = C\left[\varepsilon + 2N^{\alpha}x(1-x)\right]^{\varepsilon N^{1-\alpha}-1}. \tag{5.43}$$

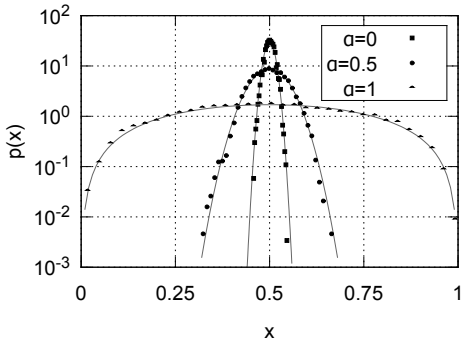

Figure 5.10: Scaling of the numerically obtained steady state PDF with three different values of mean degree scaling exponent: $\alpha = 0$ (squares), $\alpha = 0.5$ (circles) and $\alpha = 1$ (triangles). The following parameter set was used: $\sigma = 1.5$, $h = 1$, $N = 3000$, $p_0 = 0.75$, $\Delta t = 2 \cdot 10^{-5}$ and $\gamma = 1$ ($\alpha = 0$), 0.3 ($\alpha = 0.5$) and 0 ($\alpha = 1$). Gray solid lines show the corresponding mean-field approximations of the steady state PDF, Eq. (5.43). Scaling constant, d_0, was estimated by observing scaling of the mean degree $\langle d \rangle$: $d_0 = 3.2$ ($\alpha = 0$), $d_0 = 1.24$ ($\alpha = 0.5$) and $d_0 = 0.6$ ($\alpha = 1$).

See Figure 5.10 and Figure 5.11 for a comparison between the mean-field approximation, Eq. (5.43), and actual numerically obtained steady state PDF of the ABM described by Eq. (5.36). During numerical computation we have chosen a fixed time step Δt and considered transition probabilities $p_i(S \to S')\Delta t$. The time step must be chosen such that all transition probabilities would make sense, i.e. $p_i < 1$ for all i, though in order to compare this case with original Kirman's ABM one should use time step small enough for only one transition to be possible. For a given interaction topology (network structure), we synchronously update the state of each agent according to their own transition probabilities.

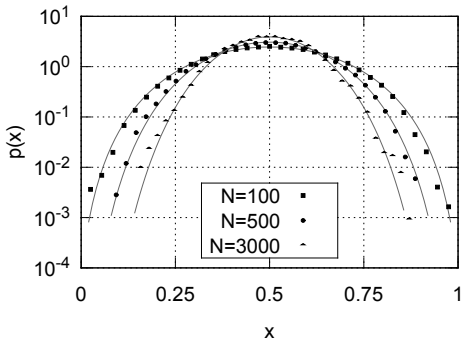

Figure 5.11: Scaling of the numerically obtained steady state PDF with the increasing number of agents in the model: $N = 100$ (squares), $N = 500$ (circles) and $N = 3000$ (triangles). The following parameter set was used: $\sigma = 1.5$, $h = 1$, $p_0 = 0.75$, $\gamma = 0.15$, $\Delta t = 2 \cdot 10^{-5}$. Gray solid lines show the corresponding mean-field approximation of the steady state PDF, Eq. (5.43). Scaling constant, d_0, was estimated to be equal to 0.9 by observing scaling of the mean degree $\langle d \rangle$.

To obtain the mean-field steady state PDF we use the parameter d_0 which is obtained by observing the scaling of the mean degree $\langle d \rangle$ during network formation. In both Figure 5.10 and Figure 5.11 we observe good agreement between the numerically obtained PDF and its mean-field approximation. The width of the steady state PDF increases with larger values of α, as is shown in Figure 5.10 and decreases with increasing number of agents N, as can be inferred from Figure 5.11. In the limit of $N \to \infty$ the PDF narrows down to Dirac's Delta function for $\alpha < 1$ or retains power-law form otherwise.

5.3.4 Continuous transition between non-extensive and extensive statistics

Note that Eq. (5.43) can be rewritten as a q-Gaussian,

$$p(x) = C' \exp_q \left[-A_q \left(x - \frac{1}{2} \right)^2 \right], \tag{5.44}$$

with

$$q = 1 - \frac{1}{\varepsilon N^{1-\alpha} - 1}, \qquad A_q = 2N^{1-\alpha} \frac{1 - \frac{1}{\varepsilon} N^{\alpha-1}}{\frac{1}{2\varepsilon} + N^{-\alpha}}. \tag{5.45}$$

In the above $\exp_q(\cdot)$ is the q-exponential function which is defined as

$$\exp_q(x) \equiv [1 + (1-q)x]_+^{\frac{1}{1-q}}, \tag{5.46}$$

here $[x]_+ = x$ if $x > 0$, and $[x]_+ = 0$ otherwise. The steady state PDF having a q-Gaussian form for finite values of N is in agreement with known fact that Tsallis generalized canonical distribution which describes systems in contact with a finite heath bath [218, 219]. The fact that we have obtained q-Gaussian distribution with finite N confirms the idea that small systems are similar to large ones with true long-range interactions.

Observe the scaling of q in Figure 5.12. Note how the $q \approx 1$ region expands with increasing N, this means that power-law distributions become lost and only Gaussian-like distribution remains as result of growing system size.

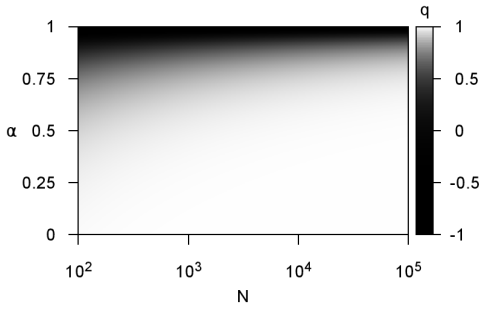

Figure 5.12: The dependence of a q-Gaussian non-extensivity parameter, q (given by Eq. (5.45)), on system size, N, and mean degree scaling exponent, α. White color represents extensive behavior $q \approx 1$, while black color non-extensive $q < 1$ (see color scale for more details).

If the interaction topology allows global interactions, $\alpha = 1$ ($\langle d \rangle \sim N$), and no matter how large the system is (though it should still be large enough for $x = X/N$ to appear continuous), then the steady-state PDF takes the following power-law form

$$p(x) = \frac{\Gamma(2\varepsilon)}{\Gamma(\varepsilon)^2}[x(1-x)]^{\varepsilon-1}. \tag{5.47}$$

This corresponds to a q-Gaussian with non-extensivity parameter given by

$$q = 1 - \frac{1}{\varepsilon - 1}. \tag{5.48}$$

On the other hand, if interaction topology allows only local interactions, $\alpha = 0$ ($\langle d \rangle \sim$ const), and the system infinitely large, $N \to \infty$, then the steady state PDF is a Dirac's Delta function centered on $x_0 = 0.5$. As real systems are never infinite, for large N the steady state PDF has a Gaussian-like form. If $\alpha < 1$ and $N \gg 1$ then

q tends to 1 and from the properties of the q-exponential function we get that the steady state PDF is approximately,

$$p(x) \sim \exp\left[-N^{1-\alpha} A \left(x - \frac{1}{2}\right)^2\right], \tag{5.49}$$

$$A = \begin{cases} \frac{2}{\frac{1}{2\varepsilon}+1}, & \alpha = 0 \\ 4\varepsilon, & 0 < \alpha < 1 \end{cases} \tag{5.50}$$

In all cases but $\alpha = 1$ we observe the so-called N-dependence problem [210], shape and variance of the distribution is lost with the increasing size of the system, N. The variance of x is lost proportionally to $1/\sqrt{N^{1-\alpha}}$ law. Fluctuations decay as usual, $1/\sqrt{N}$ if $\alpha = 0$, and decays slower as α approaches 1.

5.4 Summary

In this chapter we have discussed Kirman's ABM which was proposed in [96]. This model exhibits two distinct behavioral regimes: individualistic or herd behavior. If individualistic behavior prevails, then both of the available states are occupied by comparable numbers of agents at any given time. If herding behavior prevails, then only one state is occupied by most of agents at any given time. The occupied state is switched from time to time.

It is well known that this ABM based on herding behavior may have two different interpretations, herding interactions might be assumed to happen locally or globally. We have generalized herding interactions in respect to this dichotomy. The generalized model, with the help of novel network formation model, allows to observe what happens when interactions happen on intermediate (neither local nor global) scale. Using the generalized model we observed continuous transition from the non-extensive, characterized by q-Gaussian PDF of the population fraction, statistics to extensive, characterized by Gaussian PDF of the population fraction, statistics.

6 ABMs of the financial markets

Applicability of SDE (2.1) appears to be universal. In recent works by Gontis, Ruseckas, Kaulakys and Kononovicius it was demonstrated that by slightly modifying this SDE as well as adding some other ingredients to the stochastic model may enable reproduction of the high-frequency financial market data [134–136]. Yet the problem is that stochastic modeling itself does not provide any direct insights into microscopic origin of phenomena. Thus providing agent-based reasoning for SDE (2.1) is a rather challenging task.

In this chapter we discuss agent-based financial market setup as well as derive SDEs describing macroscopic evolution of the market. This yields an agent-based reasoning for SDE (2.1) as well as model reproducing empirical statistical properties of absolute return.

6.1 Financial market interpretation

6.1.1 Introducing price formation into Kirman's ABM

Kirman's ABM defines population dynamics in two-state agent-based system with herding interactions. In order to be able to recover financial markets observables we need to define those states in the financial market terms. In most ABMs proposed by econophysicists during the last 15 years [73] there is a common assumption that agents are of the two types: fundamentalists and chartists (sometimes referred to as noise traders). Some of the approaches, such as [93], further subdivide chartists into optimists and pessimists.

The distinction between fundamentalists and chartists arises rather naturally from the two possible extremely distinct approaches to the trading in financial markets. Some traders trade based on the released economical information about companies linked to stocks. Based on this information they estimate the true value of the stock. Other traders ignore this long term information as they try to make money fast. Namely, these traders try to anticipate the rapid changes in market moods, short term trends.

Economical information might be seen as fundamental to the market, therefore traders trading based on it might be referred to as fundamentalists. In the same

manner the value of the stock might be referred to as the fundamental price, $P_f(t)$. In the fundamentalist point of view market price, $P(t)$, given enough time, should converge towards the fundamental price. Consequently if $P_f(t) > P(t)$, then fundamentalists will expect price to grow in the future and thus they will place "buy" orders. In the opposite situation, $P_f(t) < P(t)$, fundamentalists will place "sell" orders as the price should decrease in the future. Fundamentalists' incentive to act might be assumed to be proportional to the ratio between price and value, as in the financial markets relative prices provide more information than its absolute value. Most commonly these ideas are mathematical expressed as

$$D_f(t) = X_f(t) \ln \frac{P_f(t)}{P(t)}, \tag{6.1}$$

here $D_f(t)$ is a total excess demand generated by the fundamentalists' and $X_f(t)$ gives a total number of them.

Anticipating rapid changes in the market might be compared to gamble for a short time profits. Forecasting tools, mostly based on technical analysis, are available to help traders at their gamble. Technical analysis, as opposed to fundamental analysis, is based on analyzing the market behavior related to the stock in interest. Before the computer era technical analysis was performed simply by drawing charts and looking for patterns in them, thus traders relying on technical analysis might be referred to as chartists. The selection of technical analysis tools is rather large and consequently their predictions may be wildly different. Chartists' excess demand mathematically may be expressed as

$$D_c(t) = r_0 X_c(t) \xi(t), \tag{6.2}$$

where r_0 determines the relative impact of chartist trader and $\xi(t)$ is a chartists' mood, while $X_c(t)$ gives a total number of chartists,

$$\xi(t) = \frac{X_o(t) - X_p(t)}{X_c(t)}. \tag{6.3}$$

In the above X_o is a number of chartists who have made optimistic forecast (i.e. suggesting to buy) and X_p is a number of chartists who have made pessimistic forecast (i.e. suggesting to sell).

These demands can be used to defined price via Walrassian law [220]. The original Walras law assumes that trading in the market occurs trough the market maker, who sets fair price. As fair price should stabilize the market, thus according to

the original Walras, the total demand in the market should be zero. A contemporary form Walras law relaxes this assumption by saying that market adjust itself at a certain speed β:

$$\frac{1}{P(t)}\frac{\mathrm{d}P(t)}{\mathrm{d}t} = \beta\sum_{i=1}^{N} D_i(t) = \beta\left[X_f(t)\ln\frac{P_f(t)}{P(t)} + r_0 X_c(t)\xi(t)\right], \tag{6.4}$$

$$\frac{1}{\beta N P(t)}\frac{\mathrm{d}P(t)}{\mathrm{d}t} = -x_f(t)\ln\frac{P(t)}{P_f(t)} + r_0 x_c(t)\xi(t), \tag{6.5}$$

where $x_i = X_i/N$. Assuming that total number of agents, $N = X_f(t) + X_c(t)$, (it is conserved by definition of the model) is large allows to set left hand side of equation to zero and obtain:

$$P(t) = P_f(t)\exp\left[r_0\frac{x_c(t)}{x_f(t)}\xi(t)\right]. \tag{6.6}$$

Without loss of generality let us assume that fundamental price is fixed, $P_f(t) = P_f$. Here we can introduce logarithmic relative price,

$$p(t) = \ln\frac{P(t)}{P_f}, \tag{6.7}$$

which will later on allow for a more compact notation.

Return is defined as difference between two logarithmic prices separated by some time period T. Having in mind Eq. (6.6) yields the following:

$$r_T(t) = p(t) - p(t-T) = r_0\left[\frac{x_c(t)}{x_f(t)}\xi(t) - \frac{x_c(t-T)}{x_f(t-T)}\xi(t-T)\right]. \tag{6.8}$$

Note that as the number of agents is fixed we can rewrite $x_f(t)$ in terms of $x_c(t)$: $x_f(t) = 1 - x_c(t)$. One can make adiabatic approximation of return by assuming that fundamentalist-to-chartist population dynamics are significantly slower than mood, ξ, fluctuations:

$$r_T(t) = r_0 y(t)\zeta_T(t), \tag{6.9}$$

here $y(t) = \frac{x_c(t)}{1-x_c(t)}$ is a long-term variation of return which we further refer to as modulating return (representing comparatively slow chartist-fundamentalist dynamics), and $\zeta_T(t) = \xi(t) - \xi(t-T)$ represents fast switching of the chartists' forecasts. As $\xi(t)$ process is fast, its changes may be approximated as simple, e.g., Gaussian, noise [123].

6.1.2 Introducing variable trading activity

Original Kirman model [96] assumes that agents interact at a constant rate, h. This might be true in case of an ant colony, but in the financial markets situation is quite different, the interaction rates, or in other words, trading activity noticeably vary. This variability might be accounted for by introducing macroscopic feedback function $\tau(X)$ into per agent transition rate, μ_{ij}:

$$\mu_{21}(X,N) = \sigma_1 + \frac{hX}{\tau(X)}, \quad \mu_{12}(X,N) = \frac{\sigma_2 + h(N-X)}{\tau(X)}. \tag{6.10}$$

At this point we have to assume that X represent number of chartists traders, while $N - X$ stands for the number of fundamentalists in the market. As fundamentalist traders are assumed to trade, they will switch to irrational chartist trading strategies strictly according to the plan which is represented by a fixed individual transition rate (i.e., σ_1 not being divided by $\tau(X)$).

Note that analytical treatment of Kirman's ABM does not depend on the actual form of μ_{ij} (see Section 5.2). Thus we can write down SDE for x by simply looking at Eq. (5.23):

$$\mathrm{d}\,x = \left[\varepsilon_1(1-x) - \frac{\varepsilon_2 x}{\tau(x)}\right]\mathrm{d}\,t_s + \sqrt{\frac{2x(1-x)}{\tau(x)}}\,\mathrm{d}\,W_s. \tag{6.11}$$

6.2 SDE for the modulating return

In Section 6.1 we have defined the slow component of actual returns as modulating return $y = \frac{x}{1-x}$. Using Ito variable transformation formula [119] one can obtain SDE for it:

$$\mathrm{d}\,y(x) = \left[A_x(x)\partial_x y(x) + \frac{1}{2}B_x^2(x)\partial_x^2 y(x)\right]\mathrm{d}\,t + B_x(x)\partial_x y(x)\,\mathrm{d}\,W, \tag{6.12}$$

where $A_x(x)$ and $B_x(x)$ is the old drift and diffusion functions from SDE in respect to x, Eq. (6.11), while other terms are just derivatives of y:

$$\partial_x y(x) = \frac{\mathrm{d}\,y}{\mathrm{d}\,x} = \frac{1}{1-x} + \frac{x}{(1-x)^2} = \frac{1}{1-x}(1+y), \tag{6.13}$$

$$\partial_x^2 y(x) = \frac{\mathrm{d}^2 y}{\mathrm{d}\,x^2} = \frac{2}{(1-x)^2} + \frac{2x}{(1-x)^3} = \frac{2}{(1-x)^2}(1+y). \tag{6.14}$$

By putting all of these together we obtain

$$\mathrm{d}\,y = \left[\varepsilon_1 + y\frac{2-\varepsilon_2}{\tau(y)}\right](1+y)\,\mathrm{d}\,t_s + \sqrt{\frac{2y}{\tau(y)}}(1+y)\,\mathrm{d}\,W_s. \tag{6.15}$$

It is reasonable to assume that $\tau(y) = y^{-\alpha}$, as it is well known that returns and trading activity correlate [54, 61, 221, 222]. The best correlation is reported to be achieved when trading volume is compared to squared returns, $V(r) \sim r^2$, [61]. This further suggests that $\alpha = 2$ should be a good choice.

Note that if we consider only the highest powers of y in Eq. (6.15),

$$\mathrm{d}\,y = (2-\varepsilon_2)y^{2+\alpha}\,\mathrm{d}\,t_s + \sqrt{2y^{3+\alpha}}\,\mathrm{d}\,W_s, \tag{6.16}$$

then the obtained SDE is identical to SDE (2.1). The relationship between the parameters of both SDEs are as follows:

$$\eta = \frac{3+\alpha}{2}, \quad \lambda = \varepsilon_2 + \alpha + 1. \tag{6.17}$$

The similarity between SDEs implies that PSD of y should have a frequency in range in which:

$$S(f) \sim 1/f^{\beta}, \quad \beta = 1 + \frac{\lambda - 3}{2\eta - 2} = 1 + \frac{\varepsilon_2 + \alpha - 2}{1+\alpha}. \tag{6.18}$$

Power-law PDF, of the $p(y) \sim y^{-\lambda}$ form, should also be observed.

As you can see in Figure 6.1 we are able to reproduce $1/f$ noise in three distinct cases: $\alpha = 0$ (corresponds to the original Kirman model), $\alpha = 1$ and $\alpha = 2$.

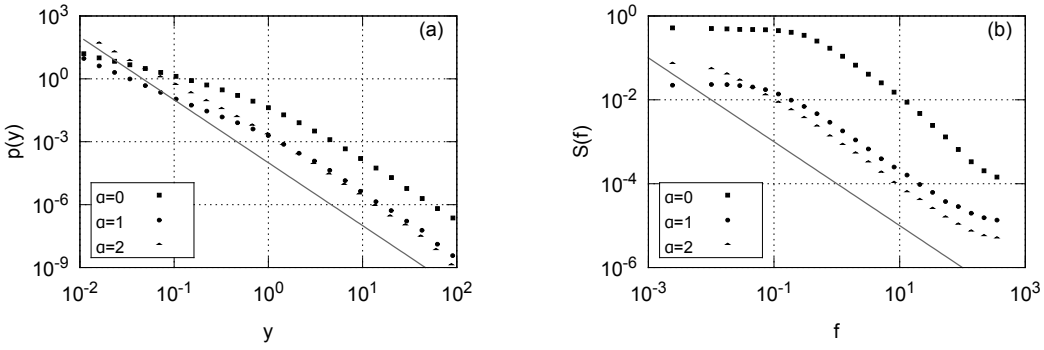

Figure 6.1: Reproducing $1/f$ noise by numerically solving Eq. (6.15) in three distinct cases – $\alpha = 0$ (squares), $\alpha = 1$ (circles) and $\alpha = 2$ (triangles). The following parameter set was used: $\varepsilon_1 = 0$, $\varepsilon_2 = 2 - \alpha$. Gray lines show expected power-law fits for (a) PDF – y^{-3}, and (b) PSD – $1/f$.

SDE (6.15) maybe also easily reduced to SDE describing a CEV process [144, 154],

$$\mathrm{d}\,x = ax\,\mathrm{d}\,t + bx^{\eta}\,\mathrm{d}\,W, \tag{6.19}$$

which is also known to provide power-law spectral densities of $1/f^{\beta}$ form with

$$\beta = 2 - \frac{1+\epsilon}{2(\eta-1)}, \tag{6.20}$$

where ϵ is arbitrary small number. By setting $\varepsilon_2 = 2$ we linearize drift function of SDE (6.15) and, for large y, obtain:

$$\mathrm{d}\,y = \varepsilon_1 y\,\mathrm{d}\,t_s + \sqrt{2y^{3+\alpha}}\,\mathrm{d}\,W_s. \tag{6.21}$$

In Figure 6.2 we show that predictions for the PSD work well in case of SDE (6.15) with $\varepsilon_2 = 2$ and $\epsilon = 0.12$.

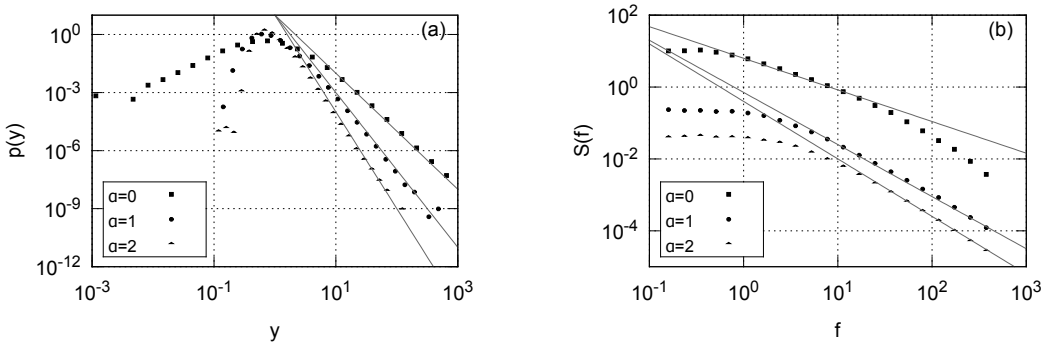

Figure 6.2: (a) PDF and (b) PSD of y obtained by numerically solving Eq. (6.15), with linearized drift function, in three distinct cases: $\alpha = 0$ (squares), $\alpha = 1$ (circles) and $\alpha = 2$ (triangles). The following parameter set was used: $\varepsilon_1 = 3$, $\varepsilon_2 = 2$. Gray lines behind the symbols provide power-law fits with exponents (a) $\lambda = 3$ (squares), $\lambda = 4$ (circles) and $\lambda = 5$ (triangles), (b) $\beta = 0.88$ (squares), $\beta = 1.45$ (circles) and $\beta = 1.6$ (triangles).

See Figure 6.3 for a highlight of possibilities to reproduce power-law PDFs and PSDs with different exponents offered by SDE Eq. (6.15).

It is important to note that similar results were previously obtained by Kirman and Teyssiere [95]. The main difference between the approaches is that Kirman and Teyssiere consider significantly more complicated version of the original herding model which cannot be treated analytically. The presense of long-range memory in absolute return time series is confirmed numerically by showing that model is capable to reproduce power-law auto-correlations. We on the other hand have proposed a simple model which we have linked to a general class of SDEs, properties of which were determined analytically.

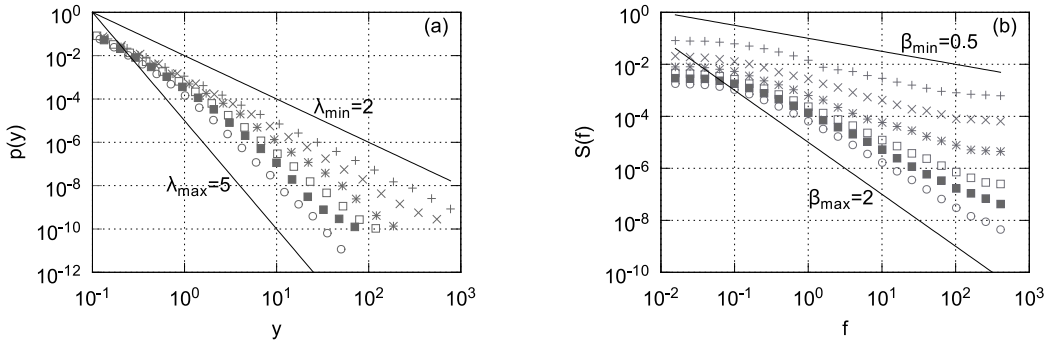

Figure 6.3: Variety of (a) PDFs and (b) PSDs with different exponents obtainable by numerically solving Eq. (6.15). Black lines represent the limiting power-law function, minimum and maximum exponent, cases with: (a) $\lambda_{min} = 2$ and $\lambda_{max} = 5$, (b) $\beta_{min} = 0.5$ and $\beta_{max} = 2$. The following parameter set was used: $\alpha = 1$, $\varepsilon_1 = 0.1$, $\varepsilon_2 = 0.1$ (plus), 0.5 (cross), 1 (star), 1.5 (open square), 2 (filled square) and 3 (open circle).

6.3 Different time scales of absolute return fluctuations

Ability to reproduce power-law statistics is great feature of the model, but in order to reproduce empirical stylized facts model needs to be more sophisticated. If mood changes, ζ, are assumed to be a simple noise, such as Gaussian, q-Gaussian or spin noise (as in [123]), then the higher frequencies of $y\zeta$ PSD become completely flat (the white noise is observed). Namely, the fracture in the model becomes too extreme (see Figure 6.4), in actual empirical data one observes that in higher frequencies PSD becomes slightly flatter (second power-law with lower exponent, see Figure 1.1). Thus assuming that ζ dynamics is just a simple noise is not sufficient to reproduce fractured PSD of absolute returns.

Recall double stochastic model discussed in Chapter 2. In the double model SDE with two exponents of multiplicativity, Eq. (2.30), was used to reproduce fracture in PSD. Due to similarity between the SDEs, we could achieve similar result by assuming specific form of $\tau(y)$ scenario. Actually by using sigmoid form of $\tau(y)$ we would obtain SDE similar to Eq. (2.30) from Kirman's ABM. But purpose is to provide microscopic (agent-based) logic for such choice.

6.3.1 Three-state ABM

To obtain a more sophisticated model chartists may be split into two groups: optimists and pessimists. These two groups may interact both among themselves

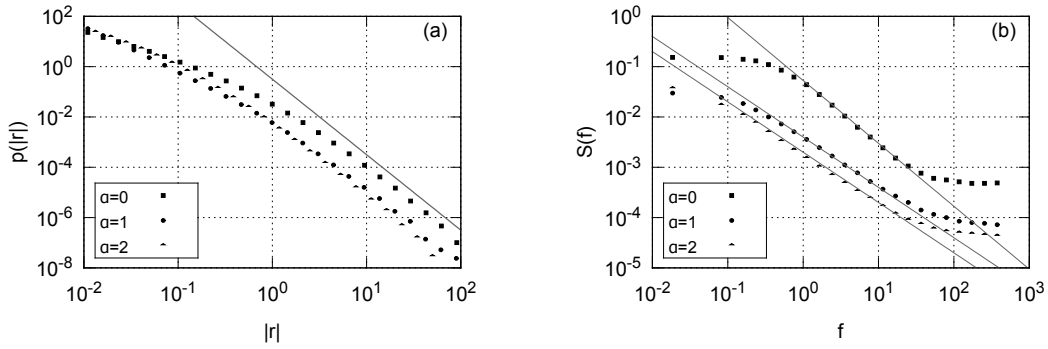

Figure 6.4: Statistical properties, (a) PDF and (b) PSD, of $r = y\zeta$ time series obtained numerically by solving Eq. (6.15) and applying q-Gaussian noise ($\zeta_0 = 1$ and $\lambda = 5$). The following parameter set was used: $\alpha = 0$ (squares), $\alpha = 1$ (circles) and $\alpha = 2$ (triangles), $\varepsilon_1 = 0$ (all cases), $\varepsilon_2 = 2 - \alpha$ (all cases). Gray lines show power-law fits: x^{-3} for PDF (a), and $1/f^{1.25}$ (line behind the squares), $1/f$ (lines behind the circles and the triangles) of PSD (b).

as well as with fundamentalists. This effectively brings us from a two-state herding model, Figure 5.1, to a three-state herding model, Figure 6.5 (a). The three-state model may be greatly simplified by using adiabatic approximation reducing model to what is seen in Figure 6.5 (b), but lets do this step by step.

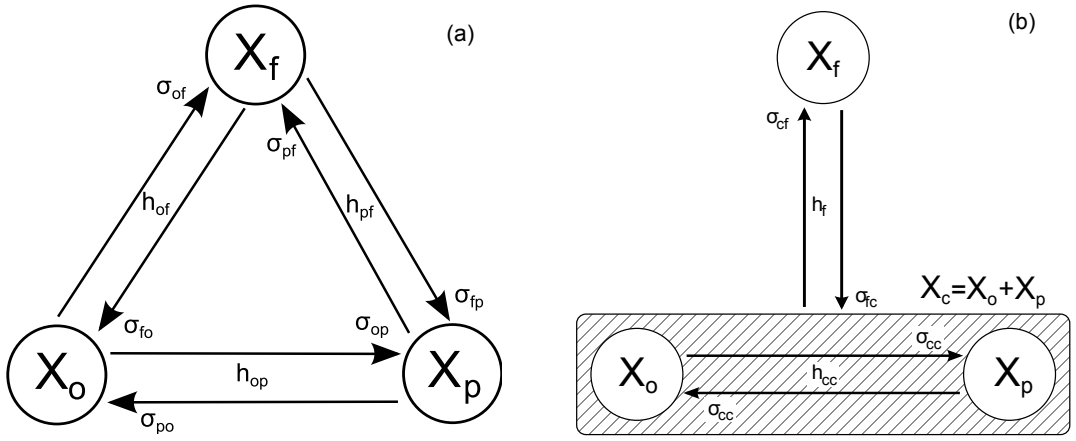

Figure 6.5: Schematic representation of the three-state model in (a) full and (b) simplified form. The arrows point in the directions of the possible transitions, note that they can be grouped into three pairs. In our modelic setup each of the transition pairs is modeled using the original Kirman's model. The relevant parameters are grouped around the corresponding pairs of arrows.

As can be seen in Figure 6.5 (a) in the three-state case we have total of six possible one step transition probabilities. In general form we can write all of these transition probabilities as:

$$p(X_i + 1, X_j - 1, X_k) = X_j(\sigma_{ji} + h_{ji}X_i)\Delta t, \tag{6.22}$$

where i, j and k subscript might take any distinct value from the set $\{f, o, p\}$. Recall that herding behavior itself is considered to be a property intrinsic to agents and not to the state, thus herding parameters are symmetric, $h_{ij} = h_{ji}$. This is important to note as there is a group of researchers examining consequences of asymmetric herding behavior [202, 203].

6.3.2 Analytical treatment of the three-state ABM

As total number of agents is fixed, $N = X_f + X_o + X_p$, one can describe three state system using two-dimensional state vector, $\{X_f, X_o\}$. Let us assume that N is large enough to secure continuity of $x_i = \frac{X_i}{N}$. Then we can introduce continuous transition probability, $\pi^{i,j}(x_f, x_o)$:

$$p(X_f + i, X_o + j, X_p + k) = N^2 \pi^{i,j}(x_f, x_o)\Delta t. \tag{6.23}$$

In the above i, j and k stand for the change of each state's occupation. As we consider only one step transition probabilities, then i, j and k must take distinct values from the set $\{-1, 0, 1\}$. Consequently, $i + j + k = 0$ holds true and vector of change, $\{i, j, k\}$, can be fully described by only two of its components $\{i, j\}$.

The transition probabilities imply the master equation for the probability to find the system in the state $\{x_f, x_o\}$ at given time t, $p(x_f, x_o, t)$:

$$\partial_t p = \sum_{i \neq j} \left(\mathbf{E}^{i,j} - 1 \right) \pi^{-i,-j} p, \tag{6.24}$$

here the sum runs over non-equal i and j which take values from the set $\{-1, 0, 1\}$. In the above we have generalized original one-dimensional one step operator for the two-dimensional case:

$$\mathbf{E}^{i,j}[f(x, y)] = f(x + i\Delta x, y + j\Delta y), \tag{6.25}$$

here i and j obey the same rule as previously, while Δx and Δy are the smallest possible increments of x and y respectively.

Expanding the two variable one step operator using the Taylor series in the limit of small increments and keeping terms up to the second order terms, allows us to rewrite Eq. (6.24) as a Fokker–Plank equation:

$$\partial_t \omega = -\sum_i \partial_{x_i} \left[D_i^1 \omega \right] + \sum_{i,j} \partial_{x_i} \left\{ \partial_{x_j} \left[D_{ij}^2 \omega \right] \right\}, \tag{6.26}$$

where i and j belong to the set $\{f, o\}$, and

$$D_f^1 = \sigma_{of} x_o + \sigma_{pf}(1 - x_o - x_f) - (\sigma_{fo} + \sigma_{fp}) x_f, \tag{6.27}$$

$$D_o^1 = \sigma_{fo} x_f + \sigma_{po}(1 - x_o - x_f) - (\sigma_{of} + \sigma_{op}) x_o, \tag{6.28}$$

$$D_{ff}^2 = h_{fo} x_f x_o + h_{fp} x_f (1 - x_o - x_f), \tag{6.29}$$

$$D_{oo}^2 = h_{fo} x_f x_o + h_{op} x_o (1 - x_o - x_f), \tag{6.30}$$

$$D_{of}^2 = D_{fo}^2 = -h_{fo} x_f x_o. \tag{6.31}$$

The Fokker–Plank equation, Eq. (6.26), can be greatly simplified by making a rather straightforward notion that there is no qualitative difference between the optimism and pessimism:

$$\begin{aligned} &\sigma_{op} = \sigma_{po} = \sigma_{cc}, \quad \sigma_{fo} = \sigma_{fp} = \sigma_{fc}/2, \quad \sigma_{of} = \sigma_{pf} = \sigma_{cf}, \\ &h_{fo} = h_{fp} = h_{fc} = h_1, \quad h_{op} = h_{cc} = H h_1. \end{aligned} \tag{6.32}$$

Further simplifications may be done by recalling the previous assumption that chartists switch between the pessimism and optimism extremely fast (adiabatic approximation):

$$H \gg 1, \quad \sigma_{cc} \gg \sigma_{cf}, \quad \sigma_{cc} \gg \sigma_{fc}, \tag{6.33}$$

where H is a transition intensity ratio between h_{cc} and h_{fc}. Under these assumptions the terms of Eq. (6.26) may be simplified to the following form:

$$D_f^1 = \sigma_{cf}(1 - x_f) - \sigma_{fc} x_f, \tag{6.34}$$

$$D_o^1 \approx \sigma_{cc}(1 - x_f - 2x_o), \tag{6.35}$$

$$D_{ff}^2 \approx h_1 (1 - x_f) x_f, \tag{6.36}$$

$$D_{oo}^2 \approx H h_1 x_o (1 - x_f - x_o) + h_1 x_f x_o, \tag{6.37}$$

$$D_{of}^2 = D_{fo}^2 \approx -h_1 x_f x_o. \tag{6.38}$$

The dynamics described by a Fokker–Plank equation, Eq. (6.26), may be also described as a set of two SDEs.

In general case a set of SDEs may be written as vector equation

$$\mathrm{d}\vec{x} = \vec{A}\,\mathrm{d}t + [\mathbf{B} \cdot \mathrm{d}\vec{W}], \tag{6.39}$$

with the state vector $\vec{x}$, vector of the drift functions $\vec{A}$, matrix of the diffusion functions **B**, and the vector of Brownian motion $\vec{W}$. While $\vec{A}$ are straightforwardly related to the first order terms of the Fokker–Plank equation, D_i^1, the problem lies in the relation between **B** and the second order terms of the Fokker–Plank equation, D_{ij}^2. It is known that they are related as [117]

$$D_{ij}^2 = \frac{1}{2}\sum_k B_{ik}B_{jk}, \quad \forall i,j, \tag{6.40}$$

but this relation provides us with only three linearly independent equations. We arbitrarily introduce forth equation into our system by requiring that our **B** would be symmetric:

$$2D_{ff}^2 = 2h_1(1-x_f-x_o)x_f + 2h_1x_fx_o = B_{ff}^2 + B_{fo}^2, \tag{6.41}$$

$$2D_{oo}^2 = 2Hh_1x_o(1-x_f-x_o) + 2h_1x_fx_o = B_{oo}^2 + B_{of}^2, \tag{6.42}$$

$$2D_{fo}^2 = 2D_{of}^2 = -2h_1x_fx_o = B_{of}B_{ff} + B_{oo}B_{fo}, \tag{6.43}$$

$$B_{fo} = B_{of}. \tag{6.44}$$

Solving the above explicitly might be somewhat problematic, thus let us solve the above by guessing mathematical form of the solutions,

$$B_{ff} = \sqrt{\mathcal{A}-C}, \quad B_{oo} = \sqrt{\mathcal{B}-C}, \quad B_{fo} = \sqrt{\mathcal{D}+C}. \tag{6.45}$$

The "guessed" form is inspired by the two-state model. Also note that with this "guess" the first two equations are solved immediately. Namely, from them we obtain the following:

$$\mathcal{A} = 2h_1x_f(1-x_f-x_o), \tag{6.46}$$

$$\mathcal{B} = 2Hh_1x_o(1-x_f-x_o), \tag{6.47}$$

$$\mathcal{D} = 2h_1x_fx_o. \tag{6.48}$$

The third equation needs to be solved to obtain C, but the exact answer has a very complicated form. The expression for C becomes more compact if adiabatic approximation is applied:

$$C \approx -2h_1x_fx_o. \tag{6.49}$$

Thus we have,

$$B_{ff}^2 = 2h_1 x_f(1 - x_f), \tag{6.50}$$

$$B_{oo}^2 = 2h_1 x_o(x_f + H[1 - x_f - x_o]) \approx 2Hh_1 x_o(1 - x_f - x_o), \tag{6.51}$$

$$B_{fo} \approx 0, \tag{6.52}$$

and the set of SDEs takes the following form

$$\mathrm{d}\, x_f = [(1 - x_f)\sigma_{cf} - x_f\sigma_{fc}]\,\mathrm{d}\, t + \sqrt{2h_1 x_f(1 - x_f)}\,\mathrm{d}\, W_1, \tag{6.53}$$

$$\mathrm{d}\, x_o = (1 - x_f - 2x_o)\sigma_{cc}\,\mathrm{d}\, t + \sqrt{2Hh_1 x_o(1 - x_f - x_o)}\,\mathrm{d}\, W_2. \tag{6.54}$$

The obtained set of SDEs is rather unwieldy, because the second SDE involves x_f which can only be obtained by solving the first SDE. SDEs might be decoupled by considering mood, ξ, as alternative variable instead of x_o. Variable substitution, which should be done in the Fokker–Planck equation (6.26), leads to the following set of decoupled SDEs:

$$\mathrm{d}\, x_f = [(1 - x_f)\sigma_{cf} - x_f\sigma_{fc}]\,\mathrm{d}\, t + \sqrt{2h_1 x_f(1 - x_f)}\,\mathrm{d}\, W_1, \tag{6.55}$$

$$\mathrm{d}\,\xi = -2\xi\sigma_{cc}\,\mathrm{d}\, t + \sqrt{2Hh_1(1 - \xi^2)}\,\mathrm{d}\, W_2. \tag{6.56}$$

6.3.3 Variable trading activity in the three-state ABM

The final ingredient is to include variable trading activity. We have already done this with the two-state model back in Section 6.1.2. At that time we assumed that chartist switching behavior is affected by the trading activity, τ function, and fundamentalists' idiosyncratic switching rate, σ_{fc}, is not. This assumption might be kept as is, but the form of τ function might be changed to reflect the more detailed information about the system available in the three-state model. Namely, we can now include chartist mood, ξ, into τ:

$$\tau(x_f, \xi) = \frac{1}{1 + \left|\frac{1-x_f}{x_f}\xi\right|^\alpha} = \frac{1}{1 + |p|^\alpha}. \tag{6.57}$$

The final form of SDEs including variable trading activity is given by:

$$\mathrm{d}\,x_f = \left[\frac{(1-x_f)\varepsilon_{cf}}{\tau(x_f,\xi)} - x_f\varepsilon_{fc}\right]\mathrm{d}\,t_s + \sqrt{\frac{2x_f(1-x_f)}{\tau(x_f,\xi)}}\,\mathrm{d}\,W_{s,1}, \tag{6.58}$$

$$\mathrm{d}\,\xi = -\frac{2\xi H\varepsilon_{cc}}{\tau(x_f,\xi)}\,\mathrm{d}\,t_s + \sqrt{\frac{2H(1-\xi^2)}{\tau(x_f,\xi)}}\,\mathrm{d}\,W_{s,2}, \tag{6.59}$$

here we have introduced scaled time $t_s = h_1 t$ as well as scaled model parameters: $\varepsilon_{cf} = \frac{\sigma_{cf}}{h_1}$, $\varepsilon_{fc} = \frac{\sigma_{fc}}{h_1}$, $\varepsilon_{cc} = \frac{\sigma_{cc}}{Hh_1}$. By numerically solving these SDEs we obtain fractured PSD of the absolute return, defined as modulus of Eq. (6.8), see Figure 6.6.

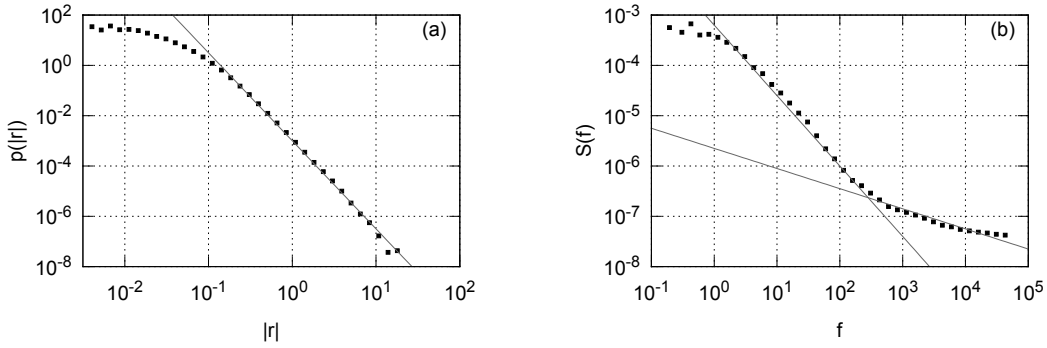

Figure 6.6: PDF (a) and PSD (b) of absolute return, defined as modulus of Eq. (6.8), numerically calculated from the three-state ABM. The squares represent the numerical results obtained by solving a system of SDEs (6.58) and (6.59). Model parameters were set as follows: $\varepsilon_{cf} = \varepsilon_{fc} = \varepsilon_{cc} = 3$, $H = 100$, $r_0 = 1$, $\alpha = 2$. The gray curves provide power-law fits: (a) $\lambda = 3.5$, (b) $\beta_1 = 1.4$ and $\beta_2 = 0.4$.

In Figure 6.6 we have shown that numerical solutions of the SDEs (6.58) and (6.59) results in fractured PSD of the absolute return. Though the power-law exponents, β_1 as well as β_2, of the numerically obtained PSD are noticeably larger than those observed in the empirical data.

6.4 Incorporating the exogenous noise

Let us recall the basic idea behind the ARCH family models (see Section 4.1): certain, heteroskedastic, economical observables might be modeled as two different processes [19, 169–175]. One of these processes, volatility process, describes comparatively long term dynamics, while the second process is just an instantaneous fluctuations, noise. Similarly we may see the three-state ABM dynamics as comparatively longer term process which shapes market volatility at a given time, while exogenous

noise accounts for various minute instantaneous factors. Similarly as it is done in ARCH family models we assume that return over given time interval, T, is given by:

$$r_T(t) = b(t)\{1 + a|p(t)|\}\zeta_q, \tag{6.60}$$

where ζ_q is a q-Gaussian noise (with zero mean and unit variance), parameter a allows to adjust the influence of endogenous three-state ABM dynamics on the observed return and $b(t)$ will be discussed in the next section (at this point one may use $b(t) = 1$). In general case variance of ζ_q should depend on return time window, T, but due to normalization procedure applied to the empirical and model data the dependence might be neglected. Empirical analysis as well as numerical modeling performed in [135, 136] shows that power-law tail of the exogenous noise should be $\lambda = 5$ (this implies $q = 1.4$), while ARCH family models frequently use Gaussian noise (which would imply $q = 1$).

As you can see in Figure 6.7 q-Gaussian noise provides good fit to the empirical PDF which appears to be better than the fit provided by the model with Gaussian noise, Figure 6.8. To show case universality of the model we also compare the numerical results, those with q-Gaussian noise, to the empirical data from smaller stock exchanges: Warsaw, Figure 6.9, and Vilnius, Figure 6.10. The obtained fits are reasonable, having in mind that discreteness effects are far stronger in smaller stock exchanges. The observed differences might be blamed on a simple fact, that "empty" time windows become more probable the smaller stock exchange is.

6.5 Introducing intra-day seasonality

It is rather straightforward to take another discrepancy (in comparison with empirical data) into account. Note that empirical PSD have spikes which coincide with the length of trading session in the respective stock exchanges. E.g., NYSE had a fixed trading session length throughout whole data set, equal to 390 minutes. The first spike appears at frequency corresponding to this period. Let us assume the following form of intra-day pattern and include them into $b(t)$ which is present in Eq. (6.60):

$$b(t) = \exp\left[-\frac{(\{t \mod 390\} - 195)^2}{w^2}\right] + 0.5, \tag{6.61}$$

where $w = 20$ quantifies the width of intra-day activity burst (spike in the PSD).

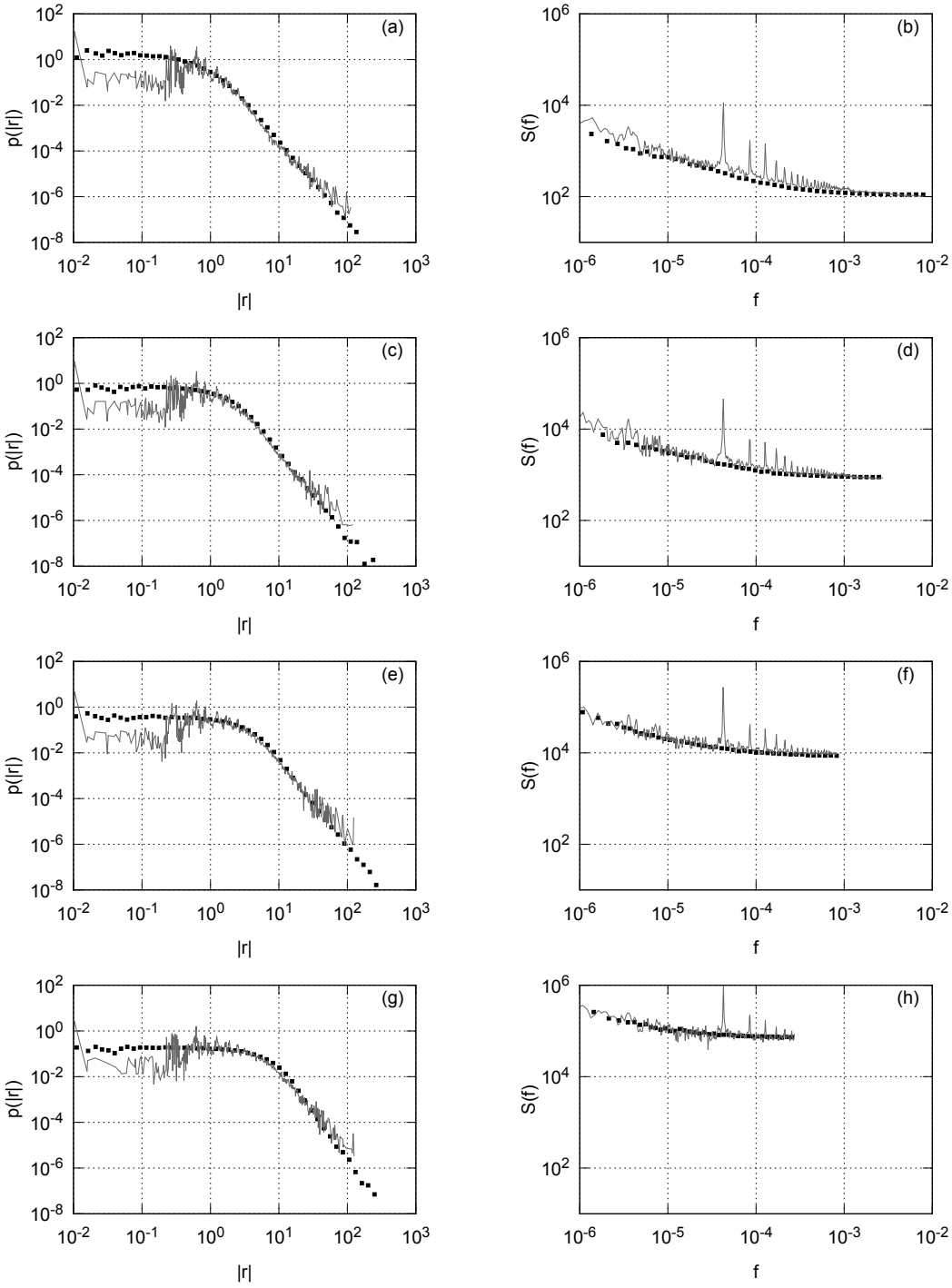

Figure 6.7: PDF and PSD of the absolute return time series for selected NYSE stocks (BMY, GM, MO, T). Empirical PDFs and PSDs (gray curves) compared to model PDFs and PSDs (black squares) in different return time windows, T: (a) and (b) 1 minute; (c) and (d) 3 minutes; (e) and (f) 10 minutes; (g) and (h) 30 minutes. Model parameters are as follows: $\varepsilon_{cf} = 0.1$, $\varepsilon_{fc} = 3$, $\varepsilon_{cc} = 3$, $H = 300$, $h = 10^{-8}s^{-1}$, $\alpha = 2$, $a = 0.5$, $\lambda = 5$ (q-Gaussian noise with $q = 1.4$ is used).

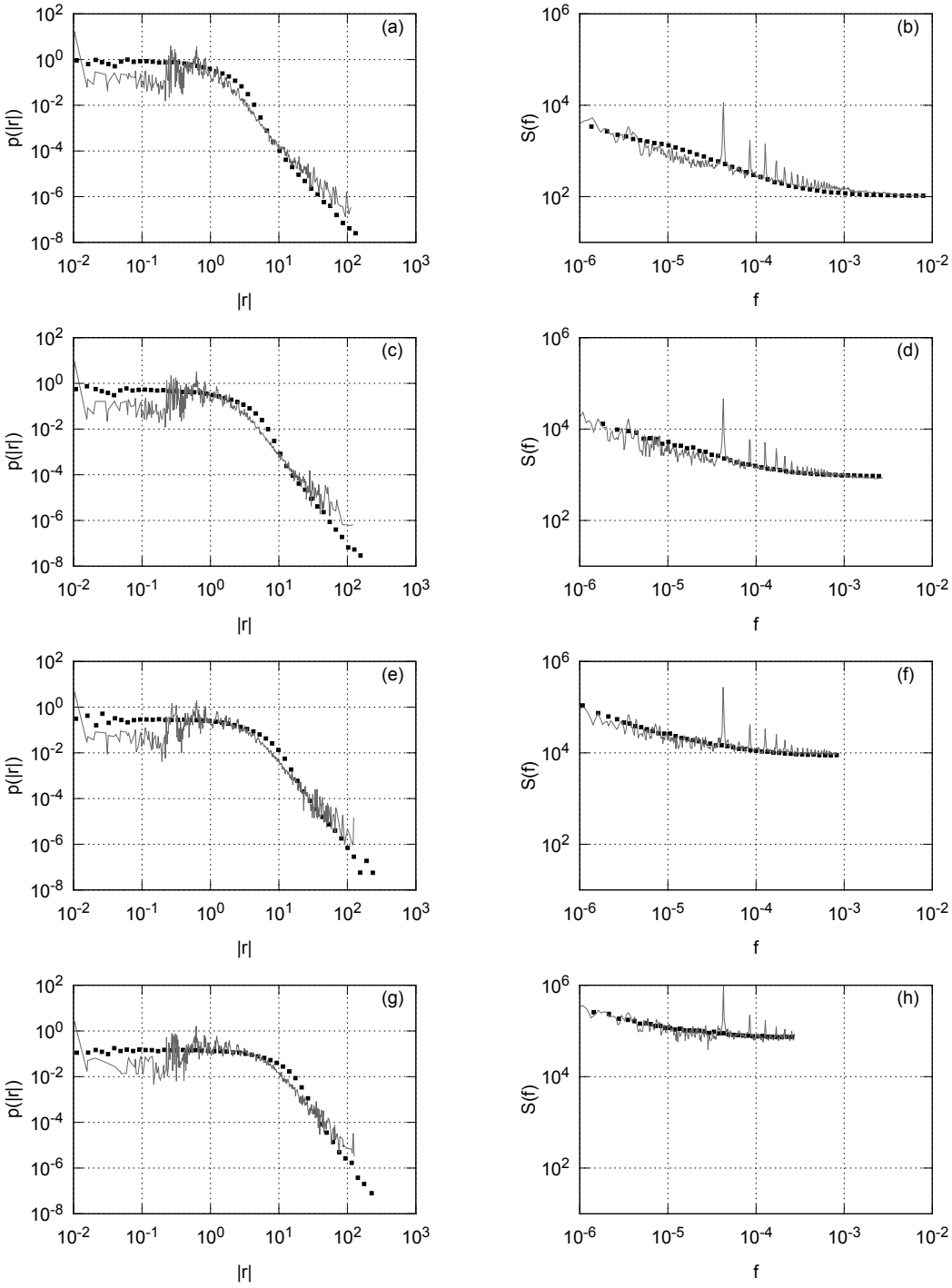

Figure 6.8: PDF and PSD of the absolute return time series for selected NYSE stocks (BMY, GM, MO, T). Empirical PDFs and PSDs (gray curves) compared to model PDFs and PSDs (black squares) in different return time windows, T:(a) and (b) 1 minute; (c) and (d) 3 minutes; (e) and (f) 10 minutes; (g) and (h) 30 minutes. Model parameters are as follows: $\varepsilon_{cf} = 0.1$, $\varepsilon_{fc} = 3$, $\varepsilon_{cc} = 3$, $H = 300$, $h = 10^{-8}s^{-1}$, $\alpha = 2$, $a = 0.5$, $q = 1$ (Gaussian noise is used).

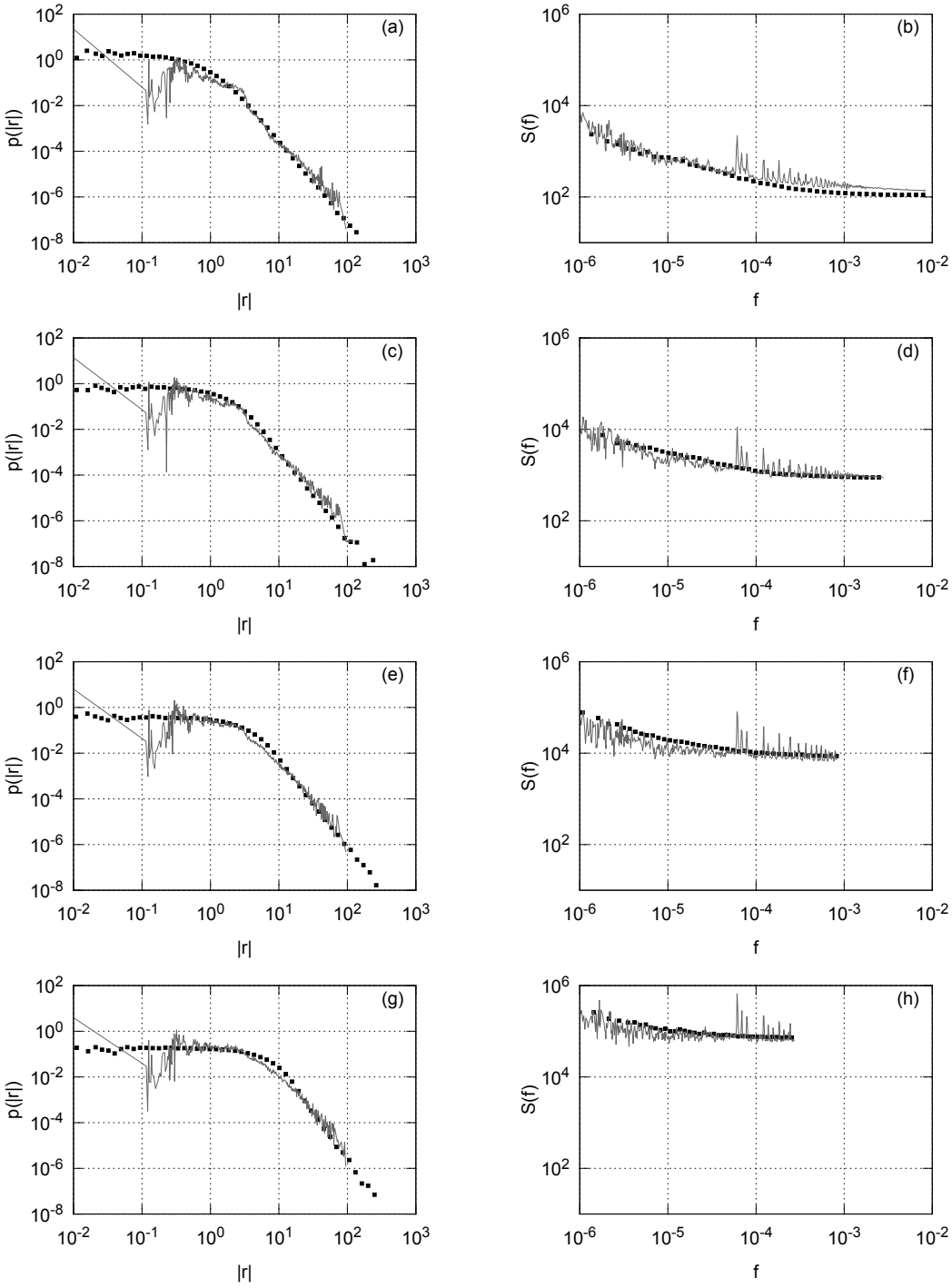

Figure 6.9: PDF and PSD of the absolute return time series for selected WSE stocks (KGHM, PZU, TPSA). Empirical PDFs and PSDs (gray curves) compared to model PDFs and PSDs (black squares) in different return time windows, T: (a) and (b) 1 minute; (c) and (d) 3 minutes; (e) and (f) 10 minutes; (g) and (h) 30 minutes. Model parameters are the same as in Figure 6.7.

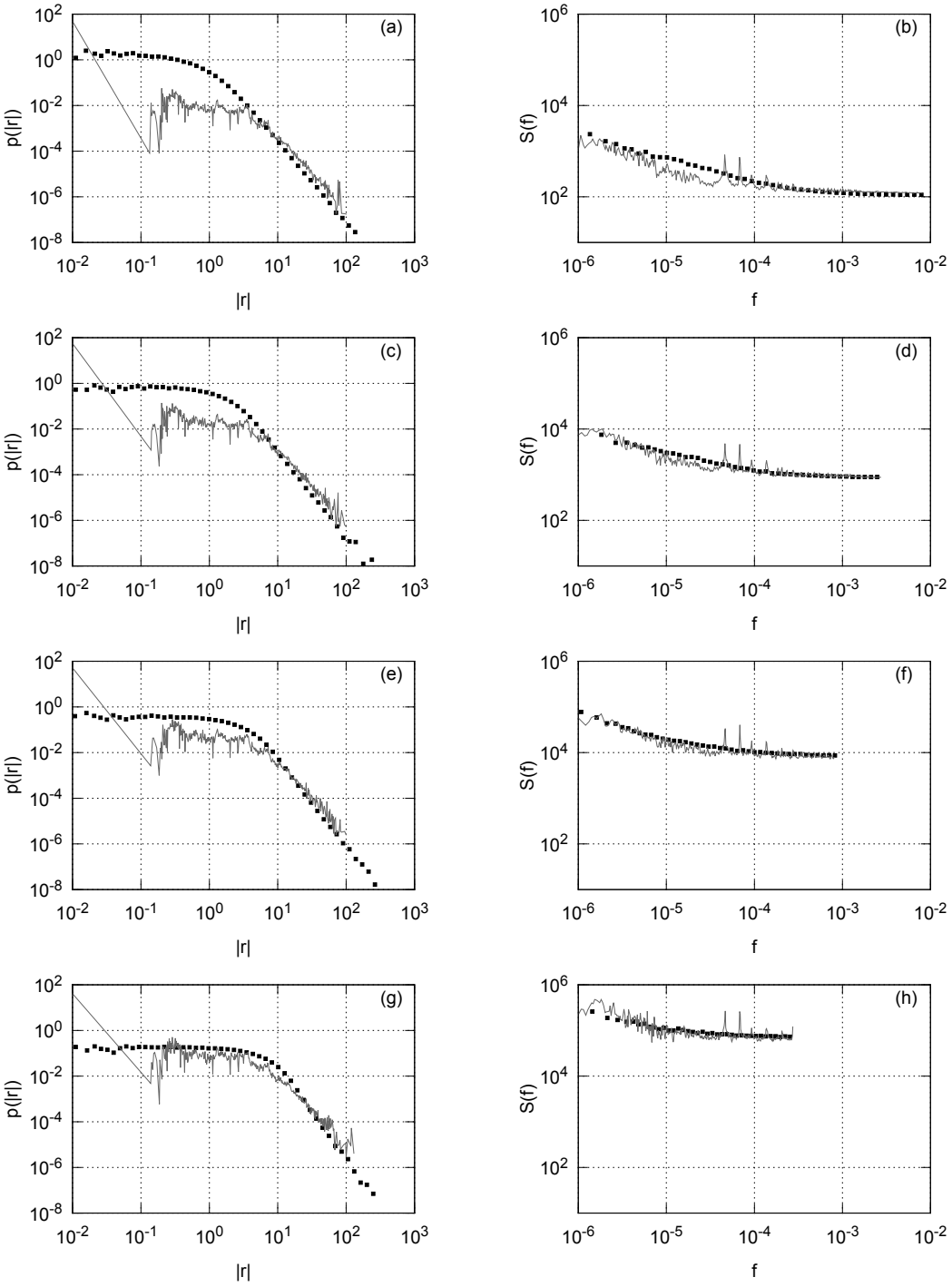

Figure 6.10: PDF and PSD of the absolute return time series for selected VSE stocks (APG1L, IVL1L, PTR1L, SAB1L, TEO1L). Empirical PDFs and PSDs (gray curves) compared to model PDFs and PSDs (black squares) in different return time windows, T: (a) and (b) 1 minute; (c) and (d) 3 minutes; (e) and (f) 10 minutes; (g) and (h) 30 minutes. Model parameters are the same as in Figure 6.7.

Note that, here time is measured in minutes. The further improved fit of the PSD is shown in Figure 6.11.

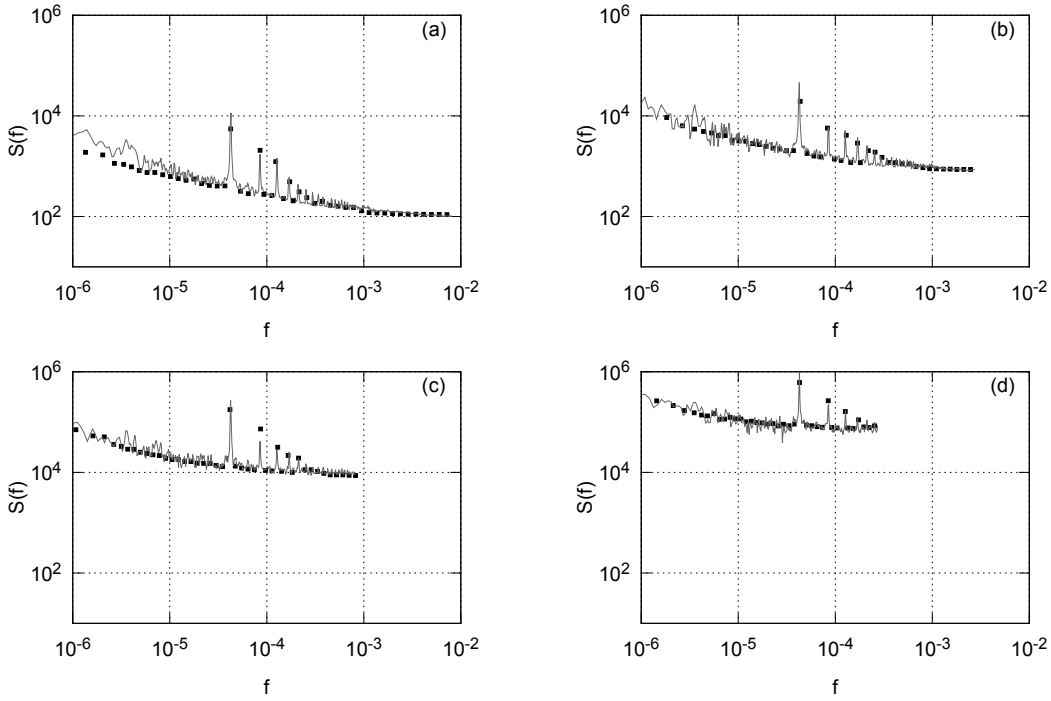

Figure 6.11: PSD of the absolute return time series for selected NYSE stocks (BMY, GM, MO, T). Empirical PSDs (gray curves) compared to model PSDs (black squares) in different return time windows, T: (a) 1 minute; (b) 3 minutes; (c) 10 minutes; (d) 30 minutes. Model parameters are the same as in Figure 6.7, $b(t)$ dependence changes according to Eq. (6.61).

6.6 Summary

In this chapter we have considered financial market interpretation based on the ABM based on herding behavior. First we discussed interpretation of the ABM based on herding behavior in terms of the financial markets. This discussion enabled us to relate certain economical variables to the endogenous population dynamics of the ABM. We have started our analysis from the simpler model for the long-term component of absolute return, so-called modulating return. The obtained SDE for the modulating return, Eq. (6.15), belongs to the general class of SDEs reproducing power-law PDF and PSD, Eq. (2.1). Thus the two-state ABM can be seen as providing agent-based reasoning, from the financial market perspective, to the aforementioned class of SDEs.

In this chapter we have also extended ABM based on herding behavior to in-

clude three state dynamics which happen on two distinct event time scales. The three-state ABM is able to generate time series with fractured PSD of absolute return. Though the exponents of the PSD were larger than those observed in the empirical time series.

Considering endogenous three-state ABM population dynamics as a source of market volatility allows to introduce exogenous noise into the model. The exogenous noise is able to decrease exponents of fractured PSD to match those observed in the empirical absolute return PSD. To show that the model is able to generate absolute return time series with the same PDF and PSD as observed in empirical data we have compared model results with three different stock exchanges: NYSE, WSE and VSE.

To reproduce spikes observed in empirical PSD we have also included intra-day seasonality into the three-state model.

7 Controlling financial fluctuations using herding interactions

Imitative behavior and peer pressure between the individuals in social systems enables a possibility for a small fraction of the system to make a significant impact on the collective behavior. The influence of the small number of individuals on the collective behavior of a crowd was studied in a series of experiments by Dyer et al. [8]. People participating in these experiments were asked to move randomly, but to stay with a crowd. Some of the people in a crowd, a small number of them, were asked to move in a certain direction. It was expected that they will be able to lead the whole crowd in that direction. The results of the experiment have shown that $4-10$ directed individuals were enough to lead the crowds of up to 200 people. It is interesting to note that the necessary number of directed individuals grows slower than the total number of people in the crowd. Consequently the movement of even larger crowds could be also controlled in a similar fashion without a further significant increase in a total number, not percentage, of the directed individuals. In the context of this dissertation we could see the directed individuals in the aforementioned experiment as the controlled individuals. Similar experiments were preformed with animals by using controlled robots [9].

The success behind these experiments encourage theoretical understanding of the possibilities to control socio-economic systems. As such understanding might suggest new policy making tools which could prevent disastrous events occurring simply due to endogenous interactions. From a mathematical point of view these ideas were tested in papers by Schweitzer et al. [133] as well as Biondo et al. [132, 223,224]. Schweitzer et al. considered the problem from the well-known Prisonner's Dilemma setup, while Biondo et al. relied on a generic earthquake, Olami-Feder-Christensen, model. While we approach from the perspective of a model which is able to reproduce main statistical features of actual empirical data of the financial markets.

7.1 Control of the two-state model

Let us start by introducing the controlled agents into the original Kirman's model discussed in Chapter 5. Suppose that we have M agents, whose choice of the

state is controlled externally, into the Kirman's model. Namely, unlike the ordinary agents, the controlled agents do not switch their state due to endogenous interactions, though they are able to trigger endogenous switches of the ordinary agents.

As we have discussed in Chapter 5 the agents may interact either locally or globally. If the interaction is local, then the herding terms disappear or become negligible in the macroscopic description of the system with large number of agents. In order for the controlled agents to make a significant impact on a whole macroscopic system they have to interact globally. In such case, depending on how the ordinary agents interact we have two set of the one-step transitions probabilities: one analogous to Eq. (5.5) (global interaction case),

$$\mu_{21}(X,N) = \sigma_1 + h(M_1 + X), \tag{7.1}$$

$$\mu_{12}(X,N) = \sigma_2 + h(N - X + M - M_1), \tag{7.2}$$

and other analogous to Eq. (5.6) (local interaction case),

$$\mu_{21}(N,X) = \sigma_1 + \frac{hX}{N} + hM_1, \tag{7.3}$$

$$\mu_{12}(N,X) = \sigma_2 + \frac{h(N-X)}{N} + h(M - M_1). \tag{7.4}$$

In the above expressions of μ_{ij} M_1 is a number of the controlled agents ($M_1 \leq M$) in the state which is occupied by X ordinary agents. From a purely mathematical point of view the influence of the controlled agents can be included into the individual behavior parameters, σ_i. Namely, one can set $\tilde{\sigma}_1 = \sigma_1 + hM_1$ and $\tilde{\sigma}_2 = \sigma_2 + h(M - M_1)$ to return to the original form of the herding model with shifted individual preferences, $\tilde{\sigma}_i$.

Similar approaches may be found in [202, 203, 211]. In [202, 203] the external forces are assumed to drive the periodic fluctuations of the herding behavior parameter, while in our case the controlled agents act on individual behavior parameters. In [211] a case where small number of core agents influence behavior of large number of periphery agents is considered, while our approach does not include any hierarchy of the agents.

The macroscopic dynamics influenced by the controlled agents, in the limit

$N \to \infty$, are given by, for the global interaction case,

$$\begin{aligned} \mathrm{d}\,x = &[(\sigma_1 + hM_1)(1-x) - (\sigma_2 + h\{M - M_1\})x]\,\mathrm{d}\,t + \\ &+ \sqrt{2hx(1-x)}\,\mathrm{d}\,W, \end{aligned} \tag{7.5}$$

and, for the local interaction case,

$$\mathrm{d}\,x = [(\sigma_1 + hM_1)(1-x) - (\sigma_2 + h\{M - M_1\})x]\,\mathrm{d}\,t. \tag{7.6}$$

It should be straightforward to determine that the mean of stationary PDF of SDE (7.5), $\bar{x}$, equals the fixed point of Eq. (7.6), x_f,

$$\bar{x} = x_f = \frac{hM_1 + \sigma_1}{hM + \sigma_1 + \sigma_2}. \tag{7.7}$$

Note that the long term impact of the controlled agents depends only on their number and on the idiosyncratic transition rates of the ordinary agents. So, if controlled agents act globally, one can use a fixed number of them to influence the behavior of an infinitely large system.

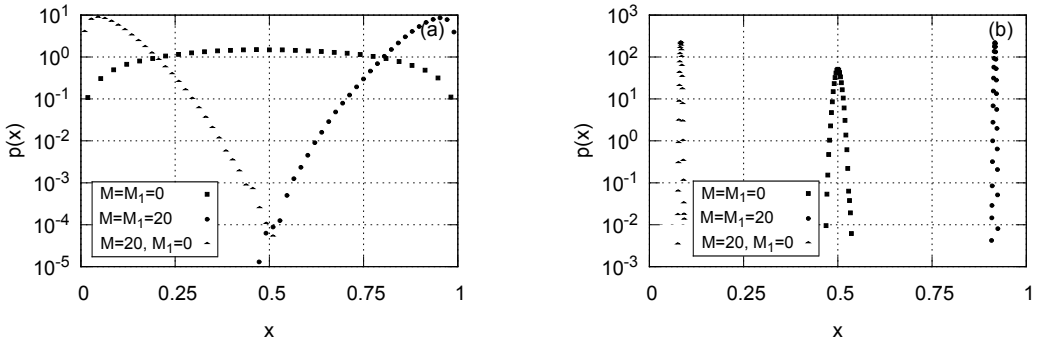

Figure 7.1: A comparison of a numerically calculated stationary PDF with no controlled agents, $M = M_1 = 0$ (squares), and stationary PDF with controlled agents, $M = M_1 = 20$ (circles) and $M = 20$ and $M_1 = 0$ (triangles), in the global interaction (a) and local interaction (b) case. Model parameters were set as follows: $\sigma_1 = \sigma_2 = 2$, $h = 1$. A stochastic model, Eq. (7.5), was used for (a) and ABM with $N = 10^4$ was used for (b).

In Figure 7.1 we numerically confirm that a fixed small number of the controlled agents ($M = 20$) enables us to significantly shift the stationary PDF of the macroscopic variable to the desired end despite the fact that the agents have strong individualistic tendencies, $\sigma_i > h$. As we can see in Figure 7.2 as few as two controlled agents are enough to significantly influence the stationary PDF of the model if herding behavior, $\sigma_i < h$, is prevalent.

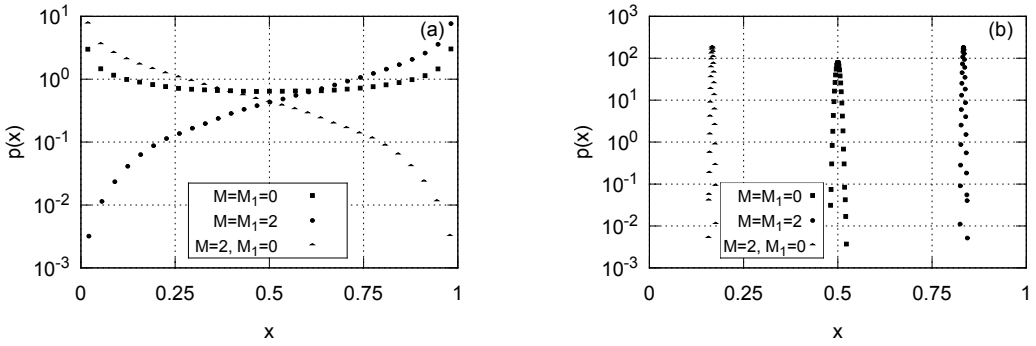

Figure 7.2: A comparison of a numerically calculated stationary PDF with no controlled agents, $M = M_1 = 0$ (squares), and stationary PDF with controlled agents, $M = M_1 = 20$ (circles) and $M = 20$ and $M_1 = 0$ (triangles), in the global interaction (a) and local interaction (b) case. Model parameters were set as follows: $\sigma_1 = \sigma_2 = 0.5$, $h = 1$. A stochastic model, Eq. (7.5), was used for (a) and ABM with $N = 10^4$ was used for (b).

An important question in this context is how fast the controlled agents are able to make the desired impact. Or namely, how fast the statistical properties of the system, PDF and mean, converge to the stationary ones. In case the ordinary agents interact locally the answer can be obtained analytically by solving corresponding ODE, Eq. (7.6). Its solution is given by:

$$x(t) = x_f + [x(0) - x_f]\exp(-[hM + \sigma_1 + \sigma_2]t), \tag{7.8}$$

here $x(0)$ is the initial condition and x_f is a fixed point of Eq. (7.6) which is given by Eq. (7.7).

It is a more complex task to solve the global interaction case, macroscopic dynamics of which is given by SDE (7.5). One would have to find the eigenvalues of the Fokker–Planck equation [117]. The problem is that the corresponding Fokker–Planck equation appears to be too complex to be dealt with analytically. A viable alternative, of course, is a numerical simulation. In Figure 7.3 we plot the results of a numerical simulation which show that the convergence times are finite for both mean and stationary PDF. Furthermore the obtained results show that the convergence of the mean is well described by Eq. (7.8), and thus the convergence in both cases happen exponentially fast.

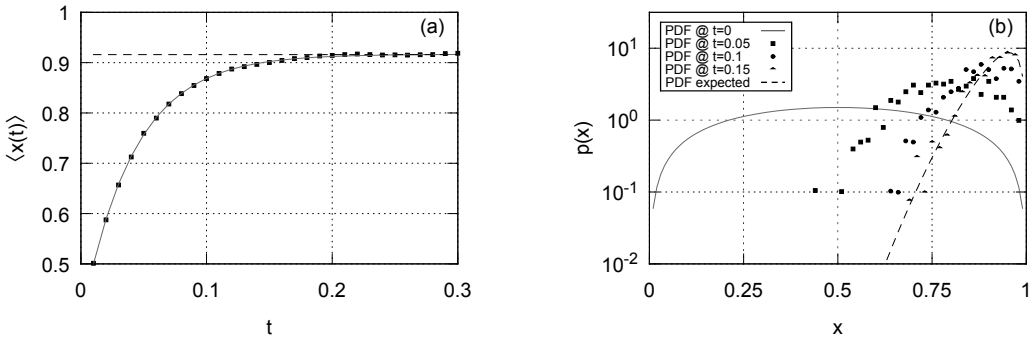

Figure 7.3: Time evolution of the mean (a) and the PDF (b) of 1000 time series obtained by numerically solving the SDE (7.5). Subfigure (a): squares represent the mean trajectory (average over ensemble of 1000 realizations), the solid curve is a plot of Eq. (7.8), while dashed line represents the expected mean. Subfigure (b): different types of points represent PDF snapshots at distinct times (squares $t = 0.05$, circles $t = 0.1$, triangles $t = 0.15$), the solid curve represents the initial condition (the PDF at $t = 0$), while dashed curve represents the expected PDF. Model parameters were set as follows: $\sigma_1 = \sigma_2 = 2$, $h = 1$, $M = M_1 = 20$.

7.2 Control of the three-state model

In previous section we have shown that even a few controlled agents are able to make significant impact on the two-state model. Thus controlling the dynamics of modulating return, see Section 6.2, is rather straightforward task from the model point of view. Implementing control in a more realistic, three-state, model is a more challenging task.

Of course it is obvious that the most effective market control method would be introduction of M agents with predefined fundamentalist trading behavior. This would increase parameter σ_{cf} by hM, or $\tilde{\varepsilon}_{cf} = \varepsilon_{cf} + M$. Observe, in Figure 7.4, that as M increases the PDF of $p(t)$ becomes narrower: larger deviations of $p(t)$ become significantly less probable and standard deviation decreases. This process may be also seen as a convergence of q-Gaussian-like (power-law asymptotic behavior) distribution towards Gaussian-like distribution (exponential asymptotic behavior), similarly to what was discussed in Section 5.3. Evidently this control strategy yields excellent results, but its main drawback is a simple fact that currently there is no conventional agreement on how to estimate fundamental price, though some approaches are being conducted by performing behavioral experiments [225–228].

The beneficial role of noise in many physical systems is widely recognized. It is a well known that certain amounts of noise allows to strengthen the actual patterns exhibited by the dynamical system [229–232]. While the idea itself is not

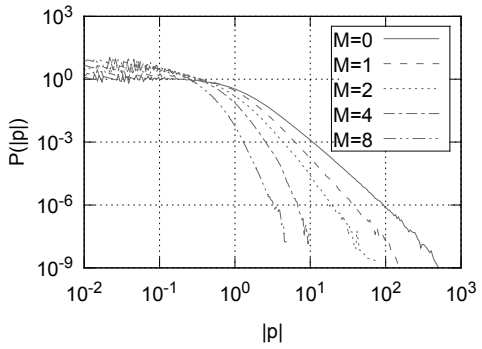

Figure 7.4: Stationary PDF of absolute log-price, $|p(t)|$, when predefined fundamentalists, $M = 0; 1; 2; 4; 8$, are present. Results were obtained by numerically solving equations Eqs. (6.58) and (6.59). Parameters were as follows: $\tilde{\varepsilon}_{cf} = 0.1 + M$, $\varepsilon_{fc} = 3$, $\varepsilon_{cc} = 3$, $H = 300$, $a = 0.5$, $\alpha = 2$.

new to physics it was just only recently applied to socio-economic systems. E.g., it was shown that random promotions might lead to more efficient hierarchical structures [233] as well as "accidental" politicians potentially improving legislature process [234]. In a couple of more recent publications this idea was applied to the financial markets. In terms of the financial markets this idea appears to be somewhat controversial as the EMH suggests that non-rational agents should be driven out from the market [235]. But the stochastic trading appears to work both as investment strategy as well as extreme event prevention strategy, at least in generic setups [132, 224]. This kind of approach would be of great value as introduction of stochastic traders, unlike fundamentalist traders, is very simple in terms of implementation. Though the realistic introduction of the stochastic agents into the three-state model, and their impact on the macroscopic behavior, is not straightforward.

The main problem is to define how the introduction of stochastic agents will impact the population dynamics between agent groups. Recall that Kirman's herding model is an ad hoc Markov process on the microscopic, individual agent, level. Agents are free of any rationality, they are assumed to have zero intelligence. Namely, they change the behavior with certain probability just in response to the contact with another agent. In the considered model this contact is equivalent to a market transaction.

Recall that we can see the three state dynamics as two independent processes (see Figure 6.5): fundamentalists-chartists process and optimists-pessimists process. As time scales of these processes are different up to three orders of magnitude we can assume them to be totally independent. In this approximation agents participate in

both two-state processes simultaneously.

We have already discussed the impact of controlled agents on the population dynamics between two agent groups. Here we apply the same logic, stochastic agents influence ordinary agents to switch to the direct opposites of the considered groups. In the slow fundamentalist-chartist process, when a fundamentalist makes a trade with a stochastic agent, he perceives stochastic agent as chartist. While, on the other hand, when a chartist makes trade with a stochastic agent, the chartist perceives stochastic agent as fundamentalist. In a similar way for the faster optimist-pessimist process, optimists perceive stochastic agents as pessimists, while pessimists perceive stochastic agents as optimists. In all cases any ordinary agent can trade with only a half of stochastic agents, those who submit opposite trade orders. Therefore in both, fast and slow, processes stochastic agents should be perceived as an additional $M/2$ agents belonging to the direct opposite of any considered group.

Mathematically the impact of stochastic agents in this setup of two independent herding processes may be formalized in the following way: $\tilde{\varepsilon}_{fc} = \varepsilon_{fc} + M/2$, $\tilde{\varepsilon}_{cf} = \varepsilon_{cf} + M/2$, $\tilde{\varepsilon}_{op} = \varepsilon_{op} + M/2$ and $\tilde{\varepsilon}_{po} = \varepsilon_{po} + M/2$. In Fig. 7.5 we demonstrate that stochastic trading has a considerable effect diminishing price deviations from the fundamental value.

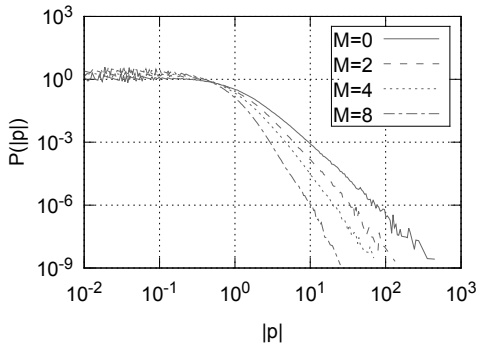

Figure 7.5: Stationary PDF of absolute log-price, $|p(t)|$, in case when stochastic traders, $M = 0; 2; 4; 8$, are assumed to have symmetric impact. Results were obtained by numerically from Eqs. (6.58) and (6.59). Parameters were set as follows: $\tilde{\varepsilon}_{cc} = 3 + M/2$ $\tilde{\varepsilon}_{fc} = 3 + M/2$, $\tilde{\varepsilon}_{cf} = 0.1 + M/2$, $H = 300$, $a = 0.5$, $\alpha = 2$.

7.3 Summary

In this chapter we have demonstrated that controlled agents are able to significantly impact the observed dynamics of the whole system. The effect may be

observed only if they interact with normal agents globally. This might be especially useful in financial market applications, were, according to the proposed model, interactions occur on global scale.

Evidently financial fluctuations are suppressed, exponents of power-law distribution decreased, if the controlled agents use fundamentalist trading strategy. Yet this is somewhat hard to implement by the policy makers as this strategy relies on economical concepts which are not clearly defined.

We have also found that financial fluctuations are suppressed, exponents of power-law distribution decreased, in the proposed three-state model , if controlled agents are trading randomly. This result is counter-intuitive and may be easily implemented by the policy makers.

8 Conclusions

1. The Bursting behavior observed in empirical a one-minute absolute return time series has a power-law nature. Statistical similar power-law dependencies were observed in the numerical time series obtained by solving Eq. (2.1) and evaluating the double stochastic model.

2. The nonlinear SDEs generating the time series exhibiting the power-law PDF and PSD, were obtained from the nonlinear modification of the GARCH(1,1) model.

3. The nonlinear SDEs generating the time series exhibiting the power-law PDF and PSD describing the long-term variability of return were obtained from ABM based on the herding behavior. The ABM was extended by considering fluctuations in agent interaction intensity.

4. Having considered the three-state ABM as a source of financial market volatility, we have obtained the financial market model generating the absolute return time series exhibiting the PDF and PSD similar to the empirical absolute return PDF and PSD.

5. Controlled agents, in the ABM based on the herding behavior, can make a significant impact on the observed dynamics, if they are allowed to interact on a global scale.

Bibliography

1. G. Akerlof, J. Shiller, *Animal Spirits: How Human Psychology Drives the Economy, and Why It Matters for Global Capitalism* (Princeton University Press, 2009).

2. J. Fox, *The Myth of the Rational Market* (HarperBusiness, 2011).

3. R. Shiller, *Finance and the Good Society* (Princeton University Press, Princeton, USA, 2012).

4. G. S. Becker, A note on restaurant pricing and other examples of social influence on price, Journal of Political Economy **99**, 1109–1116 (1991).

5. J. M. Pasteels, J. L. Deneubourg, S. Goss, Self-organization mechanisms in ant societies (I): Trail recruitment to newly discovered food sources, in J. M. Pasteels, J. L. Deneubourg (eds.), *From Individual to Collective Behaviour in Social Insects* (Birkhauser, Basel, 1987), 155–175.

6. J. M. Pasteels, J. L. Deneubourg, S. Goss, Self-organization mechanisms in ant societies (II): Learning in foraging and division of labor, in J. M. Pasteels, J. L. Deneubourg (eds.), *From Individual to Collective Behaviour in Social Insects* (Birkhauser, Basel, 1987), 177–196.

7. C. Detrain, J. L. Deneubourg, Self-organized structures in a superorganism: Do ants behave like molecules?, Physics of Life Reviews **3**, 162–187 (2006).

8. J. R. G. Dyer, A. Johansson, D. Helbing, I. D. Couzin, J. Krause, Leadership, consensus decision making and collective behaviour in humans, Phylosophical Transactions of the Royal Society B **364**, 781–789 (2009).

9. J. Krause, A. F. T. Winfield, J. L. Deneubourg, Interactive robots in experimental biology, Trends in Ecology and Evolution **26**, 369–375 (2011).

10. K. Durkin, Peer pressure, in A. S. R. Manstead, M. Hewstone (eds.), *The Blackwell Encyclopedia of Social Psychology* (Wiley–Blackwell, 1996).

11. I. Muller, *A History of Thermodynamics* (Springer, 2007).

12. J. Scott, G. Marshall, *A Dictionary of Sociology* (Oxford University Press, 2005).

13. P. Ball, The physical modelling of society: A historical perspective, Physica A **314**, 1–14 (2002).

14. C. Pellegrini, P. Cerrai, P. Freguglia (eds.), *The Application of Mathematics to the Sciences of Nature* (Springer, 2002).

15. J. Stachel (ed.), *The Collected Papers of Albert Einstein*, volume 2 (Princeton University Press, 1989).

16. S. Chandrasekhar, Marian Smoluchowski as the founder of the physics of stochastic phenomena, in *Selected Papers* (University of Chicago Press, 1989), volume 3.

17. P. H. Cootner, *The Random Character of Stock Market Prices* (MIT Press, 1964).

18. F. Black, M. Scholes, The pricing of options and corporate liabilities, Journal of Political Economy **81**, 637–654 (1973).

19. S. L. Heston, A closed-form solution for options with stochastic volatility with applications to bond and currency options, Review of Financial Studies **6**, 327–343 (1993).

20. J. Feder, *Fractals* (Plennum Press, New York, 1988).

21. H. E. Hurst, Long-term storage capacity of reservoirs, Transactions of the American Society of Civil Engineers **116**, 770–799 (1951).

22. J. P. Sethna, *Statistical Mechanics: Entropy, Order Parameters and Complexity* (Clarendon Press, Oxford, 2009).

23. E. N. Lorenz, Deterministic nonperiodic flow, Journal of the Atmospheric Sciences **20**, 130–141 (1963).

24. H. Haken, *Synergetics, an Introduction* (Springer–Verlag, New York, 1983).

25. History of complex systems research, in *Complexity Explained* (Springer–Heidelberg, Berlin, 2008), 25–55.

26. S. H. Kellert, *In the Wake of Chaos: Unpredictable Order in Dynamical Systems* (University of Chicago Press, 1993).

27. J. Persky, Retrospectives: The ethology of homo economicus, The Journal of Economic Perspectives **9**, 221–231 (1995).

28. J. Stodder, Strategic voting and coalitions: Condorcet's paradox and Ben-Gurion's tri-lemma, International Review of Economics Education **4**, 58–72 (2005).

29. W. B. Arthur, Inductive reasoning and bounded rationality, American Economic Review **84**, 406–411 (1994).

30. P. F. Drucker, *The End of Economic Man* (Transaction Publishers, Piscataway, New Jersey, 1995).

31. J. P. Bouchaud, Economics needs a scientific revolution, Nature **455**, 1181 (2008).

32. J. P. Bouchaud, The (unfortunate) complexity of the economy, Physics World **22**, 28–32 (2009).

33. J. D. Farmer, M. Gallegati, C. Hommes, A. Kirman, P. Ormerod, S. Cincotti, A. Sanchez, D. Helbing, A complex systems approach to constructing better models for managing financial markets and the economy, European Physics Journal Special Topics **214**, 295–324 (2012).

34. R. H. Nelson, *Economics as Religion: From Samuelson to Chicago and Beyond* (University Park: Pennsylvania State University Press, 2001).

35. D. Helbing, A new kind of economy is born, blog post, available at `http://www3.unifr.ch/econophysics/?q=content/new-kind-economy-born` (2013).

36. M. O. Jackson, K. Leyton-Brown, Y. Shoham, Game theory I & II, MOOCs at Coursera (2014).

37. T. Kretschmer, Competitive strategy, MOOC at Coursera (2014).

38. J. E. Hartley, *The Representative Agent in Macroeconomics* (Routledge, 1997).

39. A. Kirman, *Complex Economics: Individual and Collective Rationality* (Routledge, 2010).

40. R. Conte, N. Gilbert, G. Bonelli, C. Cioffi-Revilla, G. Deffuant, J. Kertesz, V. Loreto, S. Moat, J. P. Nadal, A. Sanchez, A. Nowak, A. Flache, M. San Miguel, D. Helbing, Manifesto of computational social science, European Physics Journal Special Topics **214**, 325–346 (2012).

41. S. Havlin, D. Y. Kenett, E. Ben-Jacob, A. Bunde, R. Cohen, H. Hermann, J. W. Kantelhardt, J. Kertesz, S. Kirkpatrick, J. Kurths, J. Portugali, S. Solomon, Challenges in network science: Applications to infrastructures, climate, social systems and economics, European Physics Journal Special Topics **214**, 273–293 (2012).

42. D. Helbing, Introduction: The FuturICT knowledge accelerator towards a more resilient and sustainable future, European Physics Journal Special Topics **214**, 5–9 (2012).

43. M. San Miguel, J. H. Johnson, J. Kertesz, K. Kaski, A. Diaz-Guilera, R. S. MacKay, V. Loreto, P. Erdi, D. Helbing, Challenges in complex systems science, European Physics Journal Special Topics **214**, 245–271 (2012).

44. V. Pareto, *Manual of Political Economy (Manuale di Economia Politica)* (Kelley, New York, 1971), translated by A. S. Schwier and A. N. Page.

45. L. Amoroso, Vilfredo Pareto, Econometrica **6**, 1–21 (1938).

46. N. Bunkley, Joseph Juran, 103, pioneer in quality control, dies, New York Times (2008).

47. P. Levy, *Calcul des Probabilites* (Gauthier–Villars, Paris, 1925).

48. H. E. Stanley, *Introduction to Phase Transitions and Critical Phenomena* (Oxford University Press, 1971).

49. B. B. Mandelbrot, *The Fractal Geometry of Nature* (W. H. Freeman, San Francisco, 1982).

50. P. Bak, C. Tang, K. Wiesenfeld, Self-organized criticality, Physical Review Letters **59**, 381–384 (1987).

51. A. L. Barabasi, M. Newman, D. J. Watts, *The Structure and Dynamics of Networks* (Princeton University Press, 2006).

52. A. Chakraborti, I. M. Toke, M. Patriarca, F. Abergel, Econophysics review: I. Empirical facts, Quantitative Finance **7**, 991–1012 (2011).

53. R. Cont, M. Potters, J. Bouchaud, Scaling in stock market data: Stable laws and beyond, in B. Dubrulle, F. Graner, D. Sornette (eds.), *Scale Invariance and Beyond* (Springer, 1997).

54. X. Gabaix, P. Gopikrishnan, V. Plerou, H. E. Stanley, A theory of power law distributions in financial market fluctuations, Nature **423**, 267–270 (2003).

55. X. Gabaix, Power laws in economics and finance, Annual Review of Economics **1**, 255–293 (2009).

56. T. Lux, M. Ausloos, Market fluctuations I: Scaling, multi-scaling and their possible origins, in A. Bunde, J. Kropp, H. Schellnhuber (eds.), *The Science of Disasters: Climate Disruptions, Heart Attacks, and Market Crashes* (Springer, 2002), 372–409.

57. M. Karsai, K. Kaski, A. L. Barabasi, J. Kertesz, Universal features of correlated bursty behaviour, NIH Scientific Reports **2**, 397 (2012).

58. D. Kondor, M. Posfai, I. Csabai, G. Vattay, Do the rich get richer? An empirical analysis of the bitcoin transaction network, PLoS ONE **9**, e86197 (2014).

59. D. R. Parisi, D. Sornette, D. Helbing, Financial price dynamics and pedestrian counterflows: A comparison of statistical stylized facts, Physical Review E **87**, 012804 (2013).

60. B. Podobnik, D. Horvatic, A. Petersen, H. Stanley, Cross-correlations between volume change and price change, Proceedings of the National Academy of Sciences of the United States of America **106**, 22079–22084 (2009).

61. R. Rak, S. Drozdz, J. Kwapien, P. Oswiecimka, Stock returns versus trading volume: Is the correspondence more general?, Acta Physica Polonica B **44**, 2035–2050 (2013).

62. J. Shao, P. C. Ivanov, B. Urosevic, H. E. Stanley, B. Podobnik, Zipf rank approach and cross-country convergence of incomes, EPL **94**, 48001 (2011).

63. K. Yamasaki, L. Muchnik, S. Havlin, A. Bunde, H. Stanley, Scaling and memory in volatility return intervals in financial markets, Proceedings of the National Academy of Sciences of the United States of America **102**, 9424–9428 (2005).

64. F. Wang, K. Yamasaki, S. Havlin, H. Stanley, Scaling and memory of intraday volatility return intervals in stock market, Physical Review E **77**, 026117 (2006).

65. F. Wang, K. Yamasaki, S. Havlin, H. Stanley, Indication of multiscaling in the volatility return intervals of stock markets, Physical Review E **77**, 016109 (2008).

66. L. Giraitis, R. Leipus, D. Surgailis, Recent advances in arch modelling, in G. Teyssiere, A. Kirman (eds.), *Long Memory in Economics* (Springer, 2007), 3–38.

67. A. J. Patton, Volatility forecast comparison using imperfect volatility proxies, Journal of Econometrics **160**, 246–256 (2011).

68. E. Jondeau, The dynamics of squared returns under contemporaneous aggregation of GARCH models, Journal of Empirical Finance **32**, 80–93 (2015).

69. D. Colander, M. Goldberg, A. Haas, K. Juselius, A. Kirman, T. Lux, B. Sloth, The financial crisis and the systemic failure of the economics profession, Critical Review **21**, 249–267 (2009).

70. T. Lux, F. Westerhoff, Economic crisis, Nature Physics **5**, 2–3 (2009).

71. ETH Zurich, Predicting economic crises with econophysics, science Daily, `http://www.sciencedaily.com/releases/2010/05/100511092406.htm` (2010).

72. A. Chakraborti, I. M. Toke, M. Patriarca, F. Abergel, Econophysics review: II. Agent-based models, Quantitative Finance **7**, 1013–1041 (2011).

73. M. Cristelli, L. Pietronero, A. Zaccaria, Critical overview of agent-based models for economics, in F. Mallnace, H. E. Stanley (eds.), *Proceedings of the School of Physics "E. Fermi", Course CLXXVI* (SIF–IOS, Bologna–Amsterdam, 2012), 235–282.

74. F. Abergel, H. Aoyama, B. K. Chakrabari (eds.), *Econophysics of Agent-Based Models* (Springer, 2014).

75. R. Frederick, Agents of influence, Proceedings of the National Academy of Sciences of the United States of America **110**, 3703–3705 (2013).

76. D. Sornette, Physics and financial economics (1776–2014): puzzles, Ising and agent-based models, Reports on Progress in Physics **77**, 062001 (2014).

77. J. von Neumann, A. W. Burks, *Theory of Self-Reproducing Automata* (University of Illinois Press, Urbana and London, 1966).

78. M. Gardner, Mathematical games – the fantastic combinations of john conway's new solitaire game "life", Scientific American **223**, 120–123 (1970).

79. S. Wolfram, *New Kind of Science* (Wolfram Media, 2002).

80. S. Bornholdt, Expectation bubbles in a spin model of markets: Intermittency from frustration across scales, International Journal of Modern Physics C **12**, 667–674 (2001).

81. T. Kaizoji, S. Bornholdt, Y. Fujiwara, Dynamics of price and trading volume in a spin model of stock markets with heterogeneous agents, Physica A **316**, 441–452 (2002).

82. S. H. Yook, H. J. Kim, Y. Kim, Agent-based generalized spin model for financial markets on two-dimensional lattices, Journal of the Korean Physical Society **52**, S150–S153 (2008).

83. S. M. Krause, P. Bottcher, S. Bornholdt, Mean-field-like behavior of the generalized voter-model-class kinetic ising model, Physical Review E **85**, 031126 (2012).

84. R. L. Liboff, *Kinetic Theory* (Prentice–Hall, New Jersey, USA, 1990).

85. A. Dragulescu, V. Yakovenko, Statistical mechanics of money, European Physical Journal B **17**, 723–729 (2000).

86. A. Chatterjee, B. K. Chakrabarti, Kinetic exchange models for income and wealth distributions, European Physical Journal B **60**, 135–149 (2007).

87. U. Garibaldi, E. Scalas, P. Viarengo, Statistical equilibrium in simple exchange games, European Physical Journal B **60**, 241–246 (2007).

88. M. Patriarca, E. Heinsalu, A. Chakraborti, Basic kinetic wealth-exchange models: common features and open problems, European Physical Journal B **73**, 145–153 (2010).

89. S. Cordier, L. Pareschi, G. Toscani, On a kinetic model for a simple market economy, Journal of Statistical Physics **120**, 253–277 (2005).

90. K. Staliūnas, Bose–Einstein condensation in financial systems, Nonlinear Analysis: Modelling and Control **10**, 247–256 (2005).

91. A. S. Chakrabarti, B. K. Chakrabarti, Microeconomics of the ideal gas like market models, Physica A **388**, 4151–4158 (2009).

92. D. Maldarella, L. Pareschi, Kinetic models for socio-economic dynamic of speculative markets, Physica A **391**, 715–730 (2012).

93. T. Lux, M. Marchesi, Scaling and criticality in a stochastic multi-agent model of a financial market, Nature **397**, 498–500 (1999).

94. D. M. Hausman, Philosophy of economics, in E. N. Zalta (ed.), *The Stanford Encyclopedia of Philosophy* (2013).

95. A. Kirman, G. Teyssiere, Microeconomic models for long memory in the volatility of financial time series, Studies in Nonlinear Dynamics and Econometrics **5**, 281–302 (2002).

96. A. P. Kirman, Ants, rationality and recruitment, Quarterly Journal of Economics **108**, 137–156 (1993).

97. L. Zhao, G. Yang, W. Wang, Y. Chen, J. P. Huang, H. Ohashi, H. E. Stanley, Herd behavior in a complex adaptive system, Proceedings of the National Academy of Sciences of the United States of America **108**, 15058–15063 (2011).

98. Y. Shapira, Y. Berman, E. Ben-Jacob, Modelling the short term herding behaviour of stock markets, New Journal of Physics **16**, 053040 (2014).

99. G. Mosquera-Donate, M. Boguna, Follow the leader: Herding behavior in heterogeneous populations, Physical Review E **91**, 052804 (2015).

100. J. Touloub, The hipster effect: When anticonformists all look the same, preprint published on arxiv 1410.8001 (2015).

101. M. O. Jackson, *Social and Economic Networks* (Princeton University Press, 2010).

102. M. J. Newman, *Networks: An Introduction* (Oxford University Press, 2010).

103. R. Cohen, S. Havlin, *Complex Networks: Structure, Robustness and Function* (Cambridge University Press, 2010).

104. A. L. Barabasi, *Network Science* (Cambridge University Press, 2015), to be published, available online.

105. P. Erdos, A. Renyi, On random graphs, Publicationes Mathematicae **6**, 290–297 (1959).

106. D. Stauffer, A. Aharony, *Introduction to Percolation Theory* (CRC Press, 1994).

107. D. J. Watts, S. H. Strogatz, Collective dynamics of small-world networks, Nature **393**, 440–442 (1998).

108. S. Milgram, The small world problem, Psychology Today **2**, 60–67 (1967).

109. R. Albert, A. L. Barabasi, Statistical mechanics of complex networks, Reviews of Modern Physics **74**, 47–97 (2002).

110. P. Holme, B. J. Kim, Growing scale-free networks with tunable clustering, Physical Review E **65**, 026107 (2002).

111. M. O. Jackson, B. W. Rogers, Meeting strangers and friends of friends: How random are social networks?, American Economic Review **97**, 890–915 (2007).

112. J. Leskovec, J. Kleinberg, C. Faloutsos, Graph evolution: Densification and shrinking diameters, Transactions on Knowledge Discovery from Data **1**, 1217301 (2007).

113. M. Balint, V. Posea, A. Dimitriu, A. Iosup, An analysis of social gaming networks in online and face to face bridge communities, in *Proceedings of the Third International Workshop on Large-scale System and Application Performance* (New York, USA, 2011), 35–42.

114. P. Moriano, J. Finke, On the formation of structure in growing networks, Journal of Statistical Mechanics **2013**, P06010 (2013).

115. P. Morters, Y. Peres, *Brownian motion* (Cambridge University Press, 2010).

116. D. S. Lemons, A. Gythiel, Paul Langevin's 1908 paper "On the theory of brownian motion", American Journal of Physics **65**, 1079 (1997).

117. H. Risken, *The Fokker–Planck Equation: Methods of Solutions and Applications* (Springer, 1996), 3 edition.

118. V. Mackevicius, *Stochastic Analysis* (Vilnius University Press, 2005).

119. C. W. Gardiner, *Handbook of Stochastic Methods* (Springer, Berlin, 2009).

120. R. Axelrod, Advancing the art of simulation in the social sciences, Complexity **3**, 16–32 (1997).

121. M. S. Pakkanen, Microfoundations for diffusion price processes, Mathematics and financial economics **3**, 89–114 (2010).

122. L. Feng, B. Li, B. Podobnik, T. Preis, H. E. Stanley, Linking agent-based models and stochastic models of financial markets, Proceedings of the National Academy of Sciences of the United States of America **22**, 8388–8393 (2012).

123. S. Alfarano, T. Lux, F. Wagner, Estimation of agent-based models: The case of an asymmetric herding model, Computational Economics **26**, 19–49 (2005).

124. S. Alfarano, T. Lux, F. Wagner, Time variation of higher moments in a financial market with heterogeneous agents: An analytical approach, Journal of Economic Dynamics and Control **32**, 101–136 (2008).

125. V. Alfi, M. Cristelli, L. Pietronero, A. Zaccaria, Minimal agent based model for financial markets I: Origin and self-organization of stylized facts, European Physical Journal B **67**, 385–397 (2009).

126. V. Alfi, M. Cristelli, L. Pietronero, A. Zaccaria, Minimal agent based model for financial markets II: Statistical properties of the linear and multiplicative dynamics, European Physical Journal B **67**, 399–417 (2009).

127. B. Kaulakys, J. Ruseckas, Stochastic nonlinear differential equation generating 1/f noise, Physical Review E **70**, 020101 (2004).

128. V. Gontis, B. Kaulakys, Modeling financial markets by the multiplicative sequence of trades, Physica A **344**, 128–133 (2004).

129. B. Kaulakys, V. Gontis, M. Alaburda, Point process model of $1/f$ noise vs a sum of Lorentzians, Physical Review E **71**, 1–11 (2005).

130. B. Kaulakys, J. Ruseckas, V. Gontis, M. Alaburda, Nonlinear stochastic models of 1/f noise and power-law distributions, Physica A **365**, 217–221 (2006).

131. B. Kaulakys, M. Alaburda, Modeling scaled processes and $1/f^{\beta}$ noise using nonlinear stochastic differential equations, Journal of Statistical Mechanics P02051 (2009).

132. A. E. Biondo, A. Pluchino, A. Rapisarda, D. Helbing, Stopping financial avalanches by random trading, Physical Review E **88**, 062814 (2013).

133. F. Schweitzer, P. Mavrodiev, C. J. Tessone, How can social herding enhance cooperation?, Advances in Complex Systems **16**, 1350017 (2013).

134. V. Gontis, B. Kaulakys, J. Ruseckas, Trading activity as driven poisson process: comparison with empirical data, Physica A **387**, 3891–3896 (2008).

135. V. Gontis, J. Ruseckas, A. Kononovicius, A long-range memory stochastic model of the return in financial markets, Physica A **389**, 100–106 (2010).

136. V. Gontis, J. Ruseckas, A. Kononovicius, A non-linear stochastic model of return in financial markets, in C. Myers (ed.), *Stochastic Control* (InTech, 2010).

137. V. Gontis, B. Kaulakys, J. Ruseckas, Point process models of 1/f noise and internet traffic, AIP Conference Proceedings **776**, 144–149 (2005).

138. B. Kaulakys, M. Alaburda, V. Gontis, T. Meskauskas, J. Ruseckas, Modeling of flows with power-law spectral densities and power-law distributions of flow intensities, in A. Schadschneider (ed.), *Traffic and Granular Flow* (Springer, 2007), volume 5, 587–594.

139. D. J. Levitin, P. Chordia, V. Menon, Musical rhythm spectra from Bach to Joplin obey a 1/f power law, Proceedings of the National Academy of Sciences of the United States of America **109**, 3716–3720 (2012).

140. B. Kaulakys, M. Alaburda, V. Gontis, Point processes modeling of time series exhibiting power-law statistics, AIP Conference Proceedings **922**, 535–538 (2007).

141. R. Kazakevicius, J. Ruseckas, Power law statistics in the velocity fluctuations of brownian particle in inhomogeneous media and driven by colored noise, Journal of Statistical Mechanics P02021 (2015).

142. R. Kazakevicius, J. Ruseckas, Anomalous diffusion in nonhomogeneous media: Power spectral density of signals generated by time-subordinated nonlinear langevin equations, Physica A **438**, 210–222 (2015).

143. T. A. Marsh, E. R. Rosenfeld, Stochastic processes for interest rates and equilibrium bond prices, The Journal of Finance **38**, 635–646 (1983).

144. M. Jeanblanc, M. Yor, M. Chesney, *Mathematical Methods for Financial Markets* (Springer, Berlin, 2009).

145. K. C. Chan, G. Andrew Karolyi, F. A. Longstaff, A. B. Sanders, An empirical comparison of alternative models of the short-term interest rate, The Journal of Finance **XLVII**, 1209–1227 (1992).

146. W. H. Press, S. A. Teukolsky, W. T. Vetterling, *Numerical Recipies* (Cambridge University Press, 2007), 3 edition.

147. P. E. Kloeden, E. Platen, *Numerical Solution of Stochastic Differential Equations* (Springer, Berlin, 1999).

148. E. W. Weinstein, Modified Bessel function of the second kind, from MathWorld – A Wolfram Web Resource: `http://mathworld.wolfram.com/ModifiedBesselFunctionoftheSecondKind.html`.

149. C. M. Gell-Mann, C. Tsallis, *Nonextensive Entropy – Interdisciplinary Applications* (Oxford University Press, New York, 2004).

150. E. W. Weinstein, Student's t-distribution, from MathWorld – A Wolfram Web Resource: http://mathworld.wolfram.com/Studentst-Distribution.html.

151. J. Ruseckas, B. Kaulakys, Scaling properties of signals as origin of 1/f noise, Journal of Statistical Mechanics **2014**, P06004 (2014).

152. V. Gontis, B. Kaulakys, Long-range memory model of trading activity and volatility, Journal of Statistical Mechanics **P10016**, 1–11 (2006).

153. D. Davydov, V. Linetsky, Pricing and hedging path-dependent options under the CEV process, Management Science **47**, 949–965 (2001).

154. S. Reimann, V. Gontis, M. Alaburda, Interplay between positive feedbacks in the generalized CEV process, Physica A **390**, 1393–1401 (2011).

155. D. O. Cajueiro, B. M. Tabak, Multifractality and herding behavior in the japanese stock market, Chaos, Solitons and Fractals **40**, 497–504 (2009).

156. J. P. Bouchaud, Crises and collective socio-economic phenomena: Simple models and challenges, Journal of Statistical Physics **151**, 567–606 (2013).

157. A. N. Borodin, P. Salminen, *Handbook of Brownian Motion* (Birkhauser, Basel, Switzerland, 2002), 2 edition.

158. S. Redner, *A guide to first-passage processes* (Cambridge University Press, 2001).

159. M. Abramowitz, I. A. Stegun, *Handbook of Mathematical Functions with Formulas, Graphs, and Mathematical Tables* (Dover, New York, 1972).

160. E. W. Weinstein, Bessel function of the first kind, from MathWorld – A Wolfram Web Resource: http://mathworld.wolfram.com/BesselFunctionoftheFirstKind.html.

161. E. W. Weinstein, Bessel function zeros, from MathWorld – A Wolfram Web Resource: http://mathworld.wolfram.com/BesselFunctionZeros.html.

162. C. S. Chou, H. J. Lin, Some properties of cir processes, Stochastic Analysis and Applications **24**, 901–912 (2006).

163. B. Mandelbrot, The variation of certain speculative prices, The Journal of Business **36**, 394 (1963).

164. E. F. Fama, The behavior of stock-market prices, The Journal of Business **38**, 34–105 (1965).

165. R. N. Mantegna, H. E. Stanley, *Introduction to Econophysics: Correlations and Complexity in Finance* (Cambridge University Press, 2000).

166. A. W. Lo, Long-term memory in stock market prices, Econometrica **59**, 1279–313 (1991).

167. Z. Ding, C. W. J. Granger, R. F. Engle, A long memory property of stock market returns and a new model, Journal of Empirical Finance **1**, 83–106 (1993).

168. J. Ruseckas, B. Kaulakys, Intermittency in relation with 1/f noise and stochastic differential equations, Chaos **23**, 023102 (2013).

169. R. Engle, Autoregresive conditional heteroscedasticity with estimates of the variance of United Kingdom inflation, Econometrica **50**, 987–1008 (1982).

170. T. Bollerslev, Generalized autoregressive conditional heteroskedasticity, Journal of Econometrics **31**, 307–327 (1986).

171. R. Engle, T. Bollerslev, Modeling the persistence of conditional variances, Econometric Reviews **5**, 1–50 (1986).

172. J. Campbell, A. Lo, A. MacKinlay, *The Econometrics of Financial Markets* (Princeton University Press, Princeton, USA, 1997).

173. M. Potters, R. Cont, J. P. Bouchaud, Financial markets as adaptive systems, EPL **41**, 239–244 (1998).

174. J. P. Fouque, K. R. Sircar, G. Papanicolaou, *Derivatives in Financial Markets with Stochastic Volatility* (Cambridge University Press, Cambridge, 2000).

175. T. Bollerslev, Glossary to ARCH (GARCH), CREATES Research Paper (2008).

176. L. Giraitis, R. Leipus, D. Surgailis, ARCH(∞) models and long memory, in T. G. Anderson, R. A. Davis, J. Kreis, T. Mikosh (eds.), *Handbook of Financial Time Series* (Springer Verlag, Berlin, 2009), 71–84.

177. C. Conrad, Non-negativity conditions for the hyperbolic garch model, Journal of Econometrics **157**, 441–457 (2010).

178. M. E. H. Arouri, S. Hammoudeh, A. Lahiani, D. K. Nguyen, Long memory and structural breaks in modeling the return and volatility dynamics of precious metals, The Quarterly Review of Economics and Finance **52**, 207–218 (2012).

179. L. Giraitis, H. L. Koul, D. Surgailis, *Large Sample Inference for Long Memory Processes* (World Scientific, 2012).

180. M. Tayefi, T. V. Ramanathan, An overview of FIGARCH and related time series models, Austrian Journal of Statistics **41**, 175–196 (2012).

181. L. Borland, Option pricing formulas based on a non-gaussian stock price model, Physical Review Letters **89**, 098701 (2002).

182. T. H. Rydberg, N. Shephard, Dynamics of trade-by-trade price movements: Decomposition and models, Journal of Financial Econometrics **1**, 2–25 (2003).

183. E. Scalas, T. Kaizoji, M. Kirchler, J. Huber, A. Tedeschi, Waiting times between orders and trades in double-auction markets, Physica A **366**, 463–471 (2006).

184. E. Jondeau, S. H. Poon, M. Rockinger, *Financial Modeling Under Non-Gaussian Distributions* (2007).

185. D. B. Nelson, ARCH models as diffusion approximations, Journal of Econometrics **45**, 7–38 (1990).

186. C. Kluppelberg, A. Lindner, R. Maller, A continuous-time GARCH process driven by a Levy process: stationarity and second-order behaviour, Journal of Applied Probability **41**, 601–622 (2004).

187. A. M. Lindner, Continuous time approximations to GARCH and stochastic volatility models, in *Handbook of Financial Time Series* (Springer, 2008).

188. C. Kluppelberg, R. Maller, A. Szimayer, The COGARCH: A review, with news on option pricing and statistical inference (2010).

189. J. Ruseckas, B. Kaulakys, 1/f noise from nonlinear stochastic differential equations, Physical Review E **81**, 031105 (2010).

190. M. L. Higgins, A. K. Bera, A class of nonlinear ARCH models, International Economic Review **33**, 137–158 (1992).

191. D. Challet, M. Marsili, R. Zecchina, Statistical mechanics of systems with heterogeneous agents: Minority games, Physical Review Letters **84**, 1824–1827 (2000).

192. J. D. Farmer, P. Patelli, I. Zovko, The predictive power of zero intelligence in financial markets, Proceedings of the National Academy of Sciences of the United States of America **102**, 2254–2259 (2005).

193. T. A. Schmitt, R. Schafer, M. C. Munnix, T. Guhr, Microscopic understanding of heavy-tailed return distributions in an agent-based model, EPL **100**, 38005 (2012).

194. S. H. Chen, S. P. Li, Econophysics: Bridges over a turbulent current, International Review of Financial Analysis **23**, 1–10 (2012).

195. M. Ortisi, V. Zuccolo, From minority game to Black–Scholes pricing, Applied Mathematical Finance **20**, 578–598 (2013).

196. L. Goldenberg, B. Libai, E. Muller, Using complex systems analysis to advance marketing theory development, Academy of Marketing Science Review **9**, 1–18 (2001).

197. G. Fibich, R. Gibori, E. Muller, *A Comparison of Stochastic Cellular Automata Diffusion with the Bass Diffusion Model*, Technical report, NYU Stern School of Business (2010).

198. P. Purplys, Mikroskopinis ir makroskopinis naujų produktų sklaidos modeliavimas, Term paper, supervisor dr. V. Gontis (2011).

199. P. Purlys, A. Kononovicius, V. Gontis, Various ways of introducing herding behavior into the agent based models of complex systems, in *Open Readings 2012* (Vilnius, Lithuania, 2012), 150.

200. M. Aoki, H. Yoshikawa, *Reconstructing Macroeconomics: A Perspektive from Statistical Physics and Combinatorial Stochastic Processes* (Cambridge University Press, 2007).

201. F. Diebold, A. Inoue, Long memory and regime switching, Journal of Econometrics **105**, 131–159 (2001).

202. A. Carro, R. Toral, M. San Miguel, Signal amplification in an agent-based herding model (2013).

203. A. Carro, R. Toral, M. San Miguel, Markets, herding and response to external information, PLoS ONE **10**, e0133287 (2015).

204. N. G. van Kampen, *Stochastic Process in Physics and Chemistry* (North Holland, Amsterdam, 2007).

205. F. M. Bass, A new product growth model for consumer durables, Management Science **15**, 215–227 (1969).

206. V. Mahajan, E. Muller, F. M. Bass, New-product diffusion models, in J. Eliashberg, G. L. Lilien (eds.), *Handbooks in Operations Research and Management Science* (North Holland, Amsterdam, 1993), volume 5, 349–408.

207. A. Prasad, V. Mahajan, How many pirates should a software firm tolerate? An analysis of piracy protection on the diffusion of software, International Journal of Research in Marketing **20**, 337–353 (2003).

208. A. Ishii, H. Arakaki, N. Matsuda, S. Umemura, T. Urushidani, N. Yamagata, N. Yoshida, The 'hit' phenomenon: A mathematical model of human dynamics interactions as a stochastic process, New Journal of Physics **14**, 063018.

209. A. Ishii, H. Koguchi, K. Uchiyama, Mathematical model of hit phenomena as a theory for human interaction in the society, in K. Glass, R. Colbaugh, P. Ormerod, J. Tsao (eds.), *Complex Sciences* (Springer International Publishing, 2013), volume 126 of *Lecture Notes of the Institute for Computer Sciences, Social Informatics and Telecommunications Engineering*, 159–164.

210. S. Alfarano, M. Milakovic, Network structure and N-dependence in agent-based herding models, Journal of Economic Dynamics and Control **33**, 78–92 (2009).

211. S. Alfarano, M. Milakovic, M. Raddant, A note on institutional hierarchy and volatility in financial markets, European Journal of Finance **19**, 449–465 (2013).

212. A. Traulsen, J. C. Claussen, C. Hauert, Coevolutionary dynamics: From finite to infinite populations, Physical Review Letters **95**, 238701 (2005).

213. A. Traulsen, J. C. Claussen, C. Hauert, Coevolutionary dynamics in large, but finite populations, Physical Review E **74**, 011901 (2006).

214. A. Traulsen, J. C. Claussen, C. Hauert, Stochastic differential equations for evolutionary dynamics with demographic noise and mutations, Physical Review E **85**, 041901 (2012).

215. L. Akoglu, C. Faloutsos, RTG: A recursive realistic graph generator using random typing, Data Mining Knowledge Discovery **19**, 194–209 (2009).

216. A. Bonato, J. Janssen, P. Pralat, A geometric model for on-line social networks, in *Proceedings of International Workshop on Modeling Social Media* (ACM, New York, USA, 2010), 1835984.

217. E. R. Colman, G. J. Rodgers, Complex scale-free networks with tunable power-law exponent and clustering, Physica A **392**, 5501–5510 (2013).

218. A. R. Plastino, A. Plastino, From Gibbs microcanonical ensemble to Tsallis generalized canonical distribution, Phys. Lett. A **193**, 140–143 (1994).

219. F. Q. Potiguar, U. M. S. Costa, Fluctuation of energy in the generalized thermostatistics, Physica A **321**, 482–492 (2003).

220. L. Walras, *Elements of Pure Economics* (Routledge, 2013).

221. J. D. Farmer, L. Gillemot, F. Lillo, S. Mike, A. Sen, What really causes large price changes, Quantitative Finance **4**, 383–397 (2004).

222. X. Gabaix, P. Gopikrishnan, V. Plerou, H. E. Stanley, Institutional investors and stock market volatility, The Quarterly Journal of Economics 461–504 (2006).

223. A. E. Biondo, A. Pluchino, A. Rapisarda, The beneficial role of random strategies in social and financial systems, Journal of Statistical Physics **151**, 607–622 (2013).

224. A. E. Biondo, A. Pluchino, A. Rapisarda, D. Helbing, Are random trading strategies more successful than technical ones?, PLoS ONE **8**, e68344 (2013).

225. C. Hommes, Heterogeneous agent models in economics and finance, in L. Tesfatsion, K. L. Judd (eds.), *Handbook of Computational Economics* (Elsevier, 2006), volume 2, chapter 23, 1109–1186.

226. C. Hommes, *Interacting Agents in Finance*, Tinbergen institute discussion papers, Tinbergen Institute (2006).

227. C. H. Hommes, Bounded rationality and learning in complex markets, in *Handbook of Economic Complexity* (Cheltenham: Edward Elgar, 2009).

228. C. Hommes, Experimental economics, behavioral economics and heterogeneity of economic and social actors, talk given at *International School on Multidisciplinary Approaches to Economic and Social Complex System* (2010).

229. R. N. Mantegna, B. Spagnolo, Noise enhanced stability in an unstable system, Physical Review Letters **76**, 563–566 (1996).

230. J. Garcia-Ojalvo, J. Sancho, *Noise in Spatially Extended Systems* (1999).

231. C. Rouvas-Nicolis, G. Nicolis, Stochastic resonance, Scholarpedia **2**, 1474 (2007).

232. F. Caruso, S. F. Huelga, M. B. Plenio, Noise-enhanced classical and quantum capacities in communication networks, Physical Review Letters **105**, 190501 (2010).

233. A. Pluchino, A. Rapisarda, C. Garofalo, The Peter principle revisited: A computational study, Physica A **389**, 467–472 (2010).

234. A. Pluchino, A. Rapisarda, C. Garofalo, S. Spagano, M. Caserta, Accidental politicians: How randomly selected legislators can improve parliament efficiency, Physica A **390**, 3944–3954 (2010).

235. M. Friedman, *A Theory of the Consumption Function* (Princeton University Press, 1956).

List of publications and presentations

Full text publications

The research covered in this dissertation was published in 15 papers. List, in chronological order, follows. 9 papers were published in ISI indexed journals [A1-A5, A7, A9, A10, A15]. [A6] paper was published in ISI indexed conference proceedings. [A8, A11-A13] papers were published in other international peer-reviewed journals. [A14] was published as a chapter in an open-access book.

A1. **A. Kononovicius**, V. Gontis, Herding interactions as an opportunity to prevent extreme events in financial markets, European Physical Journal B **88**(7), 189 (2015).

A2. **A. Kononovicius**, J. Ruseckas, Nonlinear GARCH model and 1/f noise, Physica A **427**, 74–81 (2015).

A3. **A. Kononovicius**, J. Ruseckas, Continuous transition from the extensive to the non-extensive statistics in an agent-based herding model, European Physical Journal B **87**(8), 169 (2014).

A4. V. Gontis, **A. Kononovicius**, Consentaneous agent-based and stochastic model of the financial markets, PLoS ONE **9**(7), e102201 (2014).

A5. **A. Kononovicius**, V. Gontis, Control of the socio-economic systems using herding interactions, Physica A **405**, 80–84 (2014).

A6. V. Gontis, **A. Kononovicius**, Fluctuation analysis of the three agent groups herding model, in *Noise and Fluctuations (ICNF), 2013 22nd International Conference on* (Montpeiler, France, 2013), 1–4.

A7. **A. Kononovicius**, V. Gontis, Three state herding model of the financial markets, EPL **101**, 28001 (2013).

A8. **A. Kononovicius**, V. Daniunas, Agent-based and macroscopic modeling of the complex socio-economic systems, Social Technologies **3**(1), 85–103 (2013).

A9. **A. Kononovicius**, V. Gontis, Agent based reasoning for the non-linear stochastic models of long-range memory, Physica A **391**(4), 1309–1314 (2012).

A10. V. Gontis, **A. Kononovicius**, S. Reimann, The class of nonlinear stochastic models as a background for the bursty behavior in financial markets, Advances in Complex Systems **15**(supp01), 1250071 (2012).

A11. **A. Kononovicius**, V. Gontis, V. Daniunas, Agent-based versus macroscopic modeling of competition and business processes in economics and finance, International Journal On Advances in Intelligent Systems **5**(1-2), 111–126 (2012).

A12. V. Daniunas, V. Gontis, **A. Kononovicius**, Agent-based versus macroscopic modeling of competition and business processes in economics, in *ICCGI 2011, The Sixth International Multi-Conference on Computing in the Global Information Technology* (Luxembourg, 2011), 84–88, received IARIA Best Paper Award (see `http://www.iaria.org/conferences2011/AwardsICCGI11.html`).

A13. V. Gontis, **A. Kononovicius**, Nonlinear stochastic model of return matching to the data of New York and Vilnius Stock Exchanges, Dynamics of Socio-Economic Systems **2**(1), 101–109 (2011).

A14. V. Gontis, J. Ruseckas, **A. Kononovicius**, A non-linear stochastic model of return in financial markets, in C. Myers (ed.), *Stochastic Control* (InTech, 2010).

A15. V. Gontis, J. Ruseckas, **A. Kononovicius**, A long-range memory stochastic model of the return in financial markets, Physica A **389**(1), 100–106 (2010).

Conference presentations

The research covered in this dissertation was presented in 33 conference presentations. List, in chronological order, follows. Of them 12 talks and 10 posters were presented by the author of this dissertation.

C1. A. Kononovicius, V. Gontis, Pikų statistika minučių, dienų ir mėnesių laiko skalėse, in *41-oji Lietuvos nacionalinė fizikos konferencija: Programa ir pranešimų tezės* (Vilnius, Lietuva, 2015), 355. // Poster by A. Kononovicius

C2. A. Kononovicius, J. Ruseckas, Long-range memory in non-linear GARCH(1,1) models, in *Open Readings 2015* (Vilnius, Lithuania, 2015), 247. // Poster by A. Kononovicius

C3. A. Kononovicius, V. Gontis, J. Ruseckas, Complexity and statistical physics of herding behavior, in *Naujametė fizikos konferencija* (Vilnius, Lithuania, 2015), 11. // Talk given by A. Kononovicius

C4. A. Kononovicius, V. Gontis, Controlling the dynamics of herding dominant financial market, in *International Conference on Statistical Physics* (Rhodes, Greece, 2014), 80. // Talk given by A. Kononovicius

C5. V. Gontis, A. Kononovicius, Financial herding of three agent groups under the impact of exogenous noise, in *International Conference on Statistical Physics* (Rhodes, Greece, 2014), 54–55. // Talk given by V. Gontis

C6. A. Kononovicius, J. Ruseckas, Non-extensive and extensive statistics in the agent-based herding model, in *Open Readings 2014* (Vilnius, Lithuania, 2014), 52. // Talk given by A. Kononovicius

C7. A. Kononovicius, V. Gontis, Leadership phenomenon in the agent-based herding model, in *Open Readings 2014* (Vilnius, Lithuania, 2014), 201. // Poster by A. Kononovicius

C8. A. Kononovicius, V. Gontis, Controlling the collective behavior in the agent-based herding model, in *Verhandlungen DPG (VI) 49* (Dresden, Germany, 2014), SOE 6.15. // Poster by A. Kononovicius

C9. A. Kononovicius, V. Gontis, Sudėtingų socialinių vyksmų aiškinimas siejant jų mikroskopinius ir makroskopinius aprašymus, in *Fizinių ir technologijos mokslų tarpdalykiniai tyrimai (4-oji jaunųjų mokslininkų konferencija): Fizinių mokslų sekcija* (Lietuvos mokslų akademija, Vilnius, Lietuva, 2014), 11–13. // Talk given by A. Kononovicius

C10. A. Kononovicius, V. Gontis, Mikroskopinis ir makroskopinis sudėtingų sistemų modeliavimas, in *40-oji Lietuvos nacionalinė fizikos konferencija: Programa ir pranešimų tezės* (Vilnius, Lietuva, 2013), 28. // Talk given by A. Kononovicius

C11. A. Kononovicius, V. Gontis, Generalizing binary choice agent-based herding model, in *WEHIA 2013: Conference Program* (Reykjavik, Iceland, 2013), 8. // Talk given by A. Kononovicius

C12. A. Kononovicius, V. Daniunas, Agent-based and macroscopic modeling of the complex socio-economic systems, in *Social Transformations in Contemporary Society 2013* (Vilnius, Lithuania, 2013). // Talk given by A. Kononovicius

C13. A. Kononovicius, V. Gontis, Bursting behavior of the non-linear stochastic models applicable to the financial markets, in *Open Readings 2013* (Vilnius, Lithuania, 2013), 57. // Talk given by A. Kononovicius

C14. A. Kononovicius, V. Gontis, Inter-burst times of the empirical high-frequency financial market data and non-linear stochastic models, in *Verhandlungen DPG (VI) 48* (Regensburg, Germany, 2013). // Poster by A. Kononovicius

C15. V. Gontis, A. Kononovicius, The class of nonlinear stochastic equations as a background modeling financial systems, in *ETH Zurich Latsis Symposium 2012 Satellite Workshop* (ETH Zurich, Zurich, Switzerland, 2012), 37. // Talk given by V. Gontis

C16. A. Kononovicius, V. Gontis, J. Ruseckas, B. Kaulakys, Bursting dynamics of the high-frequency empirical return and non-linear stochastic model, in *COST Action MP0801 Annual Meeting 2012* (Galway, Ireland, 2012), 31. // Poster by A. Kononovicius

C17. V. Gontis, A. Kononovicius, B. Kaulakys, Agent-based versus macroscopic modeling of competition and business processes in economics and finance, in *COST Action MP0801 Annual Meeting 2012* (Galway, Ireland, 2012), 19. // Talk given by V. Gontis

C18. A. Kononovicius, V. Gontis, B. Kaulakys, Herding behavior of agents as a background of financial fluctuations, in *25th European Conference on Operational Research* (Vilnius, Lithuania, 2012), 75. // Talk given by A. Kononovicius

C19. V. Gontis, A. Kononovicius, Agent-based versus macroscopic modeling of competition and business processes in economics and finance, in *Meeting of Workgroup 3 of COST Action MP0801* (Jerusalem, Izrael, 2012). // Talk given by V. Gontis

C20. B. Kaulakys, V. Gontis, A. Kononovicius, J. Ruseckas, Microscopic herding model leading to long-range processes and 1/f noise with application to abso-

lute return in financial markets, in *Verhandlungen DPG (VI) 47* (Berlin, Germany, 2012), 403. // Talk given by A. Kononovicius

C21. A. Kononovicius, V. Gontis, J. Ruseckas, B. Kaulakys, Bursting behavior of non-linear stochastic model and empirical high-frequency return, in *Verhandlungen DPG (VI) 47* (Berlin, Germany, 2012), 401. // Poster by A. Kononovicius

C22. P. Purlys, A. Kononovicius, V. Gontis, Various ways of introducing herding behavior into the agent based models of complex systems, in *Open Readings 2012* (Vilnius, Lithuania, 2012), 150. // Poster by P. Purlys

C23. B. Kaulakys, M. Alaburda, V. Gontis, A. Kononovicius, J. Ruseckas, Modeling by the nonlinear stochastic differential equation of the power-law distribution of extreme events in the financial systems, in *6th International Conference on Unsolved Problems on Noise* (Kolkata, India, 2012). // Talk given by B. Kaulakys

C24. A. Kononovicius, V. Gontis, B. Kaulakys, Agent based reasoning of the nonlinear stochastic models, in *Verhandlungen DPG (VI) 46* (Dresden, Germany, 2011), 502. // Poster by A. Kononovicius

C25. A. Kononovicius, V. Gontis, Mikroskopinis stochastinių modelių aiškinimas, in *39-oji Lietuvos nacionalinė fizikos konferencija: Programa ir pranešimų tezės* (Vilnius, Lietuva, 2011), 34. // Talk given by A. Kononovicius

C26. V. Gontis, A. Kononovicius, B. Kaulakys, Minimal agent based models as a microscopic reasoning of nonlinear stochastic models, in *3rd Annual Meeting COST Action MP0801: Physics of Competition and Conflicts* (Eindhoven, Holland, 2011). // Talk given by V. Gontis

C27. A. Kononovicius, V. Gontis, Stochastic model of return matching to the data of financial markets with differing liquidity, in *Open Readings 2010* (Vilnius, Lithuania, 2010). // Talk given by A. Kononovicius

C28. V. Gontis, J. Ruseckas, A. Kononovicius, M. Alaburda, B. Kaulakys, Nonextensive statistics with application to financial processes from nonlinear stochastic differential equations, in *Verhandlungen DPG Spring Meeting* (Regensburg, Germany, 2010). // Poster by V. Gontis

C29. A. Kononovicius, V. Gontis, Empirical analysis of Vilnius stock exchange absolute return time series, in *2nd Annual Meeting COST Action MP0801: Physics of Competition and Conflicts* (Sunny Beach, Bulgaria, 2010). // Poster by A. Kononovicius

C30. V. Gontis, B. Kaulakys, A. Kononovicius, Scaled nonlinear stochastic model of return versus empirical data, in *2nd Annual Meeting COST Action MP0801: Physics of Competition and Conflicts* (Sunny Beach, Bulgaria, 2010). // Talk given by V. Gontis

C31. A. Kononovicius, V. Gontis, J. Ruseckas, Grąžos statistinių savybių, stebimų finansų rinkoje, modeliavimas stochastiniu modeliu su ilga atmintimi, in *Laisvieji skaitymai 2009* (Vilnius, Lietuva, 2009). // Talk given by A. Kononovicius

C32. V. Gontis, J. Ruseckas, A. Kononovicius, Long range memory stochastic model of return in financial markets, in *Applications of Physics in Financial Analysis 7* (Tokyo, Japan, 2009). // Talk given by V. Gontis

C33. V. Gontis, J. Ruseckas, A. Kononovicius, Stochastic modeling of trading activity and volatility in financial markets, in *4th International Conference on News, Expectations and Trends in Statistical Physics* (Crete, Greece, 2008). // Talk given by V. Gontis

Personal contribution of the author

The author of the dissertation has performed all of the numerical simulations as well as most of the analytical derivations presented in this dissertation. The author suggested studying control possibilities (research presented in [A1, A5, C4, C7]) of the ABM proposed in earlier papers.

Acknowledgements

Foremost I would like to express my gratitude to my scientific supervisor dr. Vygintas Gontis. I am utmostly thankful for his supervision, overwhelming support and valuable lessons in science and life.

I would like to thank professor Bronislovas Kaulakys and dr. Julius Ruseckas for insightful discussions and helpful advice. Many thanks goes to fellow students, researchers and other staff of Vilnius University for creative and friendly atmosphere.

I acknowledge the financial support by the Research Council of Lithuania and Vilnius University Doctoral Studies Mobility Fund.

I am grateful to dr. Tomas Žalandauskas, my physics teacher Stanislovas Vičas and my informatics teacher Danguolė Milkintienė for pointing me to my current track.

Last but not the least, I would like to thank my family and friends for their patience, kind support and love. My special thanks go to Lina Abaravičiūtė.